



universität  
wien

# MASTERARBEIT

Titel der Masterarbeit

Spatially homogenous cosmology and dynamical systems

Verfasser

Gernot Heißel, BSc

angestrebter akademischer Grad

Master of Science (MSc)

Wien, 2012

Studienkennzahl lt. Studienblatt:

A 066 876

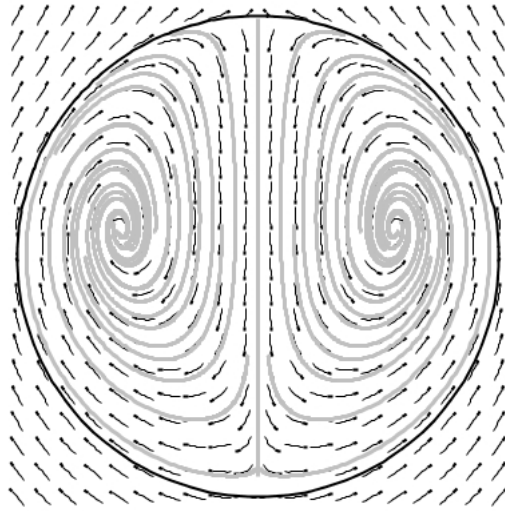
Studienrichtung lt. Studienblatt:

Masterstudium Physik

Betreuer:

MMag. Dr. Johannes Markus Heinzle





To the precise and approximate symmetries of nature



## Acknowledgements

It is my wish to express my gratitude to all those who helped and supported me in my research for and the creation of this thesis:

First and foremost, I owe my deepest gratitude to my thesis advisor Dr. Mark Heinzle. He clearly declared the goals of my thesis and simultaneously gave me plenty of rope for proceeding with my research so I could find my own way to reach them. He was always available to me to give guidance, for an informative discussion or when I wanted to pose a question.

I also wish to thank Prof. Dr. Robert Beig for spending his time answering my questions when Mark was abroad.

I highly appreciated the friendly and pleasant atmosphere in the gravitational physics group. I will keep the many discussions during the common lunch breaks in the group's library in good memory, which never failed to be at least as amusing as they were interesting. Among the other members, I especially want to thank Dr. Michael Pürner and Ingomar Gutmann, whom I was happy to join in their office.

In addition to all this support from the academical side, it is invaluable to be lucky to also have the support from my private side. I thus wish to express my deepest thanks to my parents, Reinhild and Gunther, for their constant support and encouragement during my work on this thesis. I also wish to thank my girlfriend Lucinda for her encouragement, for being with me in my spare time and for her understanding when I did not have much of it.

Finally I wish to thank the creators and users of the MaplePrimes.com and tex.stackexchange.com forum boards, where I profited a lot from discussions about techniques in the computer algebra system Maple, which I extensively used during my studies, and in the document markup language  $\text{\LaTeX}$ , in which I typeset this text.

Thank you!



## Preface

Now when the work is done, and the thesis is written, I can look back and reflect on how it evolved into the present form: The thesis is organised into three parts. Part 1, is concerned with a short introduction to spatially homogenous cosmology and the application of methods from the mathematical theory of dynamical systems in this research field, which builds a branch of mathematical cosmology. These techniques are then applied in part 2 to analyse the dynamics of a certain class of spatially homogenous cosmologies (locally rotationally symmetric Bianchi type VIII) with anisotropic matter. Part 3 deals with a tutorial on how to plot the solutions of the evolution equations encountered in part 2 as flow diagrams with the computer algebra system Maple.

Part 2 represents the core of the thesis. It contains all the results which to achieve was the declared aim specified by the theme of the thesis. It is a reprint of my research article *Dynamics of locally rotationally symmetric Bianchi type VIII cosmologies with anisotropic matter* which was published by Springer in 2012 in the journal *General Relativity and Gravitation*. As research article, part 2 is thus clearly addressed to active researchers in the field of spatially homogenous cosmology.

In contrast to this I addressed part 1 to a master student who has had a standard course on General Relativity, and is actually starting to become acquainted with the field of spatially homogenous cosmology. I therefore did not attempt to write as rigorously as possible, but rather made an effort to give a good first overview to the topic and to shed light on the central theme. After the lecture of part 1, so my goal, the above student should then have a good idea of the introduced concepts, and should be prepared to understand the content of part 2 at least along general lines. Furthermore he should be equipped and encouraged for further reading. To ease the latter, I have added some descriptive text to each piece of literature in the bibliography of part 1 that, so I hope, should help the reader with the orientation.

There are thorough introductory textbooks on spatially homogenous cosmology in the literature. However these usually assume a certain level of familiarity with concepts from semi-Riemannian geometry like isometries or Lie derivatives, or with Lie groups and Lie algebras, which my hypothetical student may not bring with him. In choosing the topics and the above explained style of presentation I thus attempted to complement the literature. For instance, for summarising the mathematical framework of General Relativity in chapter 2 I used an abstract, coordinate free approach. On one hand, this is not the way of presentation in most standard courses on General Relativity. On the other hand however, in my personal opinion this is beneficial for a demonstrative development of the concepts of symmetries of spacetime (chapter 3). For the same reasons I also incorporated a section on Lie group theory (section 2 of chapter 3) and put some effort in first developing the concepts of symmetries of spacetime in an intuitive fashion, to then go over to the more abstract description in terms of Lie groups.

Clearly none of the material presented in part 1 is new, and since most of it is standard, I did not cite a reference at every corner, but rather wrote an extended section for references and further reading at the end of this part to not break the text flow.

When working on the theorems derived in part 2, I used the computer algebra system Maple often as a tool to compare my analytical results with the numerical one which I displayed as flow diagrams in Maple. The evolution equations of part 2 depend on parameters. To get a better feeling on how the solutions change with these parameters I created a code in which I could vary their values in a quick and intuitive way, and where I could directly see the change in the flow plots as a reaction to the change in the parameters. My supervisor encouraged me to present this interactive flow plots in my thesis. I was more than satisfied to follow this suggestion, incorporated a tutorial on how to create interactive flow diagrams with Maple as part 3 of my thesis, and supplemented it with a Maple file with working examples.

I hope that I was able to reach my goals, so that part 1 is helpful for students to get started with spatially homogenous cosmology, that part 2 is of interest to researchers in the field and that part 3 is useful for those who search for an adequate way to visualise the solutions of parameter dependent dynamical systems. If this is the case or not is to be judged by the readers, to who I would be thankful for their feedback.

Vienna, September 2012

Gernot Heißel  
Gernot.Heissel@Mac.com  
Gernot.Heissel@GMX.at



# Contents

Acknowledgements	v
Preface	vii
Chapter 1. Introduction	1
<b>Part 1. A short introduction to spatially homogenous cosmology</b>	<b>3</b>
Chapter 2. Spacetime and gravitation	5
1. Smooth manifolds	5
2. Smooth tensor fields	5
3. Diffeomorphisms, tangent maps and Lie derivatives	7
4. Semi-Riemannian geometry	8
5. General Relativity in a nutshell	10
Chapter 3. Symmetries of spacetime	13
1. Intuitive notions of homogeneity and isotropy	13
2. Lie groups and Lie algebras	15
3. Symmetries in the language of Lie groups and Lie algebras	17
Chapter 4. Friedmann cosmology	19
1. The geometry of the Friedmann cosmologies	19
2. The dynamics of the Friedmann cosmologies	20
3. A qualitative analysis of the Friedmann dynamics	21
Chapter 5. Spatially homogenous cosmology	25
1. Classification of spatially homogenous cosmologies	25
2. Symmetry adapted bases	27
3. The Einstein equations of Bianchi cosmologies	27
4. Qualitative analysis of Bianchi cosmologies	28
References and further reading	33
<b>Part 2. Dynamics of locally rotationally symmetric Bianchi type VIII cosmologies with anisotropic matter</b>	<b>37</b>
1. Introduction and motivation	39
2. The LRS Bianchi type VIII setup	40
2.1 The anisotropic matter family	40
2.2 The Einstein equations as a dynamical system	42
2.3 The state space $\mathcal{X}_{\text{VIII}}$	43
2.4 The state space $\mathcal{Y}_{\text{VIII}}$	44
3. The dynamical system analysis	45
3.1 Analysis in $\overline{\mathcal{V}}_{\text{VIII}}$	45

3.2	Analysis in $\overline{\mathcal{B}}_{\text{III}}$	50
3.3	Analysis in $\overline{\mathcal{S}}_{\sharp}$	52
3.4	Analysis in $\overline{\mathcal{X}}_{\text{I}}$	52
3.5	Analysis in $\overline{\mathcal{X}}_{\text{VIII}}$ and $\overline{\mathcal{S}}_{\infty}$	53
4.	Results and discussion	53
4.1	Identification of the limit sets	54
4.2	The main results	54
4.3	Physical interpretation of the results	56
5.	Extension of the formalism to treat Vlasov matter dynamics with massive particles	56
6.	Appendix: fixed points at infinity	57
	References	59
	<b>Part 3. Plotting interactive flow diagrams with Maple</b>	61
	Chapter 6. Some basic Maple	63
	1. The Maple surface	63
	2. Some basic commands	63
	3. Embedded components	65
	Chapter 7. Plotting flow diagrams	69
	1. Simple flow diagrams	69
	2. Interactive flow diagrams	71
	References and online resources	81
	<b>Appendix</b>	83
	Abstract	85
	Zusammenfassung (German abstract)	87
	Curriculum vitae	89

## CHAPTER 1

# Introduction

With his theory of General Relativity, published in 1916, Einstein gave completely new insight to the physical nature of space, time and gravitation. In General Relativity space and time are unified as spacetime which is no longer viewed as rigid concept that merely tells when and where physics takes place, but rather is subject to physical dynamics itself. Spacetime interacts with its matter content: Matter causes spacetime to curve which in turn causes matter to move; which in detail is dictated by the Einstein equation. As the central object is spacetime itself, General Relativity is not only suited to describe gravity in isolated systems, like the gravitational attraction between celestial bodies, but also allows for a dynamical description of the evolution of the universe, so of spacetime as a whole. Hence General Relativity triggered the advent of modern physical cosmology. Soon several exact cosmological solutions of the Einstein equation were published, the most important of them being the Friedmann-Lemaître-Robertson-Walker (short Friedmann) family of solutions, which model spatially homogenous, isotropic and expanding (or contracting) universes. These models still form the basis of the current standard model of cosmology.

In the standard model, the universe is assumed to possess the spatially homogenous isotropic geometry described by the Friedmann solutions as a first approximation. Structures like galaxies are explained to have formed due to perturbations of that symmetry. During most of the evolution of the universe the matter content is modelled as a perfect fluid, which exhibits spatial homogeneity and isotropy as well. Altogether the standard model takes a typically physical approach to model reality, starting with an idealised case and modelling the details on top. Nevertheless one can ask to which extent this approach is valid: Is a universe that is ‘almost Friedmann’ at one time necessarily ‘almost Friedmann’ in the past and future as well? Are the Friedmann solutions really stable under small perturbations of isotropy and homogeneity? Attempts to answer these questions have been made by analysing the role of the Friedmann models within broader classes of spatially homogenous cosmologies, which need not necessarily be isotropic: In general the component Einstein equations form a system of non-linear partial differential equations for the gravitational field, with one time and three spatial degrees of freedom, and as such cannot be solved exactly. In the case of spatial homogenous cosmologies (for sufficiently simple matter contents) the high symmetry allows to eliminate the spatial degrees of freedom, and to formulate these equations as an autonomous system of ordinary differential equations in time. Though still not solvable exactly, equations of this kind can be rigorously analysed by applying the mathematical theory of dynamical systems. This allows to give qualitative statements for entire classes of solutions, e.g. their past and future asymptotic dynamics.

These analyses have shown many interesting aspects of cosmology, for instance: A Friedmann universe can represent an intermediate or asymptotic state for certain classes of spatially homogenous cosmologies. A spatially homogenous universe may emerge from a highly anisotropic state which isotropises more and more towards the future and approaches Friedmann geometry. Other solutions may be close to

Friedmann for a long intermediate time period but highly anisotropic towards both past and future.

Recent research in the field of spatially homogenous cosmology is mainly concerned with two major aspects: First, there is a conjecture that spacetime close to generic singularities, i.e. to black holes or the big bang, can be described by the evolution equations of spatially homogenous cosmologies. Research at the one hand attempts to proof this conjecture or to support it by heuristic or numerical arguments. On the other hand, research attempts to use this conjecture, presuming it to be true, to draw conclusions for a better understanding of black hole or big bang physics. Second, until recent years research in spatially homogenous cosmology has focused on vacuum spacetimes or universes whose matter content can be described by a perfect fluid. Current research moves over to more general matter contents, which for instance allow for anisotropic pressures. One particular example is collisionless matter (i.e. Vlasov matter) which is believed to be very well suited for a global description of the galaxies in the universe. Among other contents, the present thesis contributes to this latter branch of current research in spatially homogenous cosmology:

The following text is organised in three parts: Part 1 is concerned with a short introduction to spatially homogenous cosmology and the use of methods from the mathematical theory of dynamical systems in this research field. It aims to assist the reader who is just starting to become acquainted with spatially homogenous cosmology to get a good overview and to become familiar with the basic ideas and concepts. After the lecture of part 1 the reader should then be able to read and understand part 2 at least along general lines. Part 2 is a reprint of my research article *Dynamics of locally rotationally symmetric Bianchi type VIII cosmologies with anisotropic matter* which was published by Springer in 2012 in the journal *General Relativity and Gravitation*. It deals with the analysis of one particular class of spatially homogenous cosmologies. The therefor chosen matter contents are in general anisotropic and comprise a larger family of models in which for instance also perfect fluids are contained as special cases. The results allow to draw conclusions on how the grade of anisotropy of the matter content effects the past and future asymptotic evolution of these models. Part 3 gives a tutorial on how to visualise the solutions of the evolution equations examined in part 2 in an interactive flow diagram with the computer algebra system Maple. The such produced diagrams allow the user to see a change in the behaviour of the solutions as a direct reaction to the change in the matter parameters, where one of them essentially gives the grade of matter anisotropy. They are therefore well suited to clearly represent the complex space of solutions, and most notably to present the physical conclusions which were drawn out of the analysis in a comprehensible fashion. Part 3 is also supplemented by a Maple file, which has the same content than presented in this part, with working examples.

## Part 1

# **A short introduction to spatially homogenous cosmology**



## CHAPTER 2

# Spacetime and gravitation

The main purpose of this chapter is to define the mathematical tools that are used to introduce the notions of symmetries of spacetime in chapter 3. These are mainly the concepts of diffeomorphisms (especially one-parameter Lie groups of diffeomorphisms), tangent maps and Lie derivatives treated in section 3, and in particular the notion of an isometry given in definition 6 in section 4. The rest of this chapter embeds these concepts into their natural context in smooth manifold theory and semi-Riemannian geometry, making it a brief introduction to the mathematical backgrounds of General Relativity tailored to the purposes of this text.

### 1. Smooth manifolds

The mathematical concept that underlies spacetime in General Relativity is a certain kind of smooth manifold. A precise definition of this term can be given as follows:

DEFINITION 1. *A smooth manifold  $\Sigma$  is a Hausdorff space endowed with a complete (or maximal) atlas.* smooth manifolds

The elements of  $\Sigma$  are called points. That  $\Sigma$  is Hausdorff means that it is a topological space where for each two points in  $\Sigma$  there exist disjoint neighbourhoods of these points. So intuitively speaking no pair of distinct points is ‘arbitrarily close’ to each other. This gives a manifold the character of a continuum of points, as one would intuitively expect to be true for spacetime. That  $\Sigma$  is equipped with a complete atlas means that the whole manifold can be patched with coordinate systems over subsets of  $\Sigma$ , called charts, that have a smooth overlap. More precisely, a chart is a pair  $(\mathcal{U}, \eta)$ , consisting of some open subset  $\mathcal{U}$  of  $\Sigma$  and a map  $\eta : \mathcal{U} \rightarrow \mathbb{R}^n$ , called the coordinate system of the chart. Two charts  $(\mathcal{U}, \eta)$  and  $(\mathcal{V}, \zeta)$  for that  $\mathcal{U} \cap \mathcal{V} \neq \emptyset$  have a smooth overlap iff both maps  $\zeta \circ \eta^{-1}$  and  $\eta \circ \zeta^{-1}$  are smooth ( $\mathcal{C}^\infty$ ). Intuitively that means that coordinates can be assigned to each point  $p \in \Sigma$ . The number  $n$  of coordinates needed to do so is called the dimension of the manifold. This gives a manifold the feature that it ‘looks like’  $\mathbb{R}^n$  in the neighbourhood of any point, and in connection with the smoothness condition allows one to do calculus on this structure. A schematic of the notion of overlapping charts is depicted in figure 1. charts, coordinate systems

### 2. Smooth tensor fields

Having defined a basic underlying structure, the next thing to do is to define useful maps with it: A function  $f : \Sigma \rightarrow \mathbb{R}$  is called a smooth function on  $\Sigma$  iff its coordinate expression  $f \circ \eta^{-1}$ , where  $\eta$  is a coordinate system, is smooth ( $\mathcal{C}^\infty$ ) in the sense of ordinary calculus. The set of all such functions is denoted by  $\mathcal{F}(\Sigma)$ . A tangent vector to  $\Sigma$  at  $p$  is a function  $v_p : \mathcal{F}(\Sigma) \rightarrow \mathbb{R}$  that is  $\mathbb{R}$ -linear and Leibnizian. The set of all tangent vectors to a point  $p$  is denoted by  $T_p(\Sigma)$  and forms a vector space over  $\mathbb{R}$ . It is called the tangent space to  $\Sigma$  at  $p$ . Each tangent smooth functions, tangent vectors, tangent spaces, cotangent spaces, covectors

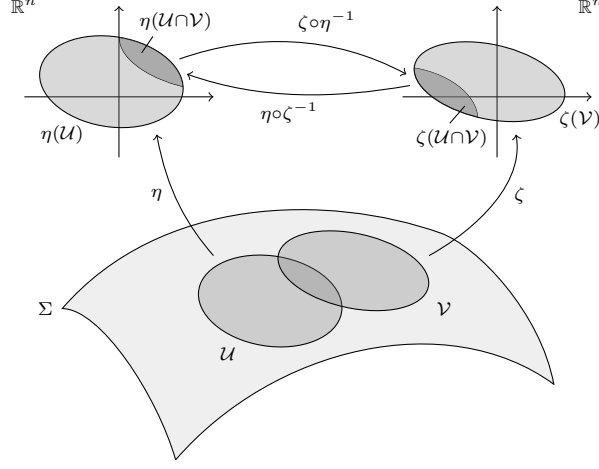


FIGURE 1. Two overlapping charts  $(\mathcal{U}, \eta)$  and  $(\mathcal{V}, \zeta)$  on a manifold  $\Sigma$ . The overlap is smooth iff both maps  $\zeta \circ \eta^{-1}$  and  $\eta \circ \zeta^{-1}$  are smooth.

space  $T_p(\Sigma)$  gives rise to yet another vector space, the cotangent space  $T_p(\Sigma)^*$  to  $\Sigma$  at  $p$ . It is defined as the set of all linear functionals  $\omega_p : T_p(\Sigma) \rightarrow \mathbb{R}$  on  $T_p(\Sigma)$ , called covectors, or 1-forms at  $p$ . The following definition generalises the notion of vectors and covectors:

tensors      DEFINITION 2. *Let  $r$  and  $s$  be nonnegative integers, not both zero. A tensor of type  $(r, s)$  at a point  $p$  of a smooth manifold  $\Sigma$  is an  $\mathbb{R}$ -multilinear functional*

$$A_p : \underbrace{T_p(\Sigma)^* \times \cdots \times T_p(\Sigma)^*}_{r\text{-times}} \times \underbrace{T_p(\Sigma) \times \cdots \times T_p(\Sigma)}_{s\text{-times}} \rightarrow \mathbb{R}.$$

tensor spaces      The tensor space of type  $(r, s)$  at  $p$  is denoted by  $T_p^{(r,s)}(\Sigma)$  and forms a vector space over  $\mathbb{R}$ . In particular  $T_p^{(0,1)}(\Sigma) = T_p(\Sigma)^*$ , and  $T_p^{(1,0)}(\Sigma)$  can be identified with  $T_p(\Sigma)$  by interpreting a tangent vector  $v_p$  as a functional  $T_p(\Sigma)^* \rightarrow \mathbb{R}$  that maps a covector  $\omega_p$  to the real number  $v_p(\omega_p) := \omega_p(v_p)$ .

smooth tensor fields      In General Relativity, physical quantities are described by smooth tensor fields on spacetime: A tensor field  $A$  on a smooth manifold  $\Sigma$  is a map  $\Sigma \rightarrow \bigcup_{p \in \Sigma} T_p^{(r,s)}(\Sigma)$  that assigns to each point  $p$  a tensor  $A_p$  of type  $(r, s)$  at  $p$ . Smooth tensor fields can be defined as follows: A vector field  $v$  is smooth iff the function  $v(f) : \Sigma \rightarrow \mathbb{R}$  defined by  $v(f)(p) := v_p(f)$  is smooth for any smooth function  $f \in \mathcal{F}(\Sigma)$ . A covector field or 1-form  $\omega$  is smooth iff the function  $\omega(v) : \Sigma \rightarrow \mathbb{R}$  defined by  $\omega(v)(p) := \omega_p(v_p)$  is smooth for any smooth vector field  $v$ . Smooth tensor fields of type  $(r, s)$  are then defined straight forwardly. The set of all smooth tensor fields of type  $(r, s)$  on  $\Sigma$  is denoted by  $\mathcal{T}^{(r,s)}(\Sigma)$ . From the  $\mathbb{R}$ -multilinearity of an  $A_p \in T_p^{(r,s)}(\Sigma)$  it follows that an  $A \in \mathcal{T}^{(r,s)}(\Sigma)$  is  $\mathcal{F}(\Sigma)$ -multilinear. One can also define smooth tensor fields on an open subset  $\mathcal{U} \subset \Sigma$  in the same way than they are defined on the whole of  $\Sigma$ .

local basis of smooth vector fields      A local basis of smooth vector fields on an open subset  $\mathcal{U} \subset \Sigma$  is a set of smooth vector fields  $\{e_a\}_{a=1}^n$  such that the set of members  $\{(e_a)_p\}_{a=1}^n$  at each point  $p \in \Sigma$  spans  $T_p^{(1,0)}(\Sigma)$ , where  $n = \dim(\Sigma)$ . The corresponding dual basis field is defined as the set of 1-forms  $\{\varepsilon^a\}_{a=1}^n$  such that  $\varepsilon^a(e_b) = \delta_b^a$ , and spans  $T_p^{(0,1)}(\Sigma)$ .

components of tensor fields      A smooth tensor field  $A$  of type  $(r, s)$  on  $\mathcal{U}$  can then be written as an expansion in these bases, where the components are given by the action on the basis fields  $A^{a_1 \cdots a_r b_1 \cdots b_s} = A(\varepsilon^{a_1}, \dots, \varepsilon^{a_r}, e_{b_1}, \dots, e_{b_s})$  and are smooth functions on  $\mathcal{U}$ .



Two smooth vector fields  $v$  and  $w$  on  $\Sigma$  give rise to a new vector field  $[v, w]$  called their commutator, which is defined by  $[v, w](f) := (v \circ w)(f) - (w \circ v)(f)$  for  $f \in \mathcal{F}(\Sigma)$ . Being again a smooth vector field, the commutator of two local basis fields  $e_a$  and  $e_b$  can itself be expanded in this basis,

$$(1) \quad [e_a, e_b] = \gamma^c_{ab} e_c,$$

where here and henceforth the Einstein summation convention is used (summation over repeated upper and lower indices from 1 to  $n$ ). The components  $\gamma^c_{ab}$  are called the commutation functions of the local basis  $\{e_a\}_{a=1}^n$ . Given any three smooth vector fields  $u, v, w$ , they satisfy the Jacobi identity

$$[u, [v, w]] + [w, [u, v]] + [v, [w, u]] = 0.$$

There is an operation  $C_j^i$  called contraction over  $i, j$  that maps smooth tensor fields of type  $(r, s)$  to smooth tensor fields of type  $(r-1, s-1)$  defined by  $C_j^i(A)(\dots, \omega, \dots, v, \dots) := A(\dots, \varepsilon^a, \dots, e_a, \dots)$ , where  $\varepsilon^a$  is inserted in the  $i^{\text{th}}$  1-form argument, and  $e_a$  in the  $j^{\text{th}}$  vector field argument, and the Einstein summation convention is used. Hence the components of  $C_j^i(A)$  in a local basis are given by  $C_j^i(A)^{a_1 \dots a_{r-1}}_{b_1 \dots b_{s-1}} = A^{\dots a \dots}_{\dots a \dots}$ . The indices  $i, j$  on  $C$  are thus not to be confused with tensor components; they merely indicate over which arguments the contraction is acting.

### 3. Diffeomorphisms, tangent maps and Lie derivatives

The following definitions will turn out to be particularly useful in the treatment of symmetries of spacetime in chapter 3:

A smooth bijection  $\phi : \Sigma \rightarrow \Sigma$  that has a smooth inverse is called a diffeomorphism on  $\Sigma$ , where smoothness is defined via the coordinate expression  $\eta \circ \phi \circ \zeta^{-1}$  of  $\phi$  in some coordinate systems  $\eta$  and  $\zeta$ . A diffeomorphism induces linear maps

$$\begin{aligned} \phi_p^{(r,s)} : T_p^{(r,s)}(\Sigma) &\rightarrow T_{\phi(p)}^{(r,s)}(\Sigma) \\ A_p &\mapsto \phi_p^{(r,s)}(A_p)_{\phi(p)} \end{aligned}$$

between tensors of type  $(r, s)$  at a point  $p$  and tensors of type  $(r, s)$  at  $\phi(p)$ , called the tangent map of type  $(r, s)$  of  $\phi$  at  $p$  (see also figure 4 in chapter 3). Thereby the respective actions on a tangent vector  $v_p$  and on a covector  $\omega_p$  are defined by (the square brackets are set for easier readability)

$$\begin{aligned} \phi_p^{(1,0)}(v_p)_{\phi(p)}(f) &:= v_p(f \circ \phi) && \text{with } f \in \mathcal{F}(\Sigma), \\ \phi_p^{(0,1)}(\omega_p)_{\phi(p)}(v_{\phi(p)}) &:= \omega_p \left( \left[ (\phi^{-1})_{\phi(p)}^{(1,0)}(v_{\phi(p)}) \right]_p \right) && \text{with } v_p \in T_p^{(1,0)}(\Sigma). \end{aligned}$$

This generalises to the action on arbitrary tensors of type  $(r, s)$  as follows:

$$\begin{aligned} \phi_p^{(r,s)}(A_p)_{\phi(p)}(\omega_{\phi(p)}, \dots, v_{\phi(p)}, \dots) &:= \\ A_p \left( \left[ (\phi^{-1})_{\phi(p)}^{(0,1)}(\omega_{\phi(p)}) \right]_p, \dots, \left[ (\phi^{-1})_{\phi(p)}^{(1,0)}(v_{\phi(p)}) \right]_p, \dots \right) \end{aligned}$$

It is convenient to unify all these maps to a single tangent map  $\tilde{\phi}$  that acts on the union of all tensor spaces to  $\Sigma$  at all points, and let it also act pointwise on tensor fields. This brings a tremendous simplification in notation with it since the points of application are omitted. However for the understanding of the tangent map it is necessary to keep track with the pointwise definition above.

Let now  $\{\phi_\lambda\}_{\lambda \in \mathbb{R}}$  be a one-parameter Lie group of diffeomorphisms, or flow, on  $\Sigma$ . This means that the action of all group elements  $\phi_\lambda$  on a point  $p \in \Sigma$  defines a smooth, parameterised curve  $\phi_\lambda(p) : \mathbb{R} \rightarrow \Sigma$ , called the orbit of  $p$  under

commutators of vector fields

commutation functions

Jacobi identity

contractions

diffeomorphisms

tangent maps

one-parameter Lie group of diffeomorphisms, flows

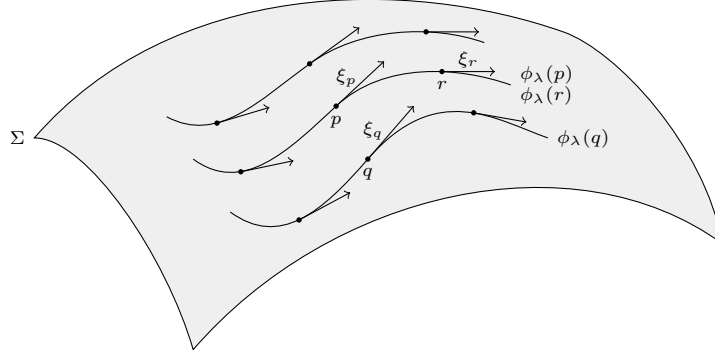


FIGURE 2. The action of the elements of a one-parameter Lie group of diffeomorphisms, or flow,  $\{\phi_\lambda\}_{\lambda \in \mathbb{R}}$  on a point  $p \in \Sigma$  defines a parameterised curve  $\phi_\lambda(p)$  in the manifold. This gives rise to a tangent vector  $\xi_p$  which is tangent to this curve at  $p$ . Pointwise, the group thus gives rise to a vector field  $\xi$  on  $\Sigma$ .

the flow  $\{\phi_\lambda\}_{\lambda \in \mathbb{R}}$ , where the group elements obey the abelian multiplication law  $\phi_\delta \circ \phi_\lambda := \phi_{\delta+\lambda}$ . From the latter it follows that  $\phi_0(p) = p$  and that  $\phi_\lambda^{-1} = \phi_{-\lambda}$ . This orbit gives rise to a tangent vector  $\xi_p$  tangent to this curve at  $p$  given by  $\xi_p(f) := \left. \frac{df(\phi_\lambda(p))}{d\lambda} \right|_{\lambda=0}$ , for  $f \in \mathcal{F}(\Sigma)$ . The orbit of a neighbouring point  $q$  that doesn't lie on  $\phi_\lambda(p)$  defines a neighbouring curve and a tangent vector  $\xi_q$  tangent to this curve at that point in the same way. The orbit of a point  $r$  that does lie on the curve  $\phi_\lambda(p)$  recovers the same curve, but with a translated parametrisation, and gives rise to a tangent vector  $\xi_r$  at that point. Pointwise, a flow  $\{\phi_\lambda\}_{\lambda \in \mathbb{R}}$  gives thus rise to a smooth vector field  $\xi$  whose members lie tangent to the orbits.

local flows

All of the above said is depicted in figure 2. A local one-parameter Lie group of diffeomorphisms, or local flow, on some open subset  $\mathcal{U} \subset \Sigma$  is defined analogously, for  $\lambda \in (-\epsilon, \epsilon) \subset \mathbb{R}$ . It turns out that any smooth vector field locally corresponds to a local flow. Conversely, any smooth vector field generates a local flow in the neighbourhood of any point. One can use these notions to define the rate of change of a smooth tensor field  $A$  when one moves the point of application  $p$  along the flow generated by a smooth vector field  $\xi$ :

Lie derivatives

DEFINITION 3. Let  $\{\phi_\lambda\}_{\lambda \in (-\epsilon, \epsilon)}$  be a local flow on an open neighbourhood  $\mathcal{U}$  of a point  $p$  on a smooth manifold  $\Sigma$ , which is generated by a smooth vector field  $\xi$ . Let  $\tilde{\phi}_\lambda$  be the induced tangent map of  $\phi_\lambda$ . Let further  $A$  be a smooth tensor field of type  $(r, s)$  on  $\Sigma$ . The Lie derivative of  $A$  with respect to  $\xi$  at  $p$  is given by

$$L_\xi(A)_p := \lim_{\lambda \rightarrow 0} \frac{\left[ \tilde{\phi}_\lambda^{-1} (A_{\phi_\lambda(p)}) \right]_p - A_p}{\lambda},$$

and defines a tensor of type  $(r, s)$  at  $p$ . The pointwise extension  $L_\xi(A)$  defines a smooth tensor field of type  $(r, s)$  on  $\Sigma$ .

One can show that  $L_v(w) = [v, w]$  for smooth vector fields  $v$  and  $w$ .

#### 4. Semi-Riemannian geometry

Geometry on a smooth manifold starts by endowing it with a structure called metric, that measures lengths and angles on it:

metrics

DEFINITION 4. A metric  $g$  on a smooth manifold  $\Sigma$  is a symmetric nondegenerate tensor field of type  $(0, 2)$  on  $\Sigma$  of constant signature.

That  $g$  is symmetric means that  $g(v, w) = g(w, v)$  for any two smooth vector fields  $v$  and  $w$ . Nondegeneracy means that if  $g(v, w) = 0$  for all  $w$  then this implies that  $v = 0$ . The latter is equivalent to the statement that the component matrix of  $g$  in any basis has an inverse. The signature of the metric is defined as the tuple of signs of the eigenvalues of  $g$ . Definition 4 implies that each member  $g_p$  of  $g$  defines a (pseudo-)scalar product on the corresponding tangent space  $T_p^{(1,0)}(\Sigma)$ , which measures the lengths of tangent vectors at  $p$  and angles between them. A smooth manifold with a metric defined on it is given its own name:

DEFINITION 5. *A semi-Riemannian manifold  $(\Sigma, g)$  is a smooth manifold  $\Sigma$  that is endowed with a metric  $g$ . (The manifold is called Riemannian iff the signature of  $g$  consists of positive signs only, i.e. when  $g$  is positive definite.)*

semi-Riemannian manifolds

In a semi-Riemannian manifold the metric provides a natural way to uniquely identify a smooth vector field  $v$  with a 1-form  $v^*$  and vice versa, via  $g(v, w) = v^*(w)$ . In component notation this equation reads  $g_{ab}v^a w^b = v_b w^b$  where  $v_b$  denotes the components of  $v^*$ . Because of that, this operation is also called the lowering of an index. Analogously one can raise an index with the inverse metric which has components  $g^{ab}$ . These operations can be extended to raise and lower an index of a smooth tensor field of arbitrary type. In the coordinate free language, when raising an index, a smooth tensor field of type  $(r, s)$  is mapped to a smooth tensor field of type  $(r + 1, s - 1)$  which contains the same information than the original field. An analogous statement holds for lowering an index. The metric thus allows to effectively change the type of a smooth tensor field. Furthermore, with this the operation of contraction  $C_j^i$  over a 1-form and a vector field argument can be extended to contractions  $C^{ij}, C_{ij}$  over two arguments of the same type. For instance, when  $A$  is a smooth tensor field of type  $(1, 2)$ , the contraction  $C_{12}(A)$  defines a smooth vector field with components  $C_{12}(A)^a := g^{bc}A^a_{bc}$ .

type changing, raising and lowering indices

An important class of maps on a semi-Riemannian manifold consists of those that leave the metric invariant (see also figure 4 in chapter 3):

DEFINITION 6. *Let  $(\Sigma, g)$  be a semi-Riemannian manifold. A diffeomorphism  $\phi$  on  $\Sigma$  is called an isometry iff it leaves the metric invariant in the sense that  $\tilde{\phi}(g) = g$  or equivalently  $\tilde{\phi}^{-1}(g) = g$ .*

isometries

From a mathematical perspective, semi-Riemannian geometry is traditionally described as the study of objects that are invariant under all isometries of a semi-Riemannian manifold in an appropriate sense. The most important of these for General Relativity is the Riemann curvature tensor field, whose definition requires a further structure on the manifold that generalises the divergence and directional derivative of ordinary vector calculus to smooth manifolds. The basic properties of these notions are carried over to smooth manifolds in the following definition:

DEFINITION 7. *A connection on a smooth manifold  $\Sigma$  is a map  $\nabla : \mathcal{T}^{(1,0)}(\Sigma)^2 \rightarrow \mathcal{T}^{(1,0)}(\Sigma)$  that is (i)  $\mathcal{F}(\Sigma)$ -linear in the first argument, (ii)  $\mathbb{R}$ -linear in the second argument and obeys the Leibniz rule (iii)  $\nabla(v, fw) = v(f)w + f\nabla(v, w)$ , for  $f \in \mathcal{F}(\Sigma)$  and  $v, w \in \mathcal{T}^{(1,0)}(\Sigma)$ .*

connections

The smooth vector field  $\nabla(v, w)$  is also written  $\nabla_v(w)$  and called the covariant derivative of  $w$  with respect to  $v$ . It gives the rate of change of  $w$  in the direction of  $v$ . The Lie derivative defined in definition 3 also gave such a rate of change, but despite it satisfies properties (ii) and (iii) of definition 7, it does not satisfy property (i) and thus fails to serve as the desired generalisation of the directional derivative of ordinary vector calculus.

covariant derivatives

The covariant derivative can be generalised to act on smooth tensor fields of arbitrary type: First, its action on smooth functions  $f \in \mathcal{F}(\Sigma)$  is defined by

$\nabla_v(f) := v(f)$ . Then the action on 1-forms  $\omega \in \mathcal{T}^{(0,1)}(\Sigma)$  is defined by requiring the Leibniz rule  $\nabla_v(\omega(w)) = \nabla_v(\omega)(w) + \omega(\nabla_v(w))$  for all  $v \in \mathcal{T}^{(1,0)}(\Sigma)$ . Finally, the action on arbitrary smooth tensor fields  $A \in \mathcal{T}^{(r,s)}(\Sigma)$  is defined by imposing the Leibniz rule

$$\begin{aligned} \nabla_v(A(\omega, \dots, v, \dots)) &= \nabla_v(A)(\omega, \dots, v, \dots) + A(\nabla_v(\omega), \dots, v, \dots) + \dots \\ &\quad + A(v, \dots, \nabla_v(w), \dots) + \dots \end{aligned}$$

Riemann connection

A connection is called torsion free iff  $\nabla_v(w) - \nabla_w(v) = [v, w]$ . One can show that on a semi-Riemannian manifold  $(\Sigma, g)$  there exists a unique torsion free connection  $\nabla$ , called the Riemann or Levi-Civita connection of  $(\Sigma, g)$  that is compatible with the metric in the sense that  $\nabla_v(g) = 0$  for all  $v \in \mathcal{T}^{(1,0)}(\Sigma)$ . This implies that  $\nabla_u(g(v, w)) = g(\nabla_u(v), w) + g(v, \nabla_u(w))$  for  $u, v, w \in \mathcal{T}^{(1,0)}(\Sigma)$ . Hence with respect to the Riemann connection the rate of change in the value of the metric in any direction only depends on the rate of change of the vector field arguments.

Equipped with the Riemann connection, one can now give the definition of the above mentioned Riemann curvature tensor field:

Riemann curvature

DEFINITION 8. Let  $(\Sigma, g, \nabla)$  be a semi-Riemannian manifold with Riemann connection. The smooth tensor field  $Riem : \mathcal{T}^{(0,1)}(\Sigma) \times \mathcal{T}^{(1,0)}(\Sigma)^3 \rightarrow \mathcal{F}(\Sigma)$  of type  $(1, 3)$  defined by

$$Riem(\cdot, w, u, v) := (\nabla_u \circ \nabla_v)(w) - (\nabla_v \circ \nabla_u)(w) - \nabla_{[u, v]}(w)$$

is called the Riemann curvature field on  $\Sigma$ .

Ricci and scalar curvature

$Riem$  gives a measure of the local curvature of the manifold. In General Relativity, gravitation is described via the curvature of spacetime. However it is not the full Riemann curvature that enters the field equation of General Relativity, but its contractions:  $Ric := C_2^1(R)$  is called the Ricci curvature field, and  $R := C_{12}(Ric)$  the scalar curvature field on  $\Sigma$ . In component equations the components of  $Ric$  are usually denoted by  $R_{ab}$  and the components of the Riemann curvature field by  $R^a{}_{bcd}$ , since there is no danger of confusion.

## 5. General Relativity in a nutshell

Spacetime is a four dimensional semi-Riemannian manifold with Riemann connection  $(M, g, \nabla)$  where the metric  $g$  has signature  $(-+++)$ . Gravitation is imposed by the Einstein equation

$$(2) \quad Ric - \frac{R}{2}g = T, \quad \text{in components} \quad R_{\mu\nu} - \frac{R}{2}g_{\mu\nu} = T_{\mu\nu},$$

where  $Ric$  and  $R$  denote the Ricci and scalar curvature fields of  $M$  respectively, and  $T$  the stress-energy tensor field of the matter content. The left hand side of this equation gives a measure of local spacetime curvature, while the right hand side gives a measure of the local energy density of the matter content. Matter causes spacetime to curve which in turn causes matter to move. This is how gravitation is described in General Relativity, the theory of spacetime and gravitation.

foliations of spacetime

General Relativity is most elegantly viewed and formulated in the above covariant language, where physical quantities are described by tensor fields on spacetime, and gravitation is imposed by a single and simple tensor field equation. This reflects the essence of the theory most clearly and directly, and emphasises that there is no unique way to globally distinguish between space and time in General Relativity. Yet in practice it is often useful to give up the aesthetics of the covariant point of view and think of spacetime  $M$  as being sliced up into a one parameter family  $\{\Sigma_t\}$  of three-dimensional spacelike hypersurfaces. The union of all slices thereby recovers the whole spacetime. It is also said, that the slices foliate spacetime; cf.

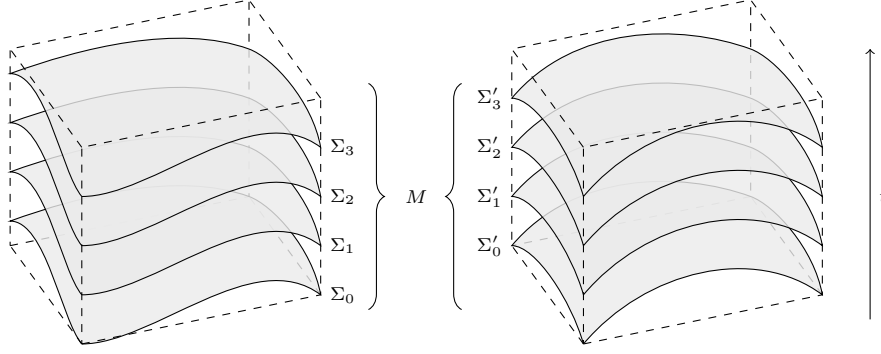


FIGURE 3. The three-dimensional spatial slices  $\Sigma_t$  and  $\Sigma'_t$  both foliate the spacetime  $M$ . One space dimension is suppressed for representability.

figure 3. The Einstein equation can then be written as a system of constraint and evolution equations for the three-dimensional geometric quantities on the slices: On the one hand the intrinsic geometry of the slices is governed by the spatial metric  $\gamma$  on them. To be able to reconstruct the full metric, one however also needs to know how the slices are embedded in spacetime. A measure of this is given by the rate of change of the spatial metric  $\gamma$  when one moves the point of application along the lines normal to the slices. Hence in terms of the Lie derivative (definition 3 in section 3) this quantity can be defined by

$$(3) \quad k := -\frac{1}{2}L_n\gamma,$$

where  $n$  denotes a smooth vector field normal to the slices of unit length. It is called the extrinsic curvature of the spatial slices. In a basis adapted to the foliation, in which the time and spatial basis fields lie normal and tangent to the slices respectively, the (component) Einstein equations (2) can then be written as a constrained system of partial differential equations for the (spatial) components  $\gamma_{ij}$  and  $k_{ij}$  of the spatial metric and extrinsic curvature of the slices. This is called the 3+1 formulation of the Einstein equations (or of General Relativity) which is particularly well explained for example in the Books [1, chapter 2] or [2, chapter 2] on numerical relativity.

As stated above, there is no unique way to foliate a given spacetime. However, in the cases where the underlying spacetime admits certain symmetries, a natural and particularly useful foliation is often at hand, which leads over to the next chapter:

spatial metric

extrinsic curvature

foliation adapted bases



## CHAPTER 3

# Symmetries of spacetime

Since this thesis deals with cosmological models that show certain symmetries, the concepts of these symmetries need to be properly defined, which is the purpose of this chapter. Section 1 starts from the intuitive notions of the important symmetries of homogeneity and isotropy, and defines them mathematically with help of the concepts of isometries and Lie derivatives, which were defined in chapter 2. After a formal treatment on Lie groups and Lie algebras in section 2 these symmetries are then redefined in the language of these mathematical theories in section 3. The reason for this is that the classification and treatment of spatially homogenous cosmologies rests on this Lie group structure that underlies the symmetries, which will be discussed in chapter 5.

If not stated differently, from now on the term manifold will always refer to a semi-Riemannian manifold with Riemann connection. Also functions, tensor fields, etc. will always understood to be smooth in the respective sense. A vector will always refer to a tangent vector at some point.

### 1. Intuitive notions of homogeneity and isotropy

What does it mean when a spacetime, or a manifold  $\Sigma$  in general, admits a certain symmetry? For the for this text most important symmetry of homogeneity an intuitive statement would be that a manifold is homogenous iff it ‘looks the same’ at every point. But what is meant here by ‘looks the same’? In a semi-Riemannian manifold this phrase can only refer to the local geometry, which is specified by the metric. Thus a manifold is homogenous iff it’s local geometry, and therefore it’s metric, is the same at every point; it is not a function of it’s point of application. This implies that the components of the metric are independent of the coordinates in any basis. The notion of isometries defined in definition 6 in chapter 2 provides a way to give a precise definition in a coordinate free fashion: Let  $\phi$  be an isometry on  $\Sigma$  that maps a point  $p$  into a point  $\phi(p)$  as depicted in figure 4. Then by definition 6 one has  $\tilde{\phi}(g_p)_{\phi(p)} = g_{\phi(p)}$  or equivalently  $\tilde{\phi}^{-1}(g_{\phi(p)})_p = g_p$ . By the definition of the tangent map in section 3 of chapter 2 this precisely expresses that the metric is the same at these two points. Consequently homogeneity can be defined as follows:

intuitive notion of homogeneity

**DEFINITION 9.** *A manifold  $\Sigma$  is homogenous iff for each two points  $p, q \in \Sigma$  there exists an isometry that maps  $p$  into  $q$ .*

homogeneity defined

Homogeneity is an example of a continuous symmetry. For those it is often useful to work with an infinitesimal concept of symmetries, the Killing fields: The notion of a one-parameter Lie group of diffeomorphisms, or flow, generated by a vector field, was discussed in section 3 of chapter 2. A vector field  $\xi$  on a manifold  $\Sigma$  is called a Killing field of  $\Sigma$  iff it generates a one-parameter Lie group of isometries, or Killing flow. A member  $\xi_p$  of a Killing field  $\xi$  is called a Killing vector. Intuitively speaking, the Killing vectors point in the direction of the symmetry, in which the metric stays the same. This intuition can be made mathematically precise: By

Killing fields, Killing vectors

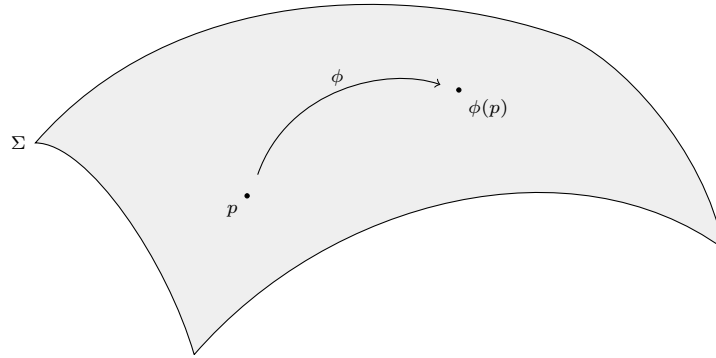


FIGURE 4. The diffeomorphism  $\phi$  on  $\Sigma$  maps the point  $p$  into the point  $\phi(p)$ . The induced tangent map  $\tilde{\phi}$  maps tensors of type  $(r, s)$  at  $p$  into tensors of type  $(r, s)$  at  $\phi(p)$ .  $\phi$  is an isometry between these two points iff  $\tilde{\phi}(g_p)_{\phi(p)} = g_{\phi(p)}$ , which states that the metric is the same at these two points.

definitions 6 and 3 in chapter 2 it follows that  $\xi$  is a Killing field iff

Killing equation (4) 
$$L_\xi(g) = 0,$$

which is called the Killing equation. This indeed states that the rate of change of the metric in the direction of a Killing field, by means of the Lie derivative, is zero. Since the Killing field generates the Killing flow and vice versa, it contains the same symmetry information than the flow itself. Homogeneity in terms of Killing fields means then the following:

homogeneity in terms of Killing vectors

PROPOSITION 1. *A manifold  $\Sigma$  is homogenous iff each of it's tangent spaces  $T_p^{(1,0)}(\Sigma)$  is spanned by Killing vectors.*

In other words, in a homogenous manifold, at each point there are Killing vectors that point in each direction and have all kind of lengths.

intuitive notion of isotropy

Apart from homogeneity also the continuous symmetry of isotropy is of major importance to cosmology. What does it mean when a manifold is isotropic around a point? An intuitive statement would be that this is the case iff 'seen from that point' the manifold 'looks the same' in all directions. Clearly a mathematically precise formulation can again be given in terms of isometries:

isotropy defined

DEFINITION 10. *A manifold  $\Sigma$  is isotropic around a point  $p \in \Sigma$  iff for each two vectors  $v_p, w_p \in T_p^{(1,0)}(\Sigma)$  there exists an isometry  $\phi$  on  $\Sigma$  such that (i)  $\phi(p) = p$  and (ii)  $\tilde{\phi}(v_p)_p = w_p$ .*

$\Sigma$  is called isotropic iff it is isotropic around any point of it.

Statement (i) expresses that, unlike for homogeneity, to check for isotropy around  $p$  one does not compare the geometry at different points, but only the geometry at  $p$ . Statement (ii) means that any vector at  $p$  can be mapped into any other vector at  $p$  by some tangent map of an isometry that satisfies (i); cf. figure 5. This precisely expresses that there is no geometrically preferred direction at  $p$ . A precise formulation of isotropy around a point in terms of Killing fields can for example be found in [3, p 378], but from (i) it is already clear that a Killing field  $\xi$  that corresponds to an isotropy around  $p$  must vanish at that point;  $\xi_p = 0$ .

Killing fields of isotropies

isotropy implies homogeneity, maximal symmetry

It can be shown that isotropy (around every point) implies homogeneity, but not vice versa. An isotropic (and homogenous) manifold is also said to be of maximal symmetry, a term which will be justified in section 3.



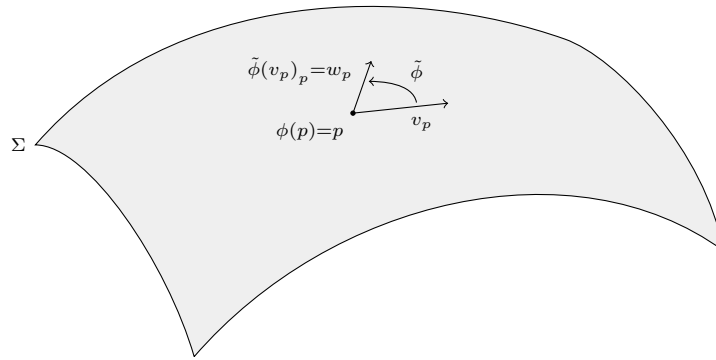


FIGURE 5. An isometry  $\phi$  that corresponds to isotropy around a point  $p \in \Sigma$  has the ability to keep this point invariant;  $\phi(p) = p$ . Furthermore it's tangent map has the ability to map each vector  $v_p$  at this point into any other vector  $w_p$  at this point;  $\tilde{\phi}(v_p)_p = w_p$ .

### 2. Lie groups and Lie algebras

The previous section discussed the continuous symmetries of homogeneity and isotropy starting from the intuitive notions. Mathematically these could then be defined equivalently in terms of Killing flows (one-parameter Lie groups of isometries) or of the corresponding Killing fields that generate these flows. This can be generalised to a formulation of continuous symmetries in the language of higher dimensional Lie groups and their corresponding Lie algebras. These formal discussions will not be of importance for the understanding of the Friedmann cosmologies in chapter 4, but will be crucial for the treatment and classification of spatially homogenous cosmologies in chapter 5. This section deals with the necessary tools from Lie group theory which are then applied to the discussion on symmetries of a manifold in section 3:

Lie groups and Lie algebras are separately defined as follows:

DEFINITION 11. A smooth manifold  $G$  is called a Lie group iff it also has the algebraic structure of a group, such that the maps  $f(g, h) := gh$  of group multiplication and  $i(g) := g^{-1}$  of inversion are both smooth for all  $g, h \in G$ . (Here  $gh$  denotes the multiplication of  $g$  with  $h$  in the group sense, and  $g^{-1}$  the inverse element of  $g$ .)

Lie groups

DEFINITION 12. A Lie algebra (over  $\mathbb{R}$ ) is a vector space  $\mathcal{G}$  (over  $\mathbb{R}$ ) together with an algebraic product  $[\cdot, \cdot]_{\mathcal{G}} : \mathcal{G}^2 \rightarrow \mathcal{G}$  called Lie bracket that is (i) anti-symmetric, (ii)  $\mathbb{R}$ -linear in both arguments and (iii) satisfies the Jacobi identity  $[u, [v, w]_{\mathcal{G}}]_{\mathcal{G}} + [w, [u, v]_{\mathcal{G}}]_{\mathcal{G}} + [v, [w, u]_{\mathcal{G}}]_{\mathcal{G}} = 0$  for all  $u, v, w \in \mathcal{G}$ .

Lie algebras

Next is to show how a Lie group naturally gives rise to a Lie algebra: Let  $G$  be an  $n$ -dimensional Lie group and  $g, h \in G$ . The map  $l_g : G \rightarrow G$  defined by  $l_g(h) := gh$  is called the left translation by  $g$  on  $G$  and is a diffeomorphism. A vector field  $v$  on  $G$  that satisfies

left translations

$$(5) \quad \tilde{l}_g(v) = v$$

left invariant vector fields

(pointwise  $\tilde{l}_g(v_h)_{gh} = v_{gh}$ ) for all  $g \in G$  is called left invariant. From the linearity of the tangent map (section 3 of chapter 2) it is clear that the set  $\mathcal{G}$  of all left invariant vector fields on  $G$  forms a vector space over  $\mathbb{R}$ . Moreover one can show ([4, Lemma 19.1]) that the commutator of two left invariant vector fields is again

left invariant;  $\tilde{l}_g([v, w]) = [v, w]$  for  $v, w \in \mathcal{G}$  and  $[\cdot, \cdot]$  the vector field commutator (section 2 of chapter 2). Hence  $\mathcal{G}$  is not only a vector space but also a Lie algebra with the commutator as Lie bracket.  $\mathcal{G}$  is called the Lie algebra of the Lie group  $G$ . It can be brought in one-to-one correspondence with the tangent space  $T_e^{(1,0)}(G)$  to  $G$  at the identity element  $e$  by observing that each  $v \in \mathcal{G}$  is uniquely determined by its member  $v_e$  at the identity since  $v_g = \tilde{l}_g(v_e)_g$  for all  $g \in G$ . Hence  $\dim(\mathcal{G}) = \dim(T_e^{(1,0)}(G)) = \dim(G) = n$ . One can then choose a basis  $\{e_a\}_{a=1}^n$  of  $\mathcal{G}$  and calculate the commutation functions (1), which in this case are actually constants since  $\mathcal{G}$  forms a vector space;

structure constants (6)  $[e_a, e_b] = C^c_{ab} e_c$  , with  $C^c_{ab} \in \mathbb{R}$ .

The  $C^c_{ab}$  are called the structure constants of  $\mathcal{G}$  in the basis  $\{e_a\}_{a=1}^n$  and transform like the components of a tensor field of type (1, 2) under a change of basis in  $\mathcal{G}$ . They fully characterise the algebraic properties of the Lie algebra  $\mathcal{G}$ , and since  $\mathcal{G}$  is endowed with the Lie group  $G$ , also encode the essential properties of  $G$ .

right translations Right translations  $r_g$  are defined analogously to left translations by  $r_g(h) := hg$  and also define diffeomorphisms on  $G$ . Consequently a vector field  $\xi$  on  $G$  is called right invariant iff

right invariant vector fields (7)  $\tilde{r}_g(\xi) = \xi$

for all  $g \in G$ . Likewise the set of all right invariant vector fields on  $G$  forms a Lie algebra  $\mathfrak{g}$  as well. Let now  $\xi$  be a right invariant vector field which generates the flow  $\{\phi_\lambda\}_{\lambda \in \mathbb{R}}$ . Since  $\xi$  is right invariant, it holds that  $r_g \circ \phi_\lambda = \phi_\lambda \circ r_g$ . This equation can be understood to be the ‘finite version’ of (7), of which (7) represents the ‘infinitesimal version’. Defining  $h(\lambda) := \phi_\lambda(e)$  one then has

$$\phi_\lambda(g) = (\phi_\lambda \circ r_g)(e) = (r_g \circ \phi_\lambda)(e) = r_g(h(\lambda)) = h(\lambda)g = l_{h(\lambda)}(g).$$

right invariant vector fields generate left translations Hence  $\phi_\lambda$  can be identified with  $l_{h(\lambda)}$ , and since  $\{\phi_\lambda\}_{\lambda \in \mathbb{R}}$  is generated by a right invariant vector field  $\xi$ , this means that right invariant vector fields are the generators of left translations. From (5) and definition 3 in chapter 2 this can equivalently be expressed as

(8)  $L_\xi(v) = [\xi, v] = 0$

for  $v$  and  $\xi$  left and right invariant, respectively. This means that a left invariant vector field does not change in the direction of a right invariant vector field in the sense of the Lie derivative.

Given a basis  $\{e_a\}_{a=1}^n$  of  $\mathcal{G}$  with structure constants  $C^c_{ab}$ , one can show ([5, section 7.2] or [6, section 6.3]) that there is always a basis  $\{\xi_a\}_{a=1}^n$  of  $\mathfrak{g}$  with structure constants  $-C^c_{ab}$ ;

equivalence of the Lie algebras of left and right invariant vector fields (9)  $[\xi_a, \xi_b] = -C^c_{ab} \xi_c$ .

In fact for this to hold, the two bases merely have to coincide at the identity  $e \in G$ . In this sense  $\mathfrak{g}$  is equivalent to  $\mathcal{G}$ .

Both the notions of left and right invariance, can be extended straight forwardly to tensor fields of type  $(r, s)$ . In analogy to (8), a left invariant tensor field  $A$  then satisfies the equation

(10)  $L_\xi(A) = 0$ ,

for a right invariant vector field  $\xi$ .

A Lie group can act on a manifold in the following way:

DEFINITION 13. Let  $G$  be a Lie group with identity element  $e$ , and  $\Sigma$  be a smooth manifold. An action of  $G$  on  $\Sigma$  is a map

$$\begin{aligned} \varphi : G \times \Sigma &\rightarrow \Sigma, \\ (g, p) &\mapsto \varphi(g, p) \equiv \varphi_g(p) \end{aligned}$$

such that (i)  $\varphi_e(p) = p$  and (ii)  $\varphi_{gh}(p) = (\varphi_g \circ \varphi_h)(p)$  for all  $g, h \in G$  and  $p \in \Sigma$ .

The set  $\varphi_G(p) := \{\varphi_g(p) | g \in G\} \subset \Sigma$  is called the orbit of  $p$  under  $G$ . It is the set of all points which can be ‘reached’ from  $p$  via the group action of  $G$ .  $G$  is said to act transitively on  $\Sigma$  iff the orbit of some point ( $\Leftrightarrow$  of all points) covers  $\Sigma$ ; that is, iff  $\varphi_G(p) = \Sigma$  for some ( $\Leftrightarrow$  for all)  $p \in \Sigma$ . Clearly in this case necessarily  $\dim(G) \geq \dim(\Sigma)$ . A transitive action where  $\dim(G) = \dim(\Sigma)$  is called simply transitive (also regular), a transitive action where  $\dim(G) > \dim(\Sigma)$  is called multiply transitive. In the case of a simply transitive action, the group action is necessarily free; (in fact simply transitive  $\Leftrightarrow$  free and transitive). That is,  $\varphi_g(p) = \varphi_h(p)$  implies  $g = h$ . Hence then, given any two points  $p, q \in \Sigma$  there is one and only one  $g \in G$  such that  $\varphi_g(p) = q$ . A simply transitive action thus allows to identify  $G$  with  $\Sigma$  in the following way: An arbitrary  $p \in \Sigma$  can be identified with the identity of  $G$  by  $\varphi_e(p) = p$ . Any other  $q \in \Sigma$  can then be identified with a unique  $g \in G$  via  $\varphi_g(p) = q$ . As a consequence, tensor fields on  $G$  can be identified with tensor fields on  $\Sigma$ .

Lie group action on a manifold

group orbits

transitive action

simply and multiply transitive action

### 3. Symmetries in the language of Lie groups and Lie algebras

This section now applies the results from Lie group theory of section 2 to the discussion on symmetries of a manifold: This is done by observing that given a manifold  $\Sigma$ , the set of all isometries on  $\Sigma$  forms a Lie group  $G$  and the set of all Killing fields associated with these isometries forms a corresponding Lie-Algebra  $\mathfrak{g}$ . Furthermore per definition 6,  $G$  acts on the underlying manifold  $\Sigma$ . From the above discussion, one can then readily express homogeneity in the language of Lie groups:

PROPOSITION 2. A manifold  $\Sigma$  is homogenous iff it’s group of isometries acts transitively on  $\Sigma$ .

homogeneity in the language of Lie groups

Let now  $\Sigma$  be a homogenous manifold,  $\dim(\Sigma) = n$  and  $\dim(G) = \dim(\mathfrak{g}) = m$ . In the case when the action is simply transitive ( $n = m$ ) the manifold has no further symmetries in addition to homogeneity. On the other hand, when the action is multiply transitive ( $n < m$ ) then there exist rotational symmetries in addition, since then there exists a subgroup  $I \subset G$  of dimension  $m - n$ , called the isotropy subgroup of  $G$ , that leaves each point in  $\Sigma$  invariant;  $\varphi_I(p) = p$  for all  $p \in \Sigma$ . This can most easily be seen by taking a look at the Killing vectors: A basis  $\{\xi_a\}_{a=1}^m$  of  $\mathfrak{g}$  consists of  $m$  linearly independent vectors in  $\mathfrak{g}$ . However in this case  $m > n$ . Hence at each point  $p \in \Sigma$ ,  $m - n$  of these basis vectors must be zero, and as argued in section 1 these Killing vectors correspond to rotational symmetries around that point, and consequently so does each element of  $I$  acting on it. By calculating the maximum number of independent Killing fields one can show ([3, section 13.1]) that

isotropy subgroup

$$(11) \quad m \leq n(n+1)/2 \quad \text{and} \quad m - n \leq n(n-1)/2.$$

Isotropy in the language of Lie groups thus means the following:

PROPOSITION 3. A manifold  $\Sigma$  of dimension  $n$  is isotropic iff it’s group of isometries admits an isotropy subgroup of dimension  $n(n-1)/2$ .

isotropy in the language of Lie groups

As already mentioned in section 1, an isotropic manifold is automatically homogenous. So when equality holds for the right equation of (11) it automatically

maximal symmetry also holds for the left equation of (11). Thus an isotropic (and homogenous) manifold possesses the maximum number of independent killing vector fields, which justifies the predicate ‘maximally symmetric’ already given to such a manifold in section 1. A manifold whose isotropy subgroup is of dimension 1 is said to be locally rotational symmetry (LRS). Intuitively speaking, such a manifold is rotationally symmetric around one and only one axis at each point.

In the light of this picture of symmetries in the language of Lie groups, the notion of a Killing flow on  $\Sigma$  given in section 1 simply represents a one parameter subgroup of the isometry group  $G$  of  $\Sigma$ , which explains why already some Lie group terminology was used beforehand.

two cases of homogenous manifolds, homogeneity subgroup Given a homogenous manifold  $\Sigma$  with isometry group  $G$  there are two possibilities: Either  $G$  admits a subgroup  $H \subset G$  of homogeneity that acts simply transitively on  $\Sigma$ , or not. In the former case the group action of  $G$  on  $\Sigma$  can be simply or multiply transitive, in the latter case it is necessarily multiply transitive. The important case for this text is the former one, in which a homogeneity subgroup  $H$  exists. Let now  $\Sigma$  be of this kind. Then  $H$  can be identified with  $\Sigma$  as described at the end of section 2 by picking an arbitrary point as the identity. Furthermore, an isometry  $\phi \in H$  that acts on  $\Sigma$  can be identified with a left multiplication  $l_\phi$  on  $H$ . Hence the tensor fields on  $\Sigma$  which are invariant under these isometries, in particular the metric, can be identified with left invariant tensor fields on  $H$ . The generators of these isometries, the Killing fields corresponding to  $H$ , can be identified with the generators of the left translations, the right invariant vector fields. The latter can also be seen by noting that for the case of the metric, equation (10) can be identified with the Killing equation (4). Hence the Lie algebra  $\mathfrak{h}$  of Killing fields on  $\Sigma$  (corresponding to  $H$ ) can be identified with the Lie algebra of right invariant vector fields on  $H$ .

## Friedmann cosmology

The purpose of this chapter is to introduce qualitative analytical methods to analyse the dynamics of spatially homogenous cosmologies on the example of the highly symmetric Friedmann models, which can also be solved exactly (for simple matter contents). Section 1 discusses the possible different geometries of the Friedmann cosmologies. Section 2 then discusses the Friedmann evolution equations, and summarises how they can be solved exactly in the case when the matter content is modelled as perfect fluid with linear equation of state. The qualitative analysis is then performed in section 3, which will be generalised to more general spatially homogenous cosmologies in chapter 5.

### 1. The geometry of the Friedmann cosmologies

In the standard model of cosmology it is assumed that the universe can be modelled to be highly symmetric as a first approximation: The Friedmann spacetime  $M$  admits a foliation  $\{\Sigma_t\}$  such that each slice  $\Sigma_t$  is a space of maximal symmetry (homogenous and isotropic). This is also called the cosmological principle, which on the one hand rests on observational data, and is on the other hand very convenient from the philosophical point of view (of science). Furthermore, the high degree of symmetry restricts the form of the possible solutions for the metric to a simple family:

cosmological principle

It is quite intuitive, that a maximally symmetric manifold, such as each slice  $\Sigma_t$  of a Friedmann spacetime, is a manifold of constant (Riemann) curvature. If this was not the case, then one could always expose a geometrically preferred point or direction, in contradiction to the cosmological principle. This is formally shown for example in [5, p 94]. Furthermore, for a three dimensional Riemannian manifold such as each  $\Sigma_t$ , there are but three qualitatively different geometries that admit such constant curvature. These are determined by the signs of their curvature: There are the three-spheres with positive curvature, flat space with zero curvature and the three-hyperboloids with negative curvature. These geometries are diagrammed in figure 6. In a basis adapted to the foliation the Friedmann

the three qualitatively different spaces of constant curvature

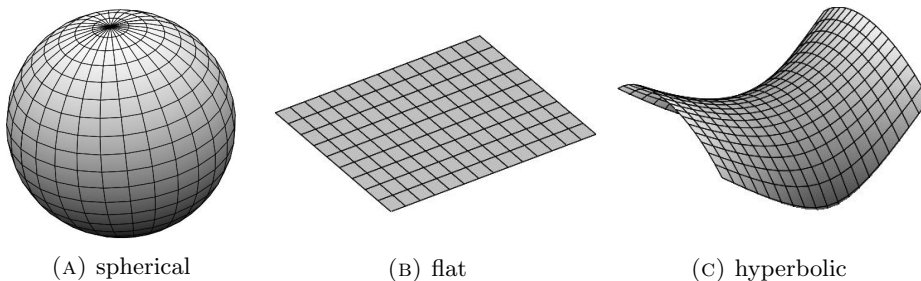


FIGURE 6. The three qualitatively different spaces of constant curvature as embeddings in a higher dimensional space, where one spatial coordinate is held constant for representability.

metric can then be written in one of the forms

$$\text{Friedmann metrics (12)} \quad g = -dt^2 + a(t)^2 \begin{cases} dr^2 + \sin^2 r^2 (d\theta^2 + \sin^2 \theta^2 d\phi^2) & , \text{ spherical} \\ dx^2 + dy^2 + dz^2 & , \text{ flat} \\ dr^2 + \sinh^2 r^2 (d\theta^2 + \sin^2 \theta^2 d\phi^2) & , \text{ hyperbolic} \end{cases} .$$

Here the spatial part is written in spherical, Cartesian and hyperbolic coordinates respectively. The function  $a$  is called scale function and determines the overall length scale of the spatial metric, as well as the magnitude of the spatial curvature in the spherical and hyperbolic cases. Clearly by the cosmological principle the scale function can be a function of time only and must be independent of the spatial coordinates.

open and closed  
Friedmann  
cosmologies

The spherical Friedmann cosmologies are also said to be closed, since the spatial slices  $\Sigma_t$  are compact, so space is finite. The flat and hyperbolic Friedmann cosmologies are said to be open, since in these cases the slices  $\Sigma_t$  are not bound, so space is infinite; cf. figure 6.

## 2. The dynamics of the Friedmann cosmologies

In the previous section it was discussed that imposing the cosmological principle on spacetime restricts the possible solutions of the Einstein equation to three qualitatively different cases determined by the sign of the Riemann curvature of the spatial slices  $\Sigma_t$  in a foliation adapted to the symmetries. Furthermore, for each of these cases, the only degree of freedom left in the metric is the scale function  $a$ . From the form of the Friedmann metrics (12) it is also clear that the sign of the curvature cannot change during the evolution of a Friedmann model: A Friedmann model that is spherical at one instant of time remains spherical during its whole evolution. Determining the dynamics of a specific Friedmann cosmology therefore reduces to finding a function  $a$ , such that (12) is subject to the Einstein equation (2):

To get the evolution equations one then has to calculate the left hand side of the Einstein equation (2) and equate it to the stress-energy tensor  $T$  of the matter content of the universe. Usually the matter is modelled as a perfect fluid,  $[T^\mu{}_\nu] = \text{diag}(-\rho, p, p, p)$ . Here  $\rho$  denotes the energy density and  $p$  the pressure of the fluid. As shown for example in [5, section 5.2], the (component) Einstein equations (2) then reduce to the Friedmann equations

$$\text{Friedmann equations (13)} \quad \frac{\dot{a}^2}{a^2} = \frac{\rho}{3} - \frac{k}{a^2} \quad \text{and} \quad \frac{\ddot{a}}{a} = -\frac{1}{6}(\rho + 3p) \quad , \quad \text{with } k = \begin{cases} 1 & , \text{ spherical} \\ 0 & , \text{ flat} \\ -1 & , \text{ hyperbolic} \end{cases} .$$

These imply the conservation equation

$$(14) \quad \dot{\rho} = -3\frac{\dot{a}}{a}(\rho + p),$$

which is often useful as an auxiliary equation. The dot denotes derivatives with respect to coordinate time  $t$ . For the case when the fluid obeys a linear equation of state  $p = w\rho$ , with  $w = \text{const}$ , the Friedmann equations (13) can be solved for  $a$ ; cf. [5, p 101 and table 5.1] for the cases of dust ( $w = 0$ ) and radiation ( $w = \frac{1}{3}$ ). Solutions for  $w > -\frac{1}{3}$  then look qualitatively as sketched in figure 7.

spatial expansion and  
contraction

As stated above, the scale factor  $a$  specifies the overall spatial length scale: The distance between two points in space that are at rest with respect to the spatial coordinates is proportional to  $a(t)$ . In particular as shown in figure 7, all Friedmann cosmologies with  $w > -\frac{1}{3}$  start with  $a(0) = 0$ , and hence from a singular state of the metric, where loosely speaking the distance between any two points in space

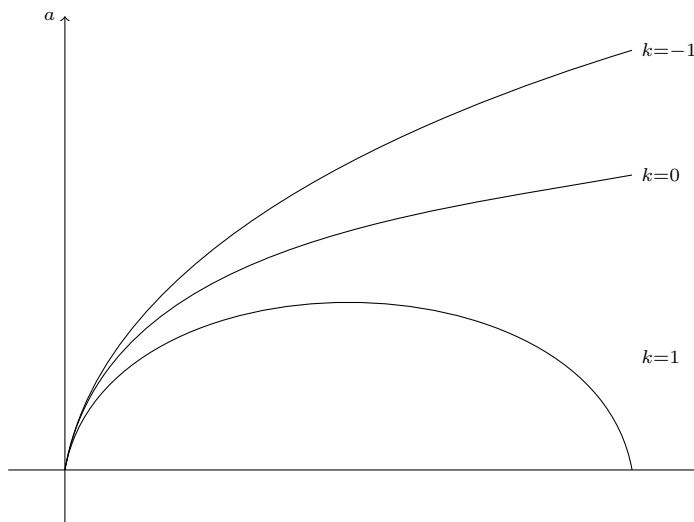


FIGURE 7. A sketch of solutions of the Friedmann equations for the spherical ( $k = 1$ ), flat ( $k = 0$ ) and hyperbolic ( $k = -1$ ) case for  $w > -\frac{1}{3}$ .

is zero. This singularity is referred to as the big bang. Then, for the open (flat and hyperbolic) Friedmann cosmologies  $a$  is strictly monotonically increasing for all  $t > 0$ . In contrast for the closed (spherical) Friedmann cosmologies  $a$  is at first strictly monotonically increasing until it attains a maximum. After that,  $a$  is strictly monotonically decreasing until it vanishes again. Hence the open Friedmann cosmologies describe forever expanding universes, while the closed Friedmann cosmologies describe universes which expand until a state of maximal spatial volume, after which they contract again down to ‘zero size’. This recollapse to another singular state that occurs in the evolution of the spherical Friedmann cosmologies is referred to as the big crunch.

### 3. A qualitative analysis of the Friedmann dynamics

Although the Friedmann equations can be solved exactly for perfect fluids with linear equation of state, many of the interesting qualitative features of the evolution of these models can be read out from the Friedmann equations (13) and the conservation equation (14) without solving; cf. [5, p 98–100]. This section deals with such a qualitative analysis, however using a method following the discussion in [7, section 2.3], that can readily be generalised for the analysis of more general spatially homogenous cosmologies, which will be discussed in chapter 5:

In order to rewrite the evolution equations in the desired way, one defines the variables

$$(15) \quad H := \frac{\dot{a}}{a}, \quad q := -\frac{\ddot{a}a}{\dot{a}^2} \quad \text{and} \quad \Omega := \frac{\rho}{3H^2}.$$

$H$  is called the Hubble scalar, and gives a measure of the rate of expansion of the underlying universe.  $q$  is called the deceleration parameter, and gives a measure of the deceleration of the expansion.  $\Omega$  is simply the expansion-normalised (or Hubble-normalised) energy density, which is often referred to as the density parameter.  $H$  has the dimension of  $\text{time}^{-1}$  while both  $q$  and  $\Omega$  are dimensionless. Differentiating  $H$  with respect to time and using  $q$  yields  $\dot{H} = -(1+q)H^2$  as an evolution equation for  $H$ . The considerations shall again be restricted to a perfect fluid with linear

Hubble scalar,  
deceleration  
parameter and  
expansion-normalised  
energy density





FIGURE 8. Flow diagram for the qualitative evolution of the Friedmann cosmologies for perfect fluids with  $p = w\rho$  and  $w > -\frac{1}{3}$ .

equation of state;  $p = w\rho$ . Then by differentiating  $\Omega$  with respect to time and using the conservation equation (14), one analogously arrives at  $\dot{\Omega} = (-3(1+w) + 2(1+q))\Omega H$  as an evolution equation for  $\Omega$ . Finally using the second Friedmann equation (13), one finds that  $q$  is related to  $\Omega$  by  $q = \frac{1+3w}{2}\Omega$ . With this, and after defining a rescaled, dimensionless time variable  $\tau$  through  $\frac{d}{d\tau} := \frac{1}{H} \frac{d}{dt}$  the two evolution equations above become

rescaled evolution equations (16) 
$$H' = -\left(1 + \frac{1+3w}{2}\Omega\right)H \quad \text{and} \quad \Omega' = (1+3w)(\Omega-1)\Omega,$$

where here and henceforth the prime denotes derivatives with respect to rescaled time  $\tau$ . These equations can be seen as the rescaled evolution equations, being equivalent to the Friedmann equations (13). However unlike the system (13), the system (16) is decoupled; there is no  $H$  appearing in the equation for  $\Omega$ . Also, the equation for  $H$  has dimension  $\text{time}^{-1}$  while the equation for  $\Omega$  is dimensionless.

To solve for the metric components exactly, one would need to solve the full system (16). However it suffices to focus on the equation for  $\Omega$  when one is merely interested in the major qualitative features of the solutions to this system. In fact for this, one does not even have to solve this equation exactly. A qualitative analysis is sufficient. This can best be seen by visualising the qualitatively different solutions of this equation in a flow diagram, which is shown in figure 8:

the state space Assuming a non-negative energy density  $\rho$ , the possible values that  $\Omega$  can attain is the non-negative part of the real line. This is also called the state space of the differential equation. Restricting again to the case  $w > -\frac{1}{3}$  one then finds that this equation has two static solutions,  $\Omega = 0$  and  $\Omega = 1$ , for which  $\Omega' = 0$ . The corresponding points in the diagram are called fixed points, since for instance if  $\Omega = 1$  at one instant of time during the evolution, then  $\Omega = 1$  during the whole evolution. Static solutions are therefore also called fixed point solutions. Solutions for which  $\Omega' \neq 0$  are called generic solutions. This is because for a solution of this type, an initial value can be out of an open subset of the state space, and does not need to be fine tuned as it has to be for the fixed point solutions. For  $\Omega \in (0, 1)$  one has  $\Omega' < 0$ . Hence for a solution with initial value in this range,  $\Omega$  is strictly monotonically decreasing with (rescaled and coordinate) time. By the uniqueness theorems of the theory of ordinary differential equations, these solutions approach the value  $\Omega = 1$  asymptotically into the past ( $\tau \rightarrow -\infty$ ) and  $\Omega = 0$  asymptotically into the future ( $\tau \rightarrow \infty$ ), however never reach these values. Hence for these solutions the matter appears to thin out with the evolution, and solutions of this type therefore seem to correspond to the open, forever expanding Friedmann cosmologies. In contrast, for  $\Omega \in (1, \infty)$  one has  $\Omega' > 0$  so that the matter density appears to diverge with the evolution. Accordingly solutions of this kind seem to correspond to the closed, recollapsing Friedmann cosmologies. However one has to take care with these assumptions, since  $\Omega$  only denotes the rescaled, Hubble-normalised energy density. To check how the actual energy density  $\rho$  evolves, one would also have to bring in information from the equation for  $H$ . Yet one can also convince oneself more easily that the above claims are indeed true by observing that the first Friedmann equation (13) can be expressed in terms of  $\Omega$  as

$$\Omega - 1 = \frac{k}{H^2 a^2},$$



from which it is clear that

$$(17) \quad \Omega < 1 \Leftrightarrow k = -1, \quad \Omega = 1 \Leftrightarrow k = 0 \quad \text{and} \quad \Omega > 1 \Leftrightarrow k = 1.$$

In summary the qualitative analysis has shown that among the generic Friedmann cosmologies there are two qualitatively different types regarding their evolution: There are the open, hyperbolic, forever expanding models for  $\Omega \in (0, 1) \Rightarrow k = -1$ , and the closed, spherical, expanding and recollapsing models for  $\Omega \in (1, \infty) \Leftrightarrow k = 1$ . Furthermore there are two non-generic fixed point solutions, one of which is the flat Friedmann model for  $\Omega = 1 \Leftrightarrow k = 0$ . The other non-generic solution for  $\Omega = 0 \Rightarrow k = -1$  corresponds to Friedmann vacuum models and is hyperbolic. The choice of taking  $\Omega$  as the dynamical variable also allows for a further physical interpretation: From (17) and the above results one sees that for a Friedmann universe to recollapse it needs a large enough energy density, such that the gravitational pull of the matter can stop the expansion of the universe. If the energy density is too small, the gravitational pull is too weak, and the universe will expand forever. The border value  $\Omega = 1$  is thus also called the critical density.

critical density

Certainly one does not get out more from the qualitative analysis than from the exact solutions. However many facets of the qualitative behaviour of solutions appear more clearly and directly in the qualitative formalism. Yet the true advantage lies in the fact that the underlying evolution equations do not need to be exactly solvable for the qualitative methods to be applicable. The Friedmann equations for perfect fluids with linear equation of state are exactly solvable due to the high symmetry of these models. But when one relaxes the symmetry, and considers more general spatially homogenous models which need not necessarily be spatially isotropic, the corresponding evolution equations are not exactly solvable in general. Then one is tied to either numerics or to qualitative analytical methods. The application of the latter to these models is the subject of the next chapter.



## Spatially homogenous cosmology

This final chapter of part 1 now makes use of the preparations of the previous chapters to arrive at a discussion on the subject of spatially homogenous cosmology. Section 1 treats the modern way to classify these models by means of the underlying Lie group of isometries. In section 2 it is explained how one can choose a basis which is adapted to the underlying Bianchi symmetry, in which the component Einstein equations take the appropriate form of a constrained system of ordinary differential equations, which is subject of section 3. Section 4 then deals with a qualitative analysis of these equations, thereby generalising the techniques applied in section 3 of chapter 4 to analyse the Friedmann cosmologies.

### 1. Classification of spatially homogenous cosmologies

With help of the preparatory work of chapter 3 a precise definition of what is meant by a spatially homogenous spacetime or cosmology is readily at hand:

DEFINITION 14. *A spacetime  $M$  is called spatially homogenous iff it admits a foliation  $\{\Sigma_t\}$  such that each spatial slice  $\Sigma_t$  is homogenous. A spatially homogenous spacetime that is subject to the Einstein equation is called a spatially homogenous cosmology.*

spatially homogenous spacetimes

The general spatially homogenous solution to the Einstein equation is not exact. Exact solutions can only be found for special cases such as the Friedmann cosmologies investigated in chapter 4. Hence when investigating general spatially homogenous solutions, one is either tied to numerics or to qualitative analytical methods, where the latter is on which this text focuses. Although the symmetry of spatial homogeneity is of course restrictive, the class of such models is still vast. To tackle the problem of getting insight into the qualitative features of generic spatially homogenous solutions one thus first wishes to classify these models into qualitatively different kinds by their spatial geometry. For the special case of the Friedmann models, the high symmetry (i.e. maximal symmetry on spatial slices) allowed to achieve such a classification simply by the sign of the spatial curvature; cf. section 1 of chapter 4. For general spatially homogenous spacetimes, a successful classification has been given by classifying the Lie group of isometries. Since this group underlies the symmetries, this classification yields a division into ‘different kinds’ of spatial homogeneity:

By the above definition and proposition 2, in a spatially homogenous spacetime  $M$  the group of isometries  $G$  on  $M$  acts transitively on the spatial slices  $\Sigma_t$ . The class of spatially homogenous spacetimes splits then up into the class of Bianchi spacetimes, for which this group admits a subgroup  $H$  of homogeneity which acts simply transitively on the slices, and into the class of Kantowski-Sachs spacetimes, for which no such subgroup exists. In the latter case the group action on the slices is necessarily multiply transitive. In fact for the Kantowski-Sachs spacetimes,  $G$  is four dimensional: It can be shown that a five dimensional Group implies the existence of a six dimensional one, and a six dimensional group possesses a homogeneity subgroup. Since by (11), a six dimensional isometry group acting on

Bianchi- and Kantowski-Sachs spacetimes

class	A						B			
type	I	II	VI <sub>0</sub>	VII <sub>0</sub>	VIII	IX	V	IV	VI <sub>h</sub>	VII <sub>h</sub>
$n_1$	0	+	0	0	-	+	0	0	0	0
$n_2$	0	0	+	+	+	+	0	0	+	+
$n_3$	0	0	-	+	+	+	0	+	-	+

TABLE 1. The classification of the Bianchi spacetimes into ten different types according to the signature  $(n_1, n_2, n_3)$  of the symmetric part  $n^{kl}$  of the independent components of the structure constants of the Lie algebra of homogeneity  $\mathfrak{h}$ . In class A the matrix of independent structure constants is purely symmetric, in class B this is not the case.

three dimensional slices means maximal symmetry (i.e. Friedmann), the isometry group of Kantowski-Sachs spacetimes can only have dimension four. Kantowski-Sachs spacetimes are therefore locally rotationally symmetric.

The case of main interest for this text is that of the Bianchi spacetimes. For these the homogeneity subgroup  $H$  can be identified with the homogenous spatial slices  $\Sigma_t$  in the way described at the end of section 2 of chapter 3. A further classification of the Bianchi models by their spatial geometry can thus naturally be achieved by classifying their Lie group of homogeneity  $H$ : The easiest way to perform this is to actually classify the associated Lie algebra of Killing fields  $\mathfrak{h}$  on the homogenous slices, which can be identified with the Lie algebra of right invariant vector fields on  $H$ . Since  $\mathfrak{h}$  generates  $H$ , and vice versa  $H$  gives rise to  $\mathfrak{h}$ , this is essentially equivalent. As described in section 2 of chapter 3, the algebraic properties of  $\mathfrak{h}$  are fully encoded in the structure constants  $-C^k_{ij}$  in some basis  $\{\xi_i\}_{i=1}^3$  of  $\mathfrak{h}$ , which are given by  $[\xi_i, \xi_j] = -C^k_{ij}\xi_k$ . (The minus sign is conventional.) The natural and probably easiest way to classify  $H$  is thus to classify the structure constants of  $\mathfrak{h}$ , which is usually performed in the following way:

The structure constants are antisymmetric in the lower two indices since the algebraic product, the vector field commutator, is antisymmetric. Hence for fixed  $k$ ,  $[C^k_{ij}]$  forms an antisymmetric  $3 \times 3$ -matrix, whose three independent components can be written in a row  $[D^{kl}]$  (for fixed  $k$ ). This can formally be achieved by a multiplication with the total antisymmetric symbol  $\epsilon^{ijl}$ ;

$$D^{kl} = C^k_{ij}\epsilon^{ijl} \quad , \text{ with } \epsilon^{ijl} := \begin{cases} 1 & , (ijl) \text{ even permutation of } (123) \\ -1 & , (ijl) \text{ odd permutation of } (123) \\ 0 & , \text{ else} \end{cases} .$$

Therefore, the nine independent components  $C^k_{ij}$  are equally well encoded in a two index object  $D^{kl}$ . The modern Bianchi classification then differs between Bianchi class A, for which  $D^{kl}$  is symmetric, and Bianchi class B where this is not the case.

Let  $n^{kl}$  denote the symmetric part of  $D^{kl}$ . Each class is then further divided into different types according to the signature, i.e. the signs of the eigenvalues, of  $[n^{kl}]$ . Under the line this yields a classification of the Bianchi spacetimes into ten types which are listed in table 1 in the modern nomenclature. (For the classification of class B some more words would be appropriate, for which it is referred to [7, section 1.5.1].)

Bianchi classification

Bianchi class A & B

Bianchi types

## 2. Symmetry adapted bases

The existence of a foliation in spatially homogenous slices  $\Sigma_t$  suggests the choice of an adapted basis, in which the components of the metric, and therefore the Einstein equations, take a particularly simple form. An example of this was given by the Friedmann metrics (12) in chapter (4). In this section it is shown how one can adapt a frame to the symmetries of a Bianchi spacetime of particular type:

Clearly at first the frame should be adapted to the foliation with the slices  $\Sigma_t$  of spatial homogeneity. This means that the basis field in time direction  $e_0$  is chosen to be of unit length and normal to the slices, and the spatial basis fields  $\{e_i\}_{i=1}^3$  tangent to the slices everywhere. The metric components then have the form

$$[g_{\mu\nu}] = \begin{bmatrix} 1 & 0 \\ 0 & [g_{ij}] \end{bmatrix}.$$

Second one wishes to choose the spatial basis fields such that it adapts to the underlying Bianchi symmetry. The goal is to reflect this symmetry in the properties of the spatial basis fields, and to therefore also mirror them in the spatial metric components. The Bianchi type is specified by the structure constants of the Lie algebra of Killing fields  $\mathfrak{h}$  on the slices, which can be identified with the Lie algebra of right invariant vector fields on  $H$ , and  $H$  can itself be identified with the slices. The equivalence of the Lie algebras of left and right invariant vector fields discussed in section 2 of chapter 3 then suggests to choose a spatial basis which corresponds to a basis of left invariant vector fields on  $H$ . Choosing this basis such that (6) and (9) hold, i.e. such that the spatial basis admits the same structure constants (modulo the sign) than the Lie algebra of homogeneity  $\mathfrak{h}$  which specifies the Bianchi type. Hence such a basis mirrors the Bianchi symmetry as desired.

When additional symmetries are present to spatial homogeneity, one would also attempt to adapt the frame to them, such that also these symmetries are reflected in the components of the metric. For instance in a locally rotationally symmetric Bianchi spacetime, one would choose the frame such that two components of the metric coincide; e.g.  $g_{22} = g_{33}$ . There are however cases where it is not possible to choose the frame such that both  $g_{ij}$  and  $n^{ij}$  have this form; cf. [8, chapter 5].

## 3. The Einstein equations of Bianchi cosmologies

In a Bianchi type adapted basis, spatial homogeneity is manifest in the spatial metric components  $g_{ij}$  by the fact that they depend on time only, and not on the spatial coordinates. By (3) the same holds for the components of the extrinsic curvature  $k_{ij}$  on the spatial slices. Therefor in an adapted basis, and for simple matter models like perfect fluids with linear equation of state, the Einstein equations for Bianchi cosmologies reduce to a constrained autonomous system of ordinary differential equations. Writing the  $m$  independent components of  $g_{ij}$  and  $k_{ij}$  in a column  $\mathbf{x} \in \mathbb{R}^m$ , the evolution equations can be written as

$$(18) \quad \dot{\mathbf{x}} = \mathbf{f}(\mathbf{x}) \quad , \quad \text{with } \mathbf{f} : \mathbb{R}^m \rightarrow \mathbb{R}^m.$$

An equation of this kind (with  $\mathbf{f}$  partially differentiable ( $\mathcal{C}^1$ )) is also called a dynamical system on  $\mathbb{R}^m$ . (It should however be mentioned, that the term ‘dynamical system’ is also often given a more general meaning.) Dynamical systems theory is a rich and well developed branch of mathematics and provides rigorous analytical methods for a qualitative analysis of these kind of equations. One example of a dynamical system analysis was already given in section 3 of chapter 4 when investigating the qualitative dynamics of the Friedmann cosmologies. The right equation of (16), which was subject to this analysis, represents a dynamical system on  $\mathbb{R}$ . For more general spatially homogenous models the system is generally of higher

foliation adapted bases

Bianchi type adapted bases

LRS adapted basis

the Einstein equations as a dynamical system

dimension. A sketch of the techniques to analyse a higher dimensional dynamical system is subject of the next section. The remainder of the present section deals with the preparation of the evolution equations for this analysis, which is a direct generalisation of the steps performed in section 3 for the Friedmann evolution equations:

First, one defines new dynamical quantities which are standard cosmological parameters and/or bring the equations into suitable shape. One of these would be the Hubble scalar  $H$ , or a related quantity that scales with  $H$ , which gives a measure of the overall rate of spatial expansion. Let  $[H, \tilde{\mathbf{x}}]^T \in \mathbb{R}^m$  denote these quantities. The next step is then to define the expansion-normalised (or Hubble normalised) quantities  $\mathbf{y} := \tilde{\mathbf{x}}/H$ . Additionally, one defines the rescaled time  $\tau$  via  $\frac{d}{d\tau} = \frac{1}{H} \frac{d}{dt}$ . The original evolution equations (18) can then be expressed as a lower dimensional (reduced) dynamical system in the rescaled variables, and a decoupled evolution equation for  $H$ ;

rescaled or reduced  
dynamical system  
and decoupled  
equation for  $H$

$$(19) \quad \mathbf{y}' = \tilde{\mathbf{f}}(\mathbf{y}) \quad \text{and} \quad H' = f(H, \mathbf{y}),$$

with  $\tilde{\mathbf{f}} : \mathbb{R}^{m-1} \rightarrow \mathbb{R}^{m-1}$  and  $f : \mathbb{R} \rightarrow \mathbb{R}$ . The prime denotes derivation with respect to rescaled time  $\tau$ . The evolution of  $\mathbf{y}$  is decoupled from the other evolution equation since  $\tilde{\mathbf{f}}$  is independent of  $H$ . Hence, for a qualitative analysis where one is not interested in details concerning the overall rate of expansion, it suffices to restrict to the rescaled dynamical system.

#### 4. Qualitative analysis of Bianchi cosmologies

This section gives a sketch on how to analyse the reduced evolution equations (left equation of (19)) of Bianchi cosmologies qualitatively with methods from dynamical systems theory. The analysis is thereby performed at the simple example of Bianchi type I with a perfect fluid with linear equation of state,  $p = w\rho$ , with  $w \in (-\frac{1}{3}, 1)$ . The goal is to draw a qualitative flow diagram in analogy to the one that was found for the Friedmann models (figure 8), and to interpret it in cosmological terms. The idea is not to reach this goal in the quickest and most elegant way. Far more the emphasis is put on presenting the techniques from dynamical systems in a general fashion:

The two dimensional reduced dynamical system for Bianchi type I with perfect fluids with linear equation of state,  $p = w\rho$ , where  $w \in (-\frac{1}{3}, 1)$ , is given by

the reduced  
dynamical system

$$(20) \quad \Sigma'_+ = -(2-q)\Sigma_+ \quad \text{and} \quad \Sigma'_- = -(2-q)\Sigma_-,$$

where the deceleration parameter  $q$  is given by

$$q = \frac{1+3w}{2} + \frac{3}{2}(1-w)(\Sigma_+^2 + \Sigma_-^2).$$

The quantities  $\Sigma_+$  and  $\Sigma_-$  represent the independent components of the expansion-normalised rate of shear tensor; cf. [7, (1.27), (6.2) and (6.8)]. They can be thought of as determining the grade of anisotropy in the geometry, where the origin  $\Sigma_+ = \Sigma_- = 0$  corresponds to an isotropic case. In addition to the evolution equations the Einstein equations dictate the constraint

the constraint

$$(21) \quad \Omega = 1 - \Sigma_+^2 - \Sigma_-^2,$$

where  $\Omega := \frac{\rho}{3H^2}$  is the expansion-normalised energy density, and is assumed to be non-negative. It should be stressed that the system (20) is non-linear and therefore not exactly solvable for generic initial conditions.

the state space

As the first step in the qualitative analysis, one needs to identify the state space. That means one needs to find the possible range of the dynamical quantities such that the constraints are satisfied, and such that all stays in accordance with any

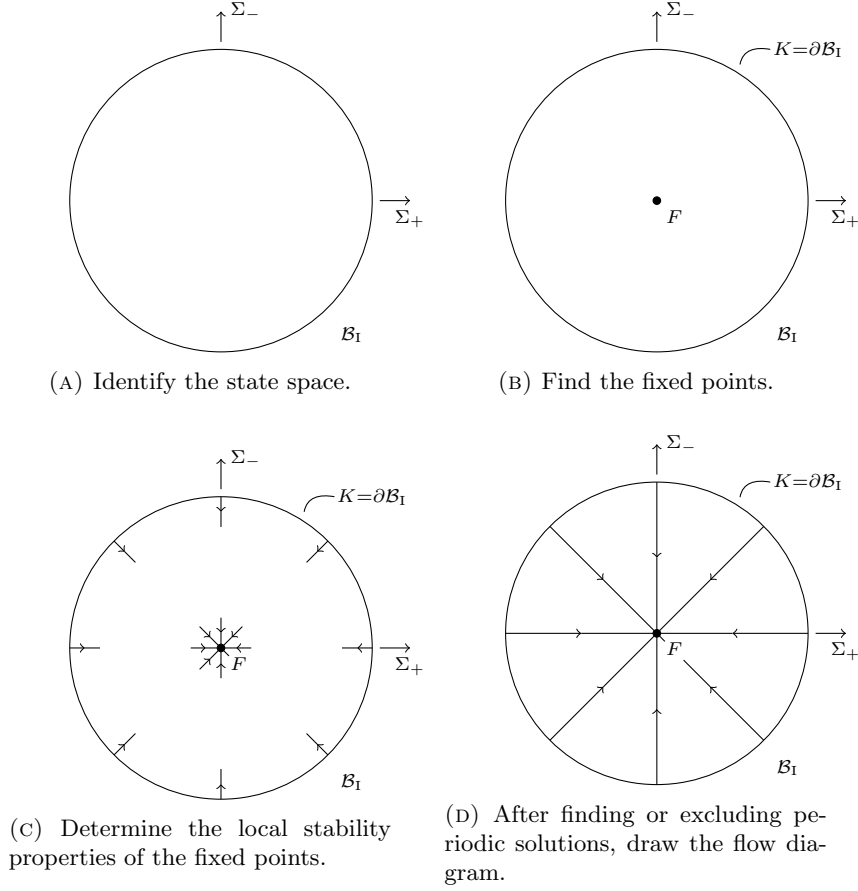


FIGURE 9. A sketch of the typical steps taken in a dynamical system analysis on the example of Bianchi type I.

additional assumptions on the variables. In the present case, the constraint (21) together with the assumption that  $\Omega \geq 0$  restricts the state space  $\mathcal{B}_1$  to the points  $(\Sigma_+, \Sigma_-)$  within the circle  $\Sigma_+^2 + \Sigma_-^2 = 1$ ; cf. figure 9a. From the constraint (21) it is clear that points on the boundary  $\partial\mathcal{B}_1$  of the state space correspond to vacuum states ( $\Omega = 0$ ).

The next step is to find the fixed point solutions of the dynamical system which are characterised by  $\mathbf{y}' = \tilde{\mathbf{f}}(\mathbf{y}) = 0$ . These are static solutions in the state space since a solution that attains the value of a fixed point during one instant of time has this value during the whole evolution. This however does not imply that the metric corresponding to a fixed point solution stays constant with time: The equation for  $H$  (right equation of (19)) can still account for dynamics in the sense of an overall rate of expansion or contraction. In the present example one finds from (20) that there is one isolated fixed point  $F$  at the origin, and that each point on the boundary  $\partial\mathcal{B}_1$  is a fixed point as well; cf. figure 9b. This circle of fixed points is called the Kasner circle, and is denoted by  $K$ ; cf. [7, section 6.2.2].

The regularity property  $\tilde{\mathbf{f}} \in \mathcal{C}^1$  of a dynamical system allows to approximate the system close to a fixed point  $\mathbf{y}^*$  by

$$(22) \quad \mathbf{y}' \approx D\tilde{\mathbf{f}}(\mathbf{y}^*)(\mathbf{y} - \mathbf{y}^*),$$

fixed points

linear approximation  
at a fixed point

local stability  
properties of the  
fixed points

where  $D\tilde{\mathbf{f}}$  denotes the derivative matrix (Jacobi matrix) of  $\tilde{\mathbf{f}}$ . As an equation, (22) is called the linear approximation of the dynamical system at the fixed point  $\mathbf{y}^*$ . At least for the generic type of fixed point (i.e. for hyperbolic fixed points; cf. [7, definition 4.9]), the flow of the linearisation indeed approximates the flow of the full system in a neighbourhood of the fixed point. This is the statement of the famous Hartman-Grobman theorem; cf. [7, section 4.3.2] or [9, section 2.8]. Linear systems are well known and exactly solvable; cf. [9, chapter 1]. For the analysis of the full dynamical system it suffices however to know about the qualitative features of (22), i.e. about the stability properties. These are encoded in the eigenvalues of  $D\tilde{\mathbf{f}}$  at the fixed point: For instance, if all these eigenvalues have negative (positive) real parts, then the solutions approach the fixed point asymptotically into the past (future), and the fixed point is called a sink (source). In the context of the full system this then holds for the local flow in some neighbourhood of the fixed point. In the present example the eigenvalues of  $D\tilde{\mathbf{f}}$  at  $F$  have both the value  $-\frac{3}{2}(1-w)$ , which is negative for  $w \in (-\frac{1}{3}, 1)$ . Hence  $F$  is a local sink in  $\mathcal{B}_I$ . Picking the fixed point  $[0, 1]^T$  on the Kasner circle  $K$  one finds a positive eigenvalue corresponding to an eigenvector in  $\Sigma_-$ -direction. The second eigenvalue is zero and corresponds to an eigenvector in  $\Sigma_+$ -direction, which is intuitively clear since the neighbouring points in these direction are fixed points as well. The symmetry of the system (20) tells that the analog holds for each point on the Kasner circle, such that all points on  $K$  play the role of a local source in  $\mathcal{B}_I$ . At this point in the analysis one would ideally know about the local stability properties of all the fixed points in the state space, and would arrive at a state of the flow diagram as in figure 9c for the present example, in which the local flow is qualitatively known in a neighbourhood of each fixed point.

periodic solutions

What is left to do is to determine the qualitative shape of the flow between the fixed points. There could be other structures than fixed points inside the state space, like periodic solutions (closed solution curves), which are approached by generic solutions asymptotically into the past or into the future. If present, one would have to find these structures, and attempt to find their local stability properties as well, which is not always trivial. Luckily in many cases there is no such additional structure. Dynamical systems theory provides several theorems to exclude their presents, e.g. the monotonicity principle; cf. [7, theorem 4.12]. In the present example the existence of periodic orbits inside  $\mathcal{B}_I$  can be excluded, and hence the only possibility for a solution curve is to approach a point on  $K$  asymptotically into the past, and to approach  $F$  asymptotically into the future; cf. figure 9d. One should note that, due to the uniqueness theorems of ordinary differential equations, these solutions however never reach  $K$  or  $F$ . For the same reason, solution curves cannot cross each other, which in particular often simplifies this last step of drawing the solution curves when the system is two dimensional.

past and future  
asymptotics

In this example one could have directly seen from (20) that the solution curves are straight lines through the origin, and would just have had to determine the direction of the flow to arrive at the final plot diagram. This would however not have served the purpose of demonstrating the general techniques of a dynamical system analysis. In general one does not get out information about the actual shape of the solution curves inside the state space, but merely information about their past and future asymptotics, which is also called the  $\alpha$ - and  $\omega$ -limit set of a solution, which are typically fixed points. The physical solution that corresponds to a fixed point can usually be given exact by involving the equation for  $H$ . In the present example one then finds that  $F$  corresponds to the flat Friedmann solution (12). (Recall that the origin corresponds to an isotropic case.) One can thus immediately draw interesting physical conclusions from the plot of the flow diagram 9d: A



Bianchi type I cosmology (with a perfect fluid out of the chosen class) is past asymptotically to an anisotropic vacuum (Kasner) solution, and future asymptotic to a flat Friedmann solution. Hence these cosmologies isotropise towards the future.



## References and further reading

The list below not only contains references to citations within part 1, but also represents a collection of literature that was useful to me to study the required mathematics and physics, and for typing the thesis. As such it is clearly not a complete list of the literature available. Never the less I want to provide the interested reader with more information on these sources, and give some personal recommendations for further reading. I therefore added some descriptive text to each item in the list below.

When writing part 1, the books [7], [4], [5] and [10] served as main references and sources for inspiration to me. For chapter 2 I mainly used [4] and [10]. Both books focus on an abstract, coordinate free point of view and choose the same approach to semi-Riemannian geometry, which I then adopted here in this text. For writing section 1 of chapter 3 I mainly used [5], but for example also [3]. [4] along with [5] were also very useful to me for writing the content of section 2 of that chapter. For writing section 3 of chapter 3 I then mainly worked with [7]. The latter source was also my main source for writing section 3 of chapter 4 and large parts of chapter 5.

For further reading on dynamical systems theory I can highly recommend the short introduction by R Tavakol; chapter 4 *Introduction to dynamical system* in [7]. For the reader who wants a thorough mathematics textbook on this topic I recommend [9].

- [1] Alcubierre M: Introduction to 3+1 Numerical Relativity; *International Series of Monographs in Physics – 104*; Oxford University Press (2008).

A textbook on numerical relativity which contains a detailed discussion on foliations in it's chapter 2 *The 3+1 formalism*. It is hence, just as [2], well suited for further reading on this topic which was only briefly touched in section 5 of chapter 2. In addition to that, this book contains a very good short introduction to General Relativity in it's chapter 1 *Brief review of general relativity*.

Cited on pages 11, 33

- [2] Baumgarte TW, Shapiro SL: Numerical Relativity: Solving Einstein's Equations on the Computer, Cambridge University Press (2010).

A textbook on numerical relativity which contains a detailed and nicely illustrated discussion on foliations in it's chapter 2 *The 3+1 decomposition of Einstein's equations*. It is hence, just as [1], well suited for further reading on this topic which was only briefly touched in section 5 of chapter 2.

Cited on pages 11, 33

- [3] Weinberg S: Gravitation and Cosmology: Principles and applications of the General Theory of Relativity, John Wiley & Sons, Inc. (1972).

This book by Weinberg is an often cited standard physics textbook on General Relativity. It stays in contrast to most other standards in that it deliberately takes a particularly non-geometric approach to the theory. It thereby sheds light on many aspects of the theory that are not treated in most other textbooks, and greatly complements the literature. Index notation is used throughout the book. Of particular interest for part 1 is it's chapter 13 *Symmetric spaces*, which comprises a very detailed discussion on Killing fields, homogenous manifolds, isotropic manifolds and maximally symmetric manifolds. The presentation of these topics is however, in the fashion of the whole book, with little emphasis on geometric aspects.

Cited on pages 14, 17, 33

- [4] Szekeres P: A course in modern mathematical physics: groups, Hilbert space and differential geometry, Cambridge University Press (2004).  
An excellent textbook on modern mathematical physics which gives a rigorous overview on many topics. It makes use of a modern notation and chooses a state of the art approach to the mathematics. It's chapters 7 *Tensors*, 15 *Differential geometry* and 18 *Connections and curvature* serve as an excellent reference to chapter 2. It's chapter 19 *Lie groups and Lie algebras* greatly supplements chapter 3.  
Cited on pages 15, 33, 34
- [5] Wald RM: General Relativity, The University of Chicago Press (1984).  
One of the standard physics textbooks on General Relativity. It is divided into two parts. *Part 1. Fundamentals* gives a thorough introduction to General Relativity and the underlying mathematics. The approach to semi-Riemannian geometry is thereby similar to those presented in [10] and [4], adopting an abstract, geometric point of view, with some differences in the way in which the concept of connections is introduced. Wald also uses a different, abstract index notation. *Part 2. Advanced topics* is then devoted to more specific aspects of the theory and also contains a section (7.2) on *Spatially homogenous cosmology*. Together with it's *Appendix C. Maps of manifolds, Lie Derivatives, and Killing Fields* this book thus serves as a good reference to all topics discussed in part 1.  
Cited on pages 16, 19, 20, 21, 33
- [6] Ryan MP, Jr; Shepley LC: Homogeneous relativistic cosmologies; *Princeton Series in Physics*; Princeton University Press (1975).  
This is still a standard textbook on spatially homogenous cosmology. The style is rigorous and self contained. The book gives many proofs, some of which are hard to find anywhere else in the literature.  
Cited on page 16
- [7] Wainwright J, Ellis GFR (editors): Dynamical Systems in Cosmology, Cambridge University Press (1997).  
This is the actual standard introductory textbook to the branch of cosmology that deals with dynamical systems techniques. The book goes far beyond of what I introduced in part 1, and is thus excellently suited for further reading. When writing section 3 of chapter 4, I adopted the discussion of section 2.3 *Qualitative analysis* (of the Friedmann dynamics) of this book. It's chapter 4 *Introduction to dynamical systems* gives an excellent short introduction to dynamical systems theory, which contains all the concepts and theorems which are essential to the purpose, and gives references to other sources for the proofs. Section 1.2 *Symmetries of space-time* of the book is a good reference to section 3 of chapter 3. Section 1.5 *Bianchi cosmologies* of the book is a good reference to sections 1, 2 and 3 of chapter 5.  
Cited on pages 21, 26, 28, 29, 30, 33
- [8] Heinzle JM: Bianchi models and generic spacelike singularities; Habilitation, Universität Wien (2010).  
The first part of this Habilitation gives a summary to the formal basics of Bianchi cosmology. It greatly complements the literature by pointing out many details on topics like local rotational symmetry, or adapted frames of reference, which can hardly be found anywhere else.  
Cited on page 27
- [9] Perko L: Differential Equations and Dynamical Systems, second edition; *Texts in applied Mathematics 7*, Springer-Verlag (1996).  
A thorough mathematics textbook on dynamical systems theory which I can highly recommend to the reader who is interested in a deeper study of this interesting branch of modern mathematics. It contains all the proofs to the theorems, and many illustrative examples.  
Cited on page 30, 33
- [10] O'Neill B: Semi-Riemannian geometry, with applications to Relativity; *Pure and Applied Mathematics*, Elsevier/Academic Press (1983).  
A thorough mathematics textbook on the subject of the title with an emphasis on an abstract and coordinate free approach. It goes way beyond of what is needed for part 1 and thus serves not only as a good reference to chapter 2 and parts of chapter 3, but also as a very good

book for further reading for the one who is interested in a deeper study of the mathematics.  
Cited on pages [33](#), [34](#)



Part 2

**Dynamics of locally rotationally  
symmetric Bianchi type VIII  
cosmologies with anisotropic matter**

### Remark

The content of this part is a reprint of my research article *Dynamics of locally rotationally symmetric Bianchi type VIII cosmologies with anisotropic matter* published by Springer in 2012 in the journal *General Relativity and Gravitation: Volume 44, Issue 11 (2012), Page 2901-2922*; DOI 10.1007/s10714-012-1430-8. It is online available at <http://www.SpringerLink.com/content/362128k038173qt2>.



## Dynamics of locally rotationally symmetric Bianchi type VIII cosmologies with anisotropic matter

Gernot Heißel

Received: 22 March 2012 / Accepted: 17 July 2012  
© Springer Science+Business Media, LLC 2012

**Abstract** This paper is a study of the effects of anisotropic matter sources on the qualitative evolution of spatially homogenous cosmologies of Bianchi type VIII. The analysis is based on a dynamical system approach and makes use of an anisotropic matter family developed by Calogero and Heinzle which generalises perfect fluids and provides a measure of deviation from isotropy. Thereby the role of perfect fluid solutions is put into a broader context. The results of this paper concern the past and future asymptotic dynamics of locally rotationally symmetric solutions of type VIII with anisotropic matter. It is shown that solutions whose matter source is sufficiently close to being isotropic exhibit the same qualitative dynamics as perfect fluid solutions. However a high degree of anisotropy of the matter model can cause dynamics to differ significantly from the vacuum and perfect fluid case.

**Keywords** Spatially homogenous cosmology · Anisotropic matter · Dynamical systems

### 1 Introduction and motivation

For spatially homogenous (SH) spacetimes the Einstein-matter equations for a large variety of matter sources reduce to an autonomous system of ordinary differential equations in time. Thus the mathematical theory of dynamical systems can be applied to gain insights into the qualitative behaviour of SH solutions. This approach has been used in mathematical cosmology, e.g. to address questions relevant for observational cosmology, in particular concerning the role the Friedmann solutions play in the more general

---

G. Heißel (✉)  
Gravitational Physics Group, Faculty of Physics, University of Vienna, Vienna,  
Austria  
e-mail: Gernot.Heissel@Mac.com

context of SH cosmologies that are not spatially isotropic in general. On the other hand the interest in SH models is nourished by the believe that the dynamics of SH cosmologies towards the initial singularity is crucial for the understanding of the behaviour of more general spacetimes close to singularities; cf. [1] and references therein.

Less is known about SH solutions with matter sources more general than perfect fluids. Calogero and Heinzle have developed a matter family naturally generalising perfect fluids that contains large classes of anisotropic matter sources and is suited for a dynamical system analysis. It includes a measure of the deviation from isotropy and thus allows to investigate the role of perfect fluid solutions in the more general context of solutions with anisotropic matter. The SH cosmologies considered were of Bianchi type I, and locally rotationally symmetric (LRS) types I, II and IX; cf. [2, 3]. While dynamical system analyses with specific anisotropic matter sources have been carried out before, the approach by Calogero and Heinzle can be regarded as a first step towards a systematic study of the effects of anisotropic matter to the qualitative dynamics of SH cosmologies.

This paper is concerned with the analysis of SH cosmologies of LRS Bianchi type VIII with anisotropic matter. In Sect. 2 the basic features of the anisotropic matter family are stated, and the state space and evolution equations for LRS type VIII are given. The dynamical system analysis is performed in Sect. 3, where some technical details on the analysis of the flow at infinity are contained in the appendix. The results are given and discussed in Sect. 4, where the main result is formulated in Theorem 1 and Corollaries 1 and 2. As a small byproduct, the results cover the future asymptotics for perfect fluids with  $p = w\rho$  and  $w \in (-\frac{1}{3}, 0)$ , which might fill a little gap in the literature. Section 5 is concerned with an extension of the formalism to treat Vlasov matter dynamics with massive particles.

Part of the material needed in Sects. 2, 3 and 5 has already been presented in [3] or [4] to analyse LRS Bianchi types I, II and IX. At these points in the text, only the crucial steps and results are quoted from there.

## 2 The LRS Bianchi type VIII setup

In a frame  $(dt, \hat{\omega}^1, \hat{\omega}^2, \hat{\omega}^3)$  adapted to the symmetries, an LRS Bianchi class A metric has the form

$${}^4g = -dt \otimes dt + g_{11}(t) \hat{\omega}^1 \otimes \hat{\omega}^1 + g_{22}(t) (\hat{\omega}^2 \otimes \hat{\omega}^2 + \hat{\omega}^3 \otimes \hat{\omega}^3).$$

In type VIII,  $d\hat{\omega}^i = -\frac{1}{2}\epsilon_{jkl}\hat{n}^{ij}\hat{\omega}^k \wedge \hat{\omega}^l$ , with  $[\hat{n}^{ij}] \equiv \text{diag}(-1, 1, 1)$ . Greek indices denote spacetime components while Latin indices label spatial components w.r.t. the adapted frame. The metric will be subject to the Einstein equations—without cosmological constant—in geometrised units ( $8\pi G = c = 1$ ), cf. [3, Eq. 2].

### 2.1 The anisotropic matter family

For a perfect fluid that is non-tilted with respect to  $dt$ , the components of the stress-energy tensor are  $[T^\mu{}_\nu] = \text{diag}(-\rho, p, p, p)$ , where  $\rho$  and  $p$  denote the energy

density and pressure of the fluid. It is an isotropic matter model since the eigenvalues of  $[T^i_j]$  are all equal. When  $p = w\rho$  with  $w = \text{const}$ , the fluid is said to obey a linear equation of state.<sup>1</sup>

The matter models considered in this paper form a family of models generalising perfect fluids with linear equation of state. This family of models is described in detail in [3, section 3]. (However it should be mentioned that several of the involved variables have already been used earlier, like  $s$  in [5].) In the following, a brief description tailored to the present purposes is given:

The components of the stress–energy tensor are  $[T^\mu_\nu] = \text{diag}(-\rho, p_1, p_2, p_2)$  where the energy density  $\rho$  (assumed to be positive) and the isotropic pressure  $p := \sum_i p_i/3$  obey a linear equation of state  $p = w\rho$ , with  $w = \text{const}$ . Defining the dimensionless rescaled principal pressures as  $w_i := p_i/\rho$  it is clear that  $w = \sum_i w_i/3$ , which in turn implies that  $w_1$  and  $w_2$  are not independent once  $w$  is given. As a consequence of the Einstein equations and some basic assumptions on the matter family given in [3, section 3],  $w_2$  (and thus  $w_1$ ) is a function of the quantity  $s := \frac{g^{22}}{\sum_i g^{ii}} \in (0, \frac{1}{2})$ . Clearly,  $s$  gives a measure of anisotropy of the spatial metric components while  $w_2$  encodes the anisotropy of the matter content.<sup>2</sup> The simple example of isotropic matter corresponds to  $w_1 = w_2 = w$ . Also, note that  $s \rightarrow 0$  and  $s \rightarrow \frac{1}{2}$  correspond to  $g_{22} \rightarrow \infty$  (or  $g_{11} \rightarrow 0$ ) and  $g_{11} \rightarrow \infty$  (or  $g_{22} \rightarrow 0$ ) respectively, i.e. to a singular metric. A basic assumption is that the limit of  $w_1$  for  $s \rightarrow \frac{1}{2}$  coincides with the limit of  $w_2$  for  $s \rightarrow 0$ , i.e. that  $w_1(\frac{1}{2}) = w_2(0)$ . Hence one can define an anisotropy parameter

$$\beta := 2 \frac{w - w_2(0)}{1 - w} \quad (1)$$

that provides a measure of deviation from an isotropic matter state in the extremal cases where the metric is singular. Note that  $\beta = 0$  corresponds to matter models that behave like a perfect fluid close to singularities.

The analysis in Sect. 3 will show that the qualitative dynamics of LRS Bianchi type VIII solutions does not depend on the whole function  $w_2$  but merely on the value  $w_2(0)$  where the metric is singular. Thus any two matter models of the anisotropic matter family that share the same parameters  $w$  and  $\beta$  also share the same qualitative dynamics, even if they have different functions  $w_i(s)$ . Accordingly,  $\beta$  serves as the parameter to investigate the influence of the anisotropy of the matter on the dynamics, even though it gives a precise measure of the anisotropy only close to singularities. Therefore, in the context of the qualitative analysis of the dynamics of solution that follows, a specific class of matter models is simply characterised by a pair  $(w, \beta)$  in the parameter space

$$\mathbb{P} := \left( -\frac{1}{3}, 1 \right) \times \mathbb{R}.$$

<sup>1</sup> For example,  $w = 0$  corresponds to dust and  $w = \frac{1}{3}$  to radiation.

<sup>2</sup> In [3]  $w_2(s)$  is called anisotropy function and denoted by  $u(s)$ .

Here  $w$  is restricted to  $(-\frac{1}{3}, 1)$  since the primary interest is in matter models that obey the standard energy conditions [6, pp. 218–220]: The weak energy condition corresponds to  $w_i \geq -1$ . The strong energy condition requires the weak energy condition to hold and  $w \geq -\frac{1}{3}$ . The dominant energy condition is  $|w_i| \leq 1$ . Therefore, by (1), for the energy conditions to hold, one has to restrict  $\beta$  to  $[\max(-2, -\frac{1+w}{1-w}), 1]$ ; cf. [3, table 2 in section 3.4]. The dominant energy condition is only marginally satisfied when  $\beta(w)$  takes the boundary values. The parameter space  $\mathbb{P}$  and the subset for which the energy conditions are satisfied is depicted in Fig. 3 together with the bifurcation lines which will be explained in Sect. 3.

## 2.2 The Einstein equations as a dynamical system

LRS Bianchi types VIII and IX share the same evolution equations which have been derived in detail in [3]. This subsection gives a brief outline:

Due to spatial homogeneity, the Einstein equations for LRS type VIII with the above matter source are a constrained autonomous system of ordinary differential equations in  $t$  for the components of the spatial metric  $g_{ij}$  and the extrinsic curvature  $k_{ij}$ . This system is then written in terms of quantities that are standard cosmological parameters and/or bring the equations into suitable shape. These quantities are the Hubble scalar  $H := -\frac{1}{3}(k^1_1 + 2k^2_2)$ , the shear variable  $\sigma_+ := \frac{1}{3}(k^1_1 - k^2_2)$  and the quantity  $m_1 := \sqrt{g_{11}/g_{22}}$ . Finally these are divided by the variable  $D := \sqrt{H^2 - 1/(3g_{22})} > 0$  to obtain the normalised variables  $(H_D, \Sigma_+, M_1) := (H, \sigma_+, m_1)/D$ . In [3] this normalisation has been taken in lieu of the Hubble normalisation [7, section 5.2] mainly because it yields a compact LRS type IX state space. Although this is not the case for LRS type VIII, the normalisation with  $D$  still has favourable properties. For example the type III form of flat spacetime which will turn out to be crucial for generic future asymptotic solutions (cf. Sect. 4) is a fixed point solution in this formulation; cf. Table 1. Also, as already stated, LRS types VIII and IX share the same evolution equations in this formulation, why many results from [3] on LRS type IX can directly be carried over to the analysis of LRS type VIII. It should also be mentioned that variables of this kind have already been used earlier; cf. [8].

The resulting representation of the Einstein equations for anisotropic matter filled LRS Bianchi type VIII spacetimes is then given by the dynamical system

$$\begin{bmatrix} H_D \\ \Sigma_+ \\ M_1 \end{bmatrix}' = \begin{bmatrix} -(1 - H_D^2)(q - H_D \Sigma_+) \\ -(2 - q)H_D \Sigma_+ - (1 - H_D^2)(1 - \Sigma_+^2) + \frac{M_1^2}{3} + 3\Omega(w_2(s) - w) \\ M_1(qH_D - 4\Sigma_+ + (1 - H_D^2)\Sigma_+) \end{bmatrix} \quad (2)$$

which represents the evolution equations, and the Hamiltonian constraint

$$\Omega + \Sigma_+^2 + \frac{M_1^2}{12} = 1. \quad (3)$$

The quantity  $\Omega := \frac{\rho}{3D^2}$  denotes the normalised energy density and  $q := 2\Sigma_+^2 + \frac{1+3w}{2}\Omega$  the deceleration parameter. The prime denotes derivatives with respect to rescaled time;  $(\cdot)' := \frac{1}{D} \frac{\partial}{\partial t}(\cdot)$ . Note that the definitions of  $M_1$  and  $D$  imply that  $s$  can be regarded as a function of  $H_D$  and  $M_1$ ,  $s = (2 - 3\frac{1-H_D^2}{M_1^2})^{-1}$ . Therefore (2) is a closed system once  $w_2(s)$  is prescribed through the ‘equation of state’ of the anisotropic matter.

### 2.3 The state space $\mathcal{X}_{\text{VIII}}$

The LRS type VIII state space is determined by the Hamiltonian constraint (3) and the relation

$$1 - H_D^2 = -\frac{1}{3D^2 g_{22}} < 0, \quad (4)$$

which follows directly from the definition of  $D$ : Since  $\rho$  is assumed to be positive (cf. Sect. 2.1) it follows by definition that  $\Omega > 0$ . And since also  $M_1 > 0$  by definition, it then follows from the Hamiltonian constraint that  $\Sigma_+^2 < 1$  and  $\Sigma_+^2 + \frac{M_1^2}{12} < 1$ . The inequality  $1 - H_D^2 < 0$  implies that the state space is the union of two disjoint sets:  $H_D > 1$  corresponds to positive  $H$  and hence to forever expanding universes, while  $H_D < -1$  corresponds to forever contracting universes. However, since (2) is invariant under the reflection  $(t, H_D, \Sigma_+) \rightarrow -(t, H_D, \Sigma_+)$  it suffices to restrict to the expanding case. Accordingly the LRS Bianchi type VIII state space is defined as

$$\mathcal{X}_{\text{VIII}} := \left\{ \begin{bmatrix} H_D \\ \Sigma_+ \\ M_1 \end{bmatrix} \in \mathbb{R}^3 \mid H_D \in (1, \infty), \Sigma_+ \in (-1, 1), M_1 \in (0, \sqrt{12(1 - \Sigma_+^2)}) \right\},$$

which forms the tunnel-like structure depicted in Fig. 1. The boundary subsets of  $\mathcal{X}_{\text{VIII}}$  are  $\mathcal{V}_{\text{VIII}}$ ,  $\mathcal{B}_{\text{III}}$  and  $\mathcal{S}_{\sharp}$ , which correspond to  $\Omega = 0$ ,  $M_1 = 0$  and  $H_D = 1$ , respectively. LRS type VIII vacuum solutions thus lie in  $\mathcal{V}_{\text{VIII}}$  while solutions in  $\mathcal{S}_{\sharp}$  and  $\mathcal{B}_{\text{III}}$  are of Bianchi types II and III respectively; cf. [3, sections 9.2 and the first remark in 10.1].

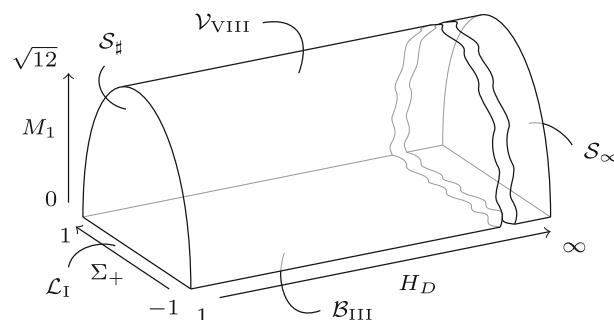


**Fig. 1** The state space  $\mathcal{X}_{\text{VIII}}$  and its boundary subsets

$\mathcal{S}_\infty$ , which corresponds to  $H_D \rightarrow \infty$ , is of course not a boundary, but one can think of it as boundary in a compactified version of the state space; cf. Appendix 6.

In this formulation LRS type IX cosmologies are subject to the same evolution Eq. (2). However there is a sign change in the relation (4) leading to a different state space  $\mathcal{X}_{IX}$  for which  $H_D \in (-1, 1)$ . Figuratively speaking  $\mathcal{X}_{IX}$  builds the tunnel connecting  $\mathcal{X}_{VIII}$  with the second disjoint LRS type VIII set. Hence both  $\mathcal{X}_{VIII}$  and  $\mathcal{X}_{IX}$  share the boundary  $\mathcal{S}_\#$ . Cf. [3, section 9].

There are two challenges in connection with the analysis of the dynamical system (2) in  $\mathcal{X}_{VIII}$ . First,  $\mathcal{X}_{VIII}$  is not compact. Hence one has to perform a careful analysis of the ‘flow at infinity’. In the present case it will be shown that there do not exist orbits that emanate from or escape to infinity. Second, the dynamical system (2) does not extend to the line  $\mathcal{L}_I$  in  $\partial\mathcal{X}_{VIII}$  for that  $H_D = 1$  and  $M_I = 0$  since  $s(H_D, M_I)$  has no limit when  $\mathcal{L}_I$  is approached from  $\mathcal{X}_{VIII}$ .<sup>3</sup> The analogous problem occurs in the context of LRS type IX, where it was overcome by introducing another set of coordinates that give regular access to this part of the boundary by ‘blowing up’  $\mathcal{L}_I$ ; cf. [3, section 10.2]. This method can be adapted to the LRS type VIII case by applying the same coordinate transformation. However the corresponding state space is again different:

#### 2.4 The state space $\mathcal{Y}_{VIII}$

The coordinate transformation used to analyse  $\mathcal{L}_I$  is

$$1 - H_D^2 = 2r \cos \theta, \quad M_I^2 = 3r \sin \theta, \quad \Sigma_+ \text{ unchanged}, \quad (5)$$

where  $r \geq 0$  and  $\theta \in [\frac{\pi}{2}, \pi]$ . Thereby,  $\mathcal{X}_{VIII}$  is transformed to the state space

$$\mathcal{Y}_{VIII} := \left\{ \left[ \begin{array}{c} r \\ \theta \\ \Sigma_+ \end{array} \right] \in \mathbb{R}^3 \mid r \in \left( 0, \frac{4(1 - \Sigma_+^2)}{\sin \theta} \right), \theta \in \left( \frac{\pi}{2}, \pi \right), \Sigma_+ \in (-1, 1) \right\}$$

which is depicted in Fig. 2. From (5) one has the following correspondences between subsets of  $\overline{\mathcal{X}}_{VIII}$  and  $\overline{\mathcal{Y}}_{VIII}$ :

$$\mathcal{X}_{VIII} \sim \mathcal{Y}_{VIII}, \quad \overline{\mathcal{V}}_{VIII} \sim \overline{\mathcal{V}}_{VIII}^{\mathcal{Y}}, \quad \overline{\mathcal{B}}_{III} \sim \overline{\mathcal{B}}_{III}^{\mathcal{Y}} \cup \overline{\mathcal{X}}_I, \quad \overline{\mathcal{S}}_\# \sim \overline{\mathcal{S}}_\#^{\mathcal{Y}} \cup \overline{\mathcal{X}}_I, \quad \overline{\mathcal{L}}_I \sim \overline{\mathcal{X}}_I. \quad (6)$$

$\mathcal{S}_\infty$  corresponds to a line at infinity in the context of  $\mathcal{Y}_{VIII}$ . Furthermore, (5) defines a diffeomorphism between  $\overline{\mathcal{X}}_{VIII} \setminus \overline{\mathcal{L}}_I$  and  $\overline{\mathcal{Y}}_{VIII} \setminus \overline{\mathcal{X}}_I$ , from which it follows that the flows in these sets are topologically equivalent. In particular,

$$\mathcal{X}_{VIII} \cong \mathcal{Y}_{VIII}, \quad \mathcal{V}_{VIII} \cong \mathcal{V}_{VIII}^{\mathcal{Y}}, \quad \mathcal{B}_{III} \cong \mathcal{B}_{III}^{\mathcal{Y}} \quad \text{and} \quad \mathcal{S}_\# \cong \mathcal{S}_\#^{\mathcal{Y}}. \quad (7)$$

<sup>3</sup> However  $s(H_D, M_I)$  has limits when  $\mathcal{L}_I$  is approached from  $\mathcal{B}_{III}$  or  $\mathcal{S}_\#$ ; cf. Sects. 3.2 and 3.3.

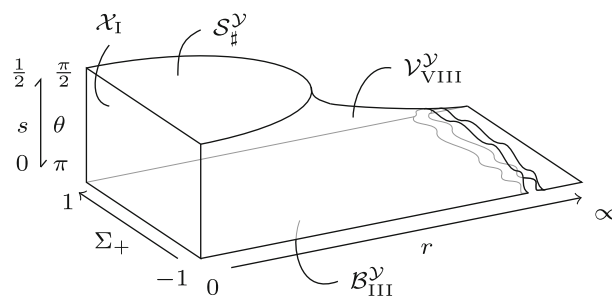


**Fig. 2** The state space  $\mathcal{V}_{\text{VIII}}^y$  and its boundary subsets

In contrast, the coordinate transformation performs a blowup of the line  $\mathcal{L}_I$  to the two-dimensional set  $\mathcal{X}_I$  defined by setting  $r = 0$ . It can be identified with the LRS Bianchi type I state space; cf. [3, section 10.2]. With (5),  $s$  can be regarded as a function of  $\theta$  alone. Therefore  $s$  has a limit as  $r \rightarrow 0$ , which implies that the dynamical system, when expressed in the coordinates  $(r, \theta, \Sigma_+)$ , extends regularly to  $\mathcal{X}_I$ .

Finally, note that since  $s(\theta)$  is a bijection on  $[\frac{\pi}{2}, \pi]$  one can as well choose  $s$  as coordinate instead of  $\theta$ ; hence the two labels on the axis in Fig. 2.

### 3 The dynamical system analysis

Whenever possible the analysis is carried out in the coordinates  $(H_D, \Sigma_+, M_1)$ , which is in all sets except  $\mathcal{X}_I$ . However the final results presented in Sect. 4 have to be interpreted in the context of the state space  $\mathcal{V}_{\text{VIII}}^y$  since the system (2) is not regular in  $\overline{\mathcal{X}_{\text{VIII}}}$ , which prevents a complete global analysis in the original state space.

Since the matter parameters  $w$  and  $\beta$  enter the evolution equations everywhere except in the vacuum boundary and at infinity, cf. Sects. 3.1 and 3.5, their values determine the qualitative properties of the flow. For instance there are fixed points that only occur in the state space iff  $(w, \beta)$  is in a certain subset of  $\mathbb{P}$ . Similarly, fixed points may have different local stability properties depending on  $(w, \beta)$ . The curves  $\beta(w) \in \mathbb{P}$  dividing  $\mathbb{P}$  into these subsets corresponding to qualitatively different dynamics shall be called bifurcation lines. These fixed points and bifurcation lines will be found in the subsequent subsections. The exact solutions corresponding to the fixed points are summarised in Table 1. These have been given in [3, appendix A] for all fixed points but  $D$ . For  $D$ , one just needs to insert the coordinates into [3, Eq. 99]. The corresponding isotropic cases to these solutions can be found in [7, section 9.1]. The bifurcation lines are plotted in Fig. 3.

#### 3.1 Analysis in $\overline{\mathcal{V}_{\text{VIII}}}$

The dynamical system in  $\overline{\mathcal{V}_{\text{VIII}}}$  is obtained by setting  $\Omega = 0$  in (2) and using (3):

$$\begin{bmatrix} H_D \\ \Sigma_+ \end{bmatrix}' = \begin{bmatrix} (1 - H_D^2)(H_D - 2\Sigma_+)\Sigma_+ \\ (1 - \Sigma_+^2)(2 + (1 - \Sigma_+^2) + (H_D - \Sigma_+)^2) \end{bmatrix} \quad (8)$$

**Table 1** The exact solutions corresponding to the fixed points

Fixed points	Corresponding solution	Type	Vacuum
$T, T_b, T_{\pm}^{\dagger}$	Taub Kasner	I	✓
$Q, Q_b, Q_{\pm}^{\dagger}$	Non-flat LRS Kasner	I	✓
$R_b, R_{\pm}^{\dagger}$	A type I anisotropic matter solution	I	
$F$	Flat Friedmann	I	
$C_{\pm}^{\dagger}$	Generalisation of Collins-Stewart	II	
$P$	Generalisation of Collins (VI <sub>-1</sub> )	III	
$D$	Type III form of flat spacetime	III	✓

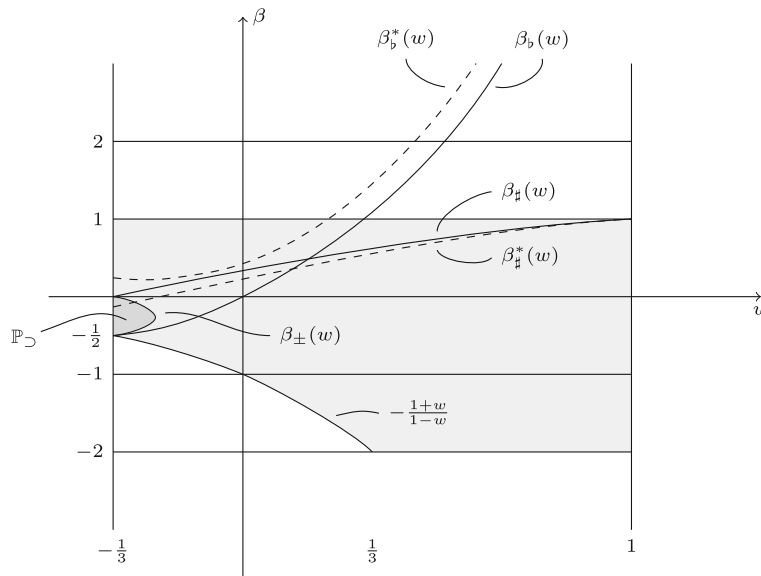


**Fig. 3** The bifurcation diagram in the parameter space  $\mathbb{P}$ . The shaded region (including  $\mathbb{P}_{\supset}$ ) marks the subset for which the energy conditions are satisfied

There are three fixed points in  $\bar{\mathcal{V}}_{\text{VIII}}$ ,  $T := [1, -1]^T$ ,  $Q := [1, 1]^T$  and  $D := [2, 1]^T$ ; cf. Table 1. The eigenvectors and eigenvalues of the linearisation of (8) at the fixed points determine their local stability properties. One finds<sup>4</sup>

$$T : \begin{bmatrix} 6 \\ 12 \end{bmatrix} \begin{bmatrix} 1 & 0 \\ 0 & 1 \end{bmatrix}, \quad Q : \begin{bmatrix} 2 \\ -4 \end{bmatrix} \begin{bmatrix} 1 & 0 \\ 0 & 1 \end{bmatrix} \quad \text{and} \quad D : \begin{bmatrix} -3 \\ -6 \end{bmatrix} \begin{bmatrix} 1 & -2 \\ 0 & 1 \end{bmatrix},$$

so  $T$  is a source,  $Q$  is a saddle repelling in  $H_D$  direction and  $D$  is a sink in  $\bar{\mathcal{V}}_{\text{VIII}}$ .

<sup>4</sup> Here and henceforth the notation follows the pattern  $P : \begin{bmatrix} \lambda_1 \\ \lambda_2 \end{bmatrix} [v_1, v_2]$  where  $\lambda_i$  and  $v_i$  denote the  $i$ th eigenvalue and eigenvector of the linearisation of the dynamical system at  $P$ .



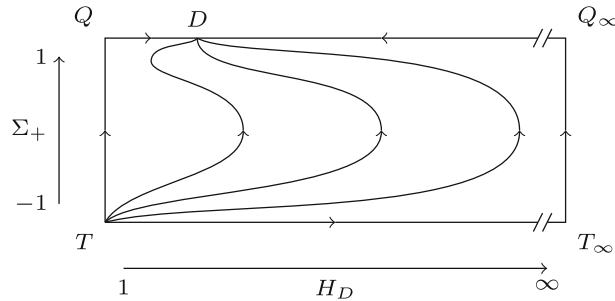


Fig. 4 The flow in  $\bar{\mathcal{V}}_{\text{VIII}}$

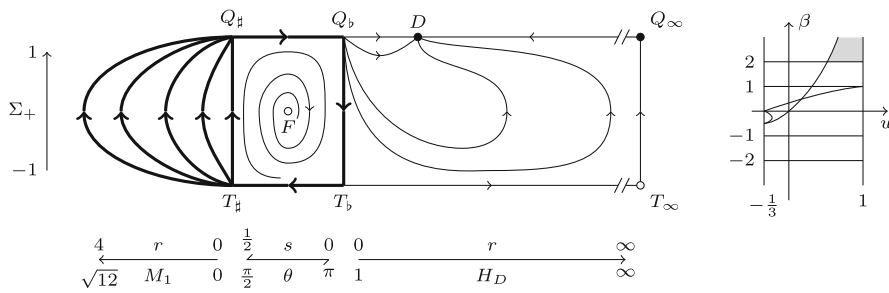


Fig. 5  $\alpha(\gamma) \subseteq \text{network}(T_b, T_\#, Q_\#, Q_b)$ .  $\omega(\gamma) = D$ , possibly  $\partial\mathcal{X}_1$

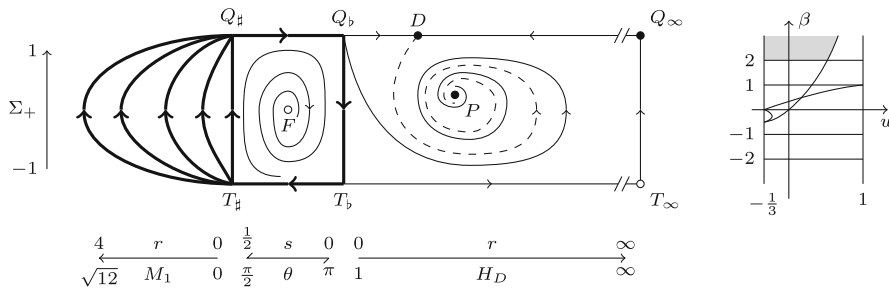
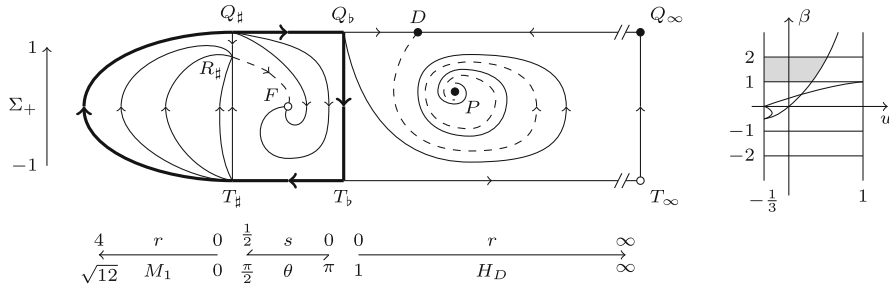


Fig. 6  $\alpha(\gamma) \subseteq \text{network}(T_b, T_\#, Q_\#, Q_b)$ .  $\omega(\gamma) = D$ , possibly  $\partial\mathcal{X}_1$

It is proven in Appendix 6.1 that there are exactly two more fixed points at infinity,  $T_\infty = [\infty, -1]^T$  and  $Q_\infty = [\infty, 1]^T$ . The stability properties then follow directly from (8): First,  $\Sigma'_+ > 0$  in  $\mathcal{V}_{\text{VIII}}$ . Second, for  $H_D > 2$  (and thus at infinity),  $H'_D \leq 0$  for  $\Sigma_+ \leq 0$ . Hence  $T_\infty$  and  $Q_\infty$  play the role of saddles for the flow in  $\bar{\mathcal{V}}_{\text{VIII}}$  given in Fig. 4.

To interpret this as flow in  $\bar{\mathcal{V}}_{\text{VIII}}^y$ , note that the fixed point  $T$  in  $\bar{\mathcal{V}}_{\text{VIII}}$  corresponds to the closure of the line  $T_b \rightarrow T_\#$  in  $\bar{\mathcal{V}}_{\text{VIII}}^y$ . Since  $T_b$  and  $T_\#$  turn out to act as a source and a saddle in  $\bar{\mathcal{V}}_{\text{VIII}}^y$  in all cases respectively, cf. Figs. 5, 6, 7, 8, 9, 10, 11, 12, 13, 14, 15, 16 and 17, the orbits in  $\mathcal{V}_{\text{VIII}}^y$  have the form  $T_b \rightarrow D$ .



**Fig. 7**  $\alpha(\gamma) = \text{cycle}(T_b, T_{\#}, Q_{\#}, Q_b)$ .  $\omega(\gamma) = P$

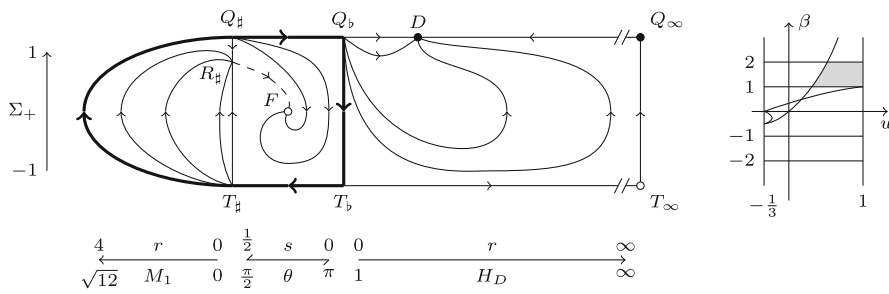


**Fig. 8**  $\alpha(\gamma) = \text{cycle}(T_b, T_{\#}, Q_{\#}, Q_b)$ .  $\omega(\gamma) = D$

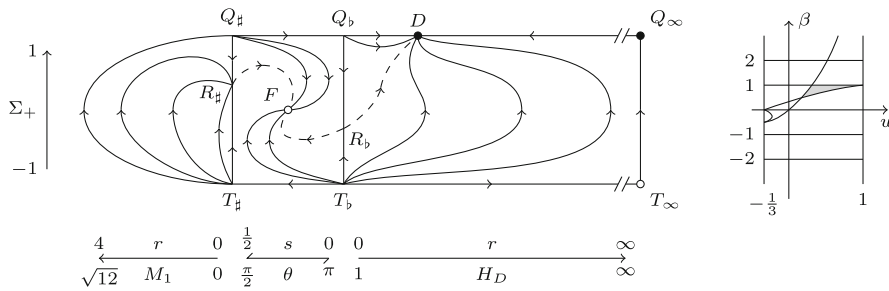


**Fig. 9**  $\alpha(\gamma) = T_b$ .  $\omega(\gamma) = D$

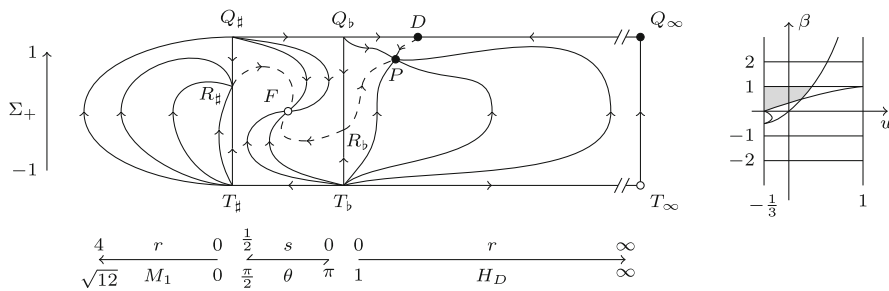


**Fig. 10**  $\alpha(\gamma) = T_b$ .  $\omega(\gamma) = P$

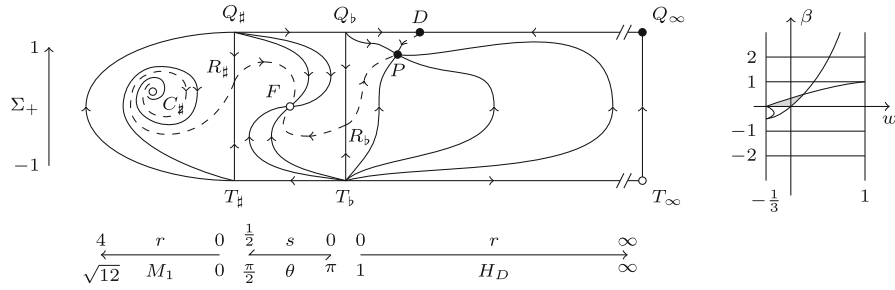


**Fig. 11**  $\alpha(\gamma) = T_b, \omega(\gamma) = P$

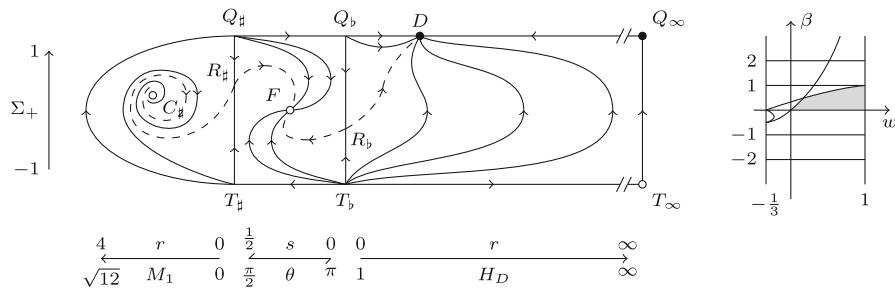


**Fig. 12**  $\alpha(\gamma) = T_b, \omega(\gamma) = D$

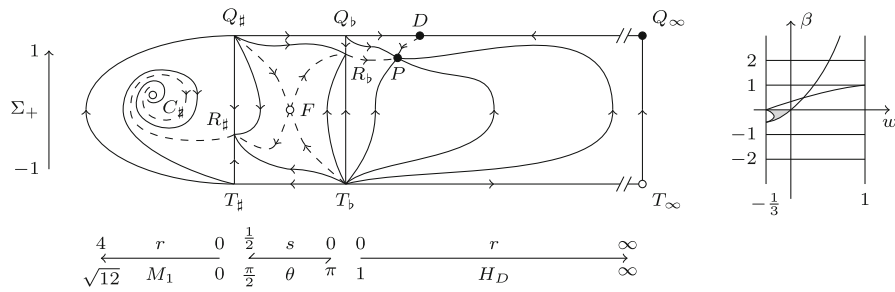


**Fig. 13**  $\alpha(\gamma) = T_b, \omega(\gamma) = P$

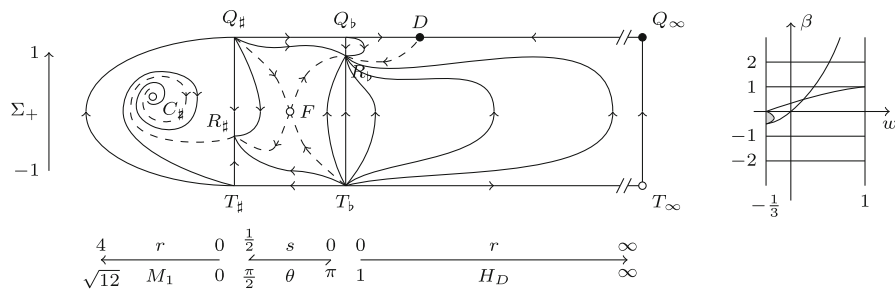


**Fig. 14**  $\alpha(\gamma) = T_b, \omega(\gamma) = R_b$

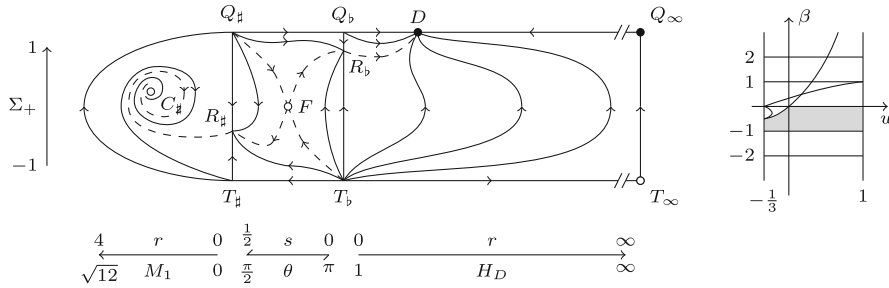


Fig. 15  $\alpha(\gamma) = T_b, \omega(\gamma) = D$

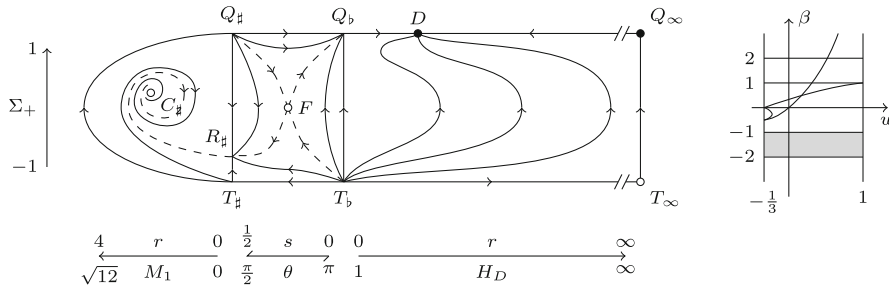


Fig. 16  $\alpha(\gamma) = T_b, \omega(\gamma) = D$

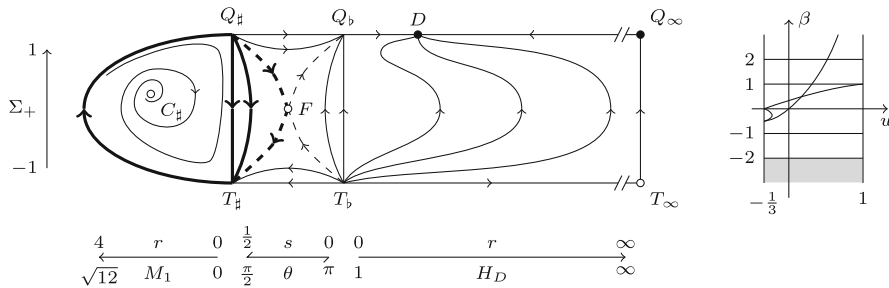


Fig. 17  $\alpha(\gamma) = T_b$ , possibly network( $T_b#, Q_b#, F$ ).  $\omega(\gamma) = D$

### 3.2 Analysis in $\bar{B}_{III}$

The dynamical system in  $\bar{B}_{III}$  is obtained from (2) by setting  $M_1 = 0 (\Leftrightarrow s = 0)$  and using (1):

$$\begin{bmatrix} H_D \\ \Sigma_+ \end{bmatrix}' = \begin{bmatrix} -(1 - H_D^2) (2 - \frac{3}{2}(1 - w)(1 - \Sigma_+^2) - H_D \Sigma_+) \\ -(1 - \Sigma_+^2) ((1 - H_D^2) + \frac{3}{2}(1 - w)(H_D \Sigma_+ + \beta)) \end{bmatrix} =: f(H_D, \Sigma_+) \tag{9}$$

This system has at least three and at most five fixed points in  $\overline{\mathcal{B}}_{\text{III}}$  depending on  $(w, \beta) \in \mathbb{P}$ , namely

$$T_b := \begin{bmatrix} 1 \\ -1 \end{bmatrix}, \quad Q_b := \begin{bmatrix} 1 \\ 1 \end{bmatrix}, \quad D = \begin{bmatrix} 2 \\ 1 \end{bmatrix}, \quad R_b := \begin{bmatrix} 1 \\ -\beta \end{bmatrix} \quad \text{and} \\ P := \begin{bmatrix} \frac{2+3\beta(1-w)}{\sqrt{(1-3w)^2+6\beta(1-w)}} \\ \frac{1+3w}{\sqrt{(1-3w)^2+6\beta(1-w)}} \end{bmatrix};$$

cf. Table 1. Clearly  $R_b$  is a fixed point in  $\overline{\mathcal{B}}_{\text{III}}$  (and different from  $T_b, Q_b$ ) iff  $\beta \in (-1, 1)$ . The conditions  $H_D|_P > 1$  and  $\Sigma_+|_P < 1$  entail that  $P$  is in  $\mathcal{B}_{\text{III}}$  iff  $\beta > \beta_b(w) := \frac{2w}{1-w}$  and  $(w, \beta) \notin \mathbb{P}_{\supset}$ , where  $\mathbb{P}_{\supset}$  refers to the small  $\supset$ -shaped subset of  $\mathbb{P}$  bounded by  $\beta_{\pm}(w) := \frac{-1 \pm \sqrt{-3 + (1-3w)^2}}{3(1-w)}$ ; cf. Fig. 3. Under these conditions the square root in the coordinates of  $P$  is automatically real and  $\Sigma_+|_P > 0$ .

The eigenvectors and eigenvalues of the linearisation  $\text{Df}(H_D, \Sigma_+)$  at  $T_b, Q_b, D$  and  $R_b$  determine their local stability properties. One finds

$$T_b : \begin{bmatrix} 6 \\ 3(1-w)(1-\beta) \end{bmatrix} \begin{bmatrix} 1 & 0 \\ 0 & 1 \end{bmatrix}, \quad D : \begin{bmatrix} -3 \\ 3\beta(1-w) - 6w \end{bmatrix} \begin{bmatrix} 1 & \frac{1-3w}{1-2w+\beta(1-w)} \\ 0 & 1 \end{bmatrix}, \\ Q_b : \begin{bmatrix} 2 \\ 3(1-w)(1+\beta) \end{bmatrix} \begin{bmatrix} 1 & 0 \\ 0 & 1 \end{bmatrix}, \quad R_b : \begin{bmatrix} 3\beta^2(1-w)+1+3w+2\beta \\ -\frac{3}{2}(1-w)(1-\beta^2) \end{bmatrix} \begin{bmatrix} \frac{3\beta^2(1-w)+5+3w+4\beta}{(1-\beta^2)(3\beta(1-w)+4)} & 0 \\ 1 & 1 \end{bmatrix}.$$

Therefore, in  $\overline{\mathcal{B}}_{\text{III}}$ ,  $T_b$  is a source for  $\beta < 1$  and a saddle repelling in  $H_D$  direction for  $\beta > 1$ ,  $Q_b$  is a saddle repelling in  $H_D$  direction for  $\beta < -1$  and a source for  $\beta > -1$ ,  $D$  is a sink for  $\beta < \beta_b(w)$  and a saddle attracting in  $H_D$  direction for  $\beta > \beta_b(w)$  and  $R_b$  is a sink  $\forall (w, \beta) \in \mathbb{P}_{\supset}$  and a saddle attracting in  $\Sigma_+$  direction  $\forall (w, -1 < \beta < 1) \in \mathbb{P} \setminus \mathbb{P}_{\supset}$ .

The eigenvalues  $\lambda_{\pm}$  of  $\text{Df}|_P$  are given in terms of trace and determinant by

$$2\lambda_{\pm} = \text{tr Df}|_P \pm \sqrt{(\text{tr Df}|_P)^2 - 4 \det \text{Df}|_P}, \quad (10)$$

where

$$\det \text{Df}|_P = \frac{9(1-w)(3\beta^2(1-w) + 1 + 3w + 2\beta)(\beta(1-w) - 2w)}{(1-3w)^2 + 6\beta(1-w)}, \quad (11)$$

$$\text{tr Df}|_P = -\frac{3(1-w)(1+2\beta)}{\sqrt{(1-3w)^2 + 6\beta(1-w)}}, \quad (12)$$

which are real whenever  $P$  exists in  $\mathcal{B}_{\text{III}}$  because the square root in (12) appears in the coordinates of  $P$  as well. Further,  $\text{tr Df}|_P < 0$  and  $\det \text{Df}|_P > 0$  whenever  $P$  is

in  $\mathcal{B}_{\text{III}}$ .<sup>5</sup> Hence the real part of (10) is always negative, whether the eigenvalues are real or complex, so  $P$  is a sink in  $\mathcal{B}_{\text{III}}$  whenever present. The eigenvalues are real for  $\beta \in (\beta_b(w), \beta_b^*(w)]$ ; cf. Fig. 3.

In order to perform the analysis of the flow in the full state space  $\mathcal{X}_{\text{VIII}}$  in Sect. 3.5, it is also necessary to know the local stability of  $P$  in the direction of  $M_1$ . From (2) one has  $(\ln M_1)'|_P = -3\Sigma_+|_P$ , which is negative so that  $P$  is attracting in the direction of  $M_1$ . This implies that  $P$  is a local sink in  $\overline{\mathcal{X}}_{\text{VIII}}$ .

It is shown in Appendix 6.1 that there are exactly two more fixed points at infinity,  $T_\infty = [\infty, -1]^T$  and  $Q_\infty = [\infty, 1]^T$ . Their stability properties then follow straightforwardly from (9). For  $H_D$  sufficiently large,  $f(H_D, \Sigma_+) \approx [-H_D^3\Sigma_+, H_D^2(1 - \Sigma_+^2)]^T$ . Hence,  $\Sigma'_+ > 0$  and  $H'_D \gtrless 0$  for  $\Sigma_+ \lesseqgtr 0$ , which implies that  $T_\infty$  and  $Q_\infty$  play the role of saddles for the flow in  $\overline{\mathcal{B}}_{\text{III}}$ .

For the cases where  $P$  does not exist in  $\mathcal{B}_{\text{III}}$ , the information suffices to draw the corresponding qualitative flow diagrams. When  $P$  exists in  $\mathcal{B}_{\text{III}}$ , periodic orbits encircling this fixed point could in principle be present. However numeric investigations strongly suggest that this is not the case. In any case, the main results of this paper are not affected by this open question; cf. Sect. 4.

The resulting qualitative dynamics in  $\overline{\mathcal{B}}_{\text{III}}$  in dependence of  $(w, \beta) \in \mathbb{P}$  is depicted in Figs. 5, 6, 7, 8, 9, 10, 11, 12, 13, 14, 15, 16 and 17 as flows in  $\overline{\mathcal{B}}_{\text{III}}^{\mathcal{Y}}$  together with the flows in  $\overline{\mathcal{S}}_{\sharp}^{\mathcal{Y}}$  and  $\overline{\mathcal{X}}_1$ . The latter two subsets will be discussed next.

### 3.3 Analysis in $\overline{\mathcal{S}}_{\sharp}$

$\overline{\mathcal{S}}_{\sharp}$  is the common boundary of the state spaces  $\mathcal{X}_{\text{VIII}}$  and  $\mathcal{X}_{\text{IX}}$  of LRS types VIII and IX. It has been analysed in detail in [3, section 10.1]. The bifurcation lines  $\beta = \pm 2$ ,  $\beta_{\sharp}(w)$  and  $\beta_{\sharp}^*(w)$  result from this analysis. The former correspond to the local stability properties of the fixed point  $R_{\sharp}$ , and the latter two to those of  $C_{\sharp}$ ; cf. Table 1. The results are depicted in Sect. 4 as flows in  $\overline{\mathcal{S}}_{\sharp}^{\mathcal{Y}}$  together with the flows in  $\overline{\mathcal{B}}_{\text{III}}^{\mathcal{Y}}$  and  $\overline{\mathcal{X}}_1$ .

### 3.4 Analysis in $\overline{\mathcal{X}}_1$

The flow in  $\overline{\mathcal{X}}_1$  has been analysed in detail in [3, section 10.2]. The only new bifurcation line in Fig. 3 resulting from this analysis is  $\beta = 0$  which corresponds to the local stability properties of the Friedmann point  $F$ ; cf. Table 1. However the qualitative dynamics in  $\overline{\mathcal{X}}_1$  is also associated with the bifurcation lines  $\beta = \pm 1$  and  $\beta = \pm 2$ . The results are depicted in Sect. 4 together with the flows in  $\overline{\mathcal{B}}_{\text{III}}^{\mathcal{Y}}$  and  $\overline{\mathcal{S}}_{\sharp}^{\mathcal{Y}}$ .

<sup>5</sup> To see the first inequality, note from Fig. 3 that  $\beta > -\frac{1}{2}$  when  $P$  is in  $\mathcal{B}_{\text{III}}$ . To see the second inequality, note that setting the middle and last factor in the numerator of (11) to zero corresponds to the bifurcation line  $\beta_{\pm}(w)$  and  $\beta_b(w)$ , respectively.

### 3.5 Analysis in $\bar{\mathcal{X}}_{\text{VIII}}$ and $\bar{\mathcal{S}}_{\infty}$

The full system (2) does not have any fixed points in  $\mathcal{X}_{\text{VIII}}$ . Furthermore, as shown in Appendix 6.2 there are only the already known fixed points  $T_{\infty} = [\infty, -1, 0]^T$  and  $Q_{\infty} = [\infty, 1, 0]^T$  at infinity. Their stability properties then follow straightforwardly from (2): For  $H_D$  sufficiently large,  $\text{rhs}(2) \approx [-H_D^3 \Sigma_+, H_D^2(1 - \Sigma_+^2), -H_D^2 \Sigma_+ M_1]^T$ . Hence  $\Sigma'_+ > 0$ ,  $H'_D \gtrless 0$  for  $\Sigma_+ \lesseqgtr 0$  and  $M'_1 \gtrless 0$  for  $\Sigma_+ \lesseqgtr 0$ , which implies that  $T_{\infty}$  and  $Q_{\infty}$  play the role of saddles for the flow in  $\bar{\mathcal{X}}_{\text{VIII}}$ . Viewing infinity as the boundary  $\bar{\mathcal{S}}_{\infty}$  in a compactified version of the state space,  $T_{\infty}$  is a source and  $Q_{\infty}$  is a sink in  $\bar{\mathcal{S}}_{\infty}$ , hence all orbits in  $\bar{\mathcal{S}}_{\infty}$  are of the form  $T_{\infty} \rightarrow Q_{\infty}$ .

An important consequence is that there is no orbit in  $\mathcal{X}_{\text{VIII}}$  that emanates from or escapes to infinity. Hence each orbit in  $\mathcal{X}_{\text{VIII}}$  lies in a compact subset. The following lemma concludes this section. It will also be used to localise the  $\alpha$ - and  $\omega$ -limit sets [7, p. 99 Def 4.12] in the next section; cf. [7, p. 91 Def 4.7] for the term ‘invariant set’:

**Lemma 1** *Let  $\gamma$  be an orbit in  $\mathcal{Y}_{\text{VIII}}$ . Then both,  $\alpha(\gamma)$  and  $\omega(\gamma)$ , is a non-empty, compact and connected invariant subset of  $\bar{\mathcal{Y}}_{\text{VIII}}$ . Furthermore,  $\alpha(\gamma) \subseteq \bar{\mathcal{S}}_{\sharp}^{\mathcal{Y}} \cup \bar{\mathcal{X}}_1$  and  $\omega(\gamma) \subseteq \bar{\mathcal{B}}_{\text{III}}^{\mathcal{Y}} \cup \bar{\mathcal{X}}_1$ .*

*Proof* First, since each orbit in  $\mathcal{X}_{\text{VIII}}$  lies in a compact subset, so does by (5) each orbit in  $\mathcal{Y}_{\text{VIII}}$ . The first statement of the lemma then follows from [7, p. 99 Thm 4.9].

Second, consider the function  $Z_5 : \mathcal{X}_{\text{VIII}} \cup \mathcal{Y}_{\text{VIII}} \rightarrow \mathbb{R}$  given by

$$Z_5 := \frac{H_D M_1^{\frac{1}{3}}}{(H_D^2 - 1)^{\frac{2}{3}}} > 0 \quad \text{with} \quad Z'_5 = -\frac{4\Sigma_+ + (1 + 3w)\Omega}{2H_D} Z_5 \leq 0.$$

One can check that  $Z''_5|_{\Sigma_+=\Omega=0} = 0$  and  $Z'''_5|_{\Sigma_+=\Omega=0} < 0$  in  $\mathcal{X}_{\text{VIII}}$ , which means that  $Z_5$  is strictly monotonically decreasing along the flow in  $\mathcal{X}_{\text{VIII}}$ . Hence the monotonicity principle [7, p. 103 Thm 4.12] implies that the limit sets lie in  $\bar{\mathcal{B}}_{\text{III}} \cup \bar{\mathcal{S}}_{\sharp}$ . Moreover, since  $Z_5 \rightarrow 0 = \inf(Z_5)$  when one approaches  $\bar{\mathcal{B}}_{\text{III}}$  and  $Z_5 \rightarrow \infty = \sup(Z_5)$  when one approaches  $\bar{\mathcal{S}}_{\sharp}$ , the monotonicity principle implies  $\alpha(\tilde{\gamma}) \subseteq \bar{\mathcal{S}}_{\sharp}$  and  $\omega(\tilde{\gamma}) \subseteq \bar{\mathcal{B}}_{\text{III}}$  for all orbits  $\tilde{\gamma}$  in  $\mathcal{X}_{\text{VIII}}$ . In the context of  $\mathcal{Y}_{\text{VIII}}$  this means that  $\alpha(\gamma) \subseteq \bar{\mathcal{S}}_{\sharp}^{\mathcal{Y}} \cup \bar{\mathcal{X}}_1$  and  $\omega(\gamma) \subseteq \bar{\mathcal{B}}_{\text{III}}^{\mathcal{Y}} \cup \bar{\mathcal{X}}_1$ ; cf. (6).  $\square$

## 4 Results and discussion

Finally all information obtained in Sect. 3 can be collected to identify the  $\alpha$ - and  $\omega$ -limit sets of generic orbits  $\gamma \in \mathcal{Y}_{\text{VIII}}$ , and hence the past and future asymptotic dynamics of generic LRS Bianchi type VIII cosmologies, for all qualitatively different anisotropic matter cases:

#### 4.1 Identification of the limit sets

Figure 3 shows that there are 13 qualitatively different cases.<sup>6</sup> These cases are listed in Figs. 5, 6, 7, 8, 9, 10, 11, 12, 13, 14, 15, 16 and 17, which show, for each case, a plot of the bifurcation diagram where the corresponding subset of  $\mathbb{P}$  is shaded and a representative flow diagram in the set  $\overline{\mathcal{S}}_{\sharp}^{\mathcal{Y}} \cup \overline{\mathcal{X}}_1 \cup \overline{\mathcal{B}}_{\text{III}}^{\mathcal{Y}}$ , on which the limit sets lie by Lemma 1. Solid (dashed) lines represent generic (non-generic) orbits in the respective boundary subset. A filled (empty) circle on a fixed point indicates that it attracts (repels) orbits in the respective orthogonal direction.<sup>7</sup> Heteroclinic cycles and networks are represented by thick lines. The axes with two labels emphasise the diffeomorphisms (7) and the bijection between  $s$  and  $\theta$ ; cf. Sect. 2.4.

By Lemma 1, the limit sets are non-empty, compact and connected invariant subsets of  $\overline{\mathcal{Y}}_{\text{VIII}}^{\mathcal{Y}}$ . This leaves fixed points, heteroclinic cycles and heteroclinic networks as candidates for the limit sets in Figs. 5, 6, 7, 8, 9, 10, 11, 12, 13, 14, 15, 16 and 17.

A single fixed point is an ( $\alpha$ -)  $\omega$ -limit set of generic orbits  $\gamma \in \mathcal{Y}_{\text{VIII}}$  iff it (repels) attracts orbits from a three dimensional neighbourhood in  $\mathcal{Y}_{\text{VIII}}$ ; e.g. a (source) sink. These can easily be identified from the figures. In the cases of Figs. 9, 10, 11, 12, 13, 14, 15, and 16, fixed points are the only possible generic limit sets. Furthermore, these cases exhibit just one source and sink respectively, which implies that these are the past/future attractors [7, p. 100 Def 4.13].

Figures 5, 6, 7, 8 and 17 show a heteroclinic cycle or network each, and hence additional candidates for limit sets. In Figs. 7 and 8 the cycle is the past attractor since there is no other candidate for a generic  $\alpha$ -limit set in  $\overline{\mathcal{S}}_{\sharp}^{\mathcal{Y}} \cup \overline{\mathcal{X}}_1$ , and as proven in Sect. 3.5  $\alpha(\gamma)$  is non-empty. Note that since the cycle is not in  $\overline{\mathcal{B}}_{\text{III}}^{\mathcal{Y}} \cup \overline{\mathcal{X}}_1$  it cannot be an  $\omega$ -limit set. The same line of arguments shows that in Figs. 5 and 6 the past attractor is a subset of the heteroclinic network.

In Fig. 17, the heteroclinic network could be an  $\alpha$ -limit set in addition to  $T_b$ . Analogously, in Figs. 5 and 6, the heteroclinic cycle  $\partial\mathcal{X}_1$  could be an  $\omega$ -limit set in addition to  $D$  and  $P$ , respectively. The nontrivial task of directly tackling the stability properties of these structures is omitted here. They are however taken into account as further candidates for generic limit sets in these three cases. Note that Fig. 17 is the only one of these three cases where the energy conditions can be satisfied; cf. Sect. 2.1 and Fig. 3.

#### 4.2 The main results

Finally one arrives at the main theorem and its corollaries:

**Theorem 1** *The  $\alpha$ - and  $\omega$ -limit sets of generic orbits  $\gamma \in \mathcal{Y}_{\text{VIII}}$  of the dynamical system (2) with parameters  $(w, \beta) \in \mathbb{P}$ , is given as stated in the captions of Figs. 5, 6,*

<sup>6</sup> The bifurcation lines  $\beta_b^*(w)$  and  $\beta_{\sharp}^*(w)$  only specify if the fixed points  $C_{\sharp}$  and  $P$  are local stable nodes or foci in  $\mathcal{S}_{\sharp}^{\mathcal{Y}}$  and  $\mathcal{B}_{\text{III}}^{\mathcal{Y}}$  respectively, which is irrelevant for identifying the limit sets.

<sup>7</sup> The colour coding of  $T_{\infty}$  and  $Q_{\infty}$  makes only sense in the context of  $\mathcal{X}_{\text{VIII}}$ . The fixed points in  $\partial\mathcal{X}_1$  are not colour coded since the orthogonal directions are represented in the figures.



7, 8, 9, 10, 11, 12, 13, 14, 15, 16 and 17. These describe the past and future asymptotic dynamics of LRS Bianchi type VIII cosmologies with anisotropic matter of the family defined in Sect. 2.1.

*Proof* Cf. Sect. 4.1. □

**Vacuum and perfect fluid cases** *LRS Bianchi type VIII vacuum solutions are past asymptotic to  $T_b$  and future asymptotic to  $D$ .*

*Generic LRS Bianchi type VIII solutions with a non-tilted perfect fluid where  $p = w\rho$  and  $w \in (-\frac{1}{3}, 1)$  are past asymptotic to  $T_b$ , future asymptotic to  $P$  for  $w \in (-\frac{1}{3}, 0)$  and to  $D$  for  $w \in [0, 1)$ .*

The vacuum part follows from Sect. 3.1; cf. Fig. 4. For the perfect fluid cases, recall from Sect. 2.1 that they correspond to the line  $\beta = 0$  in  $\mathbb{P}$ . They are therefore contained in Theorem 1 as special cases.<sup>8</sup> The only bifurcation line intersecting  $\beta = 0$  is  $\beta_b(w)$  at  $w = 0$  which yields the two qualitatively different perfect fluid cases, see Figs. 12 and 13, respectively. The statement on the future asymptotics for  $w \in (-\frac{1}{3}, 0)$  might fill a little gap in the literature. The other results are known: The past asymptotics has been given in [9, table 4 and figure 4], the future asymptotics for vacuum in [10, Prop 8.1] and the future asymptotics for perfect fluids with  $w \in [0, 1)$  in [11, Thm 3.1].

Comparison of the vacuum and perfect fluid cases with all cases of Theorem 1 shows that the dynamics with anisotropic matter differs from the vacuum and perfect fluid cases in Figs. 5, 6, 7, 8, 14 and perhaps 17. More precisely, the past asymptotic dynamics differs in all cases where  $\beta \geq 1$ , i.e. in the cases of Figs. 5, 6, 7 and 8. Additionally, depending on whether or not the heteroclinic network in Fig. 17 is a generic  $\alpha$ -limit set, the past asymptotics could also differ in the case when  $\beta \leq -2$ ; cf. the discussion at the end of Sect. 4.1. The future asymptotic dynamics differs when  $(w, \beta) \in \mathbb{P}_\triangleright$ , i.e. in the case of Fig. 14. Additionally, depending on whether or not the heteroclinic cycle  $\partial\mathcal{X}_1$  in Figs. 5 and 6 is a generic  $\omega$ -limit set, the future asymptotics could also differ in the cases when  $\beta \geq 2$ ; cf. the discussion at the end of Sect. 4.1. The strongest implications of this represent the main results of this paper stated in the following corollaries:

**Corollary 1** (past asymptotics) *The past asymptotic dynamics of generic LRS Bianchi type VIII cosmologies with anisotropic matter can differ significantly from that of the vacuum and perfect fluid cases. In particular, the approach to the initial singularity is oscillatory in the cases depicted in Figs. 5, 6, 7 and 8.*

**Corollary 2** (future asymptotics) *The future asymptotic dynamics of generic LRS Bianchi type VIII cosmologies with anisotropic matter can differ significantly from that of the vacuum and perfect fluid cases. Note in particular the case depicted in Fig. 14.*

For completeness it is necessary to elaborate on the remark at the end of Sect. 3.2 concerning the possible occurrence of periodic orbits around  $P$  in  $\mathcal{B}_{\text{III}}^\triangleright$ : such orbits are not observed numerically. However, their occurrence could change certain details

<sup>8</sup> The fact that  $\beta = 0$  is itself a bifurcation line, which is related to the stability of the Friedmann point, is not relevant for the asymptotic dynamics.

in Theorem 1, adding further  $\omega$ -limit candidates in the cases where  $P$  is in  $\mathcal{B}_{\text{III}}^{\mathcal{Y}}$ . On the other hand, Corollary 1 would be completely untouched and Corollary 2 even strengthened by the occurrence of such periodic orbits.

#### 4.3 Physical interpretation of the results

An interesting observation is that there is a neighbourhood of the line  $\beta = 0$  in  $\mathbb{P}$  for which the corresponding asymptotic dynamics is identical to that of the perfect fluid cases. Hence the perfect fluid solutions are robust under small perturbations of a vanishing anisotropy parameter. For the past asymptotics to differ from that,  $\beta$  even needs to be so high that the dominant energy condition is only marginally satisfied.

The specialisation of the results to the cases for which the energy conditions are satisfied is obtained by restricting  $\beta$  to  $[\max(-2, -\frac{1+w}{1-w}), 1]$ ; cf. Sect. 2.1. This corresponds to the shaded region in Fig. 3, and thus rules out the cases of Figs. 5 and 6. All other cases contain values  $(w, \beta)$  for which the energy conditions are satisfied.

However, it should be pointed out that the cases represented by Figs. 7 and 8 only satisfy the energy conditions for  $\beta = 1$ , and the case of Fig. 17 only for  $w \geq \frac{1}{3}$  and  $\beta = -2$ , i.e. for  $(w, \beta)$  in one-dimensional subsets of  $\mathbb{P}$  for which the dominant energy condition is only marginally satisfied. Consequently, in these cases the energy flow is necessarily lightlike asymptotically toward the singularity. A special example is given by collisionless (Vlasov) matter with massless particles, which as shown in [3, section 12.1] falls into the class of matter models with  $(w, \beta) = (\frac{1}{3}, 1)$ .

In any case, the statements of Corollaries 1 and 2 remain true under the restriction to matter satisfying the energy conditions.

This concludes the main results on the anisotropic matter analysis. Section 5 is concerned with an extension of the present formalism to treat LRS type VIII dynamics with Vlasov matter with massive particles, which does not a priori fit into the anisotropic matter family considered so far.

### 5 Extension of the formalism to treat Vlasov matter dynamics with massive particles

It was stated in Sect. 4.3 that Vlasov matter with massless particles falls into the class of matter models described in Sect. 2.1 with parameters  $(w, \beta) = (\frac{1}{3}, 1)$ . This is shown in [3, section 12.1]. However, as stated there, for Vlasov matter with massive particles the relation  $p = w\rho$  is non-linear. In [4], Calogero and Heinzle extended their formalism to treat Vlasov matter dynamics with massive particles in the case of LRS type IX. Since types VIII and IX are analogous in this formulation, and in particular share the same evolution equations, this extension of the formalism can be adopted to LRS type VIII without difficulties:

Following [4, section 3], the dynamical system representing the LRS type VIII Einstein-Vlasov system is given by the system (2) and the additional equation

$$l' = 2H_D l(1 - l). \quad (13)$$

The additional variable  $l := \frac{(\det g)^{1/3}}{1+(\det g)^{1/3}} \in (0, 1)$  corresponds to a length scale of the spatial metric. The rescaled principal pressures are functions of  $l$  and  $s$ . Their full expressions are given in [4, Eq. 13] from which it follows that

$$(w, \beta)|_{l=0} = \left(\frac{1}{3}, 1\right) \quad \text{and} \quad (w, \beta)|_{l=1} = (0, 0). \quad (14)$$

The LRS type VIII state space for Vlasov matter dynamics is given by  $\mathcal{X}_{\text{VIII}} \times (0, 1)$ .

The dynamical system can be analysed as follows: By (13),  $l$  is strictly monotonically increasing along orbits in  $\mathcal{X}_{\text{VIII}} \times (0, 1)$ . The monotonicity principle thus implies that  $\alpha(\gamma) \subseteq \overline{\mathcal{X}_{\text{VIII}}} \times \{0\}$  and  $\omega(\gamma) \subseteq \overline{\mathcal{X}_{\text{VIII}}} \times \{1\}$ .<sup>9</sup> Hence, the search for the limit sets can be restricted to these boundary subsets:

From (14), the flow in  $\overline{\mathcal{X}_{\text{VIII}}} \times \{0\}$  is equivalent to the flow for anisotropic matter with parameters  $(\frac{1}{3}, 1)$ ; cf. Fig. 8. Hence the cycle  $(T_b, T_{\sharp}, Q_{\sharp}, Q_b)$  is the past attractor of the flow in  $\mathcal{X}_{\text{VIII}} \times (0, 1)$ , since this cycle is the only candidate for an  $\alpha$ -limit set for generic orbits. Also from (14), the flow in  $\overline{\mathcal{X}_{\text{VIII}}} \times \{1\}$  is equivalent to the flow for anisotropic matter with parameters  $(0, 0)$ , i.e. to that for dust; cf. Fig. 12. Hence  $D$  is the future attractor of the flow in  $\mathcal{X}_{\text{VIII}} \times (0, 1)$ , since this fixed point is the only candidate for an  $\omega$ -limit set for generic orbits.

$l = 0$  corresponds to Vlasov dynamics with massless particles; cf. [4, section 3]. Hence the result states that Vlasov matter with massive particles behaves like Vlasov matter with massless particles asymptotically to the past, and like dust asymptotically to the future. This thereby also completes the results of [5] regarding the forever expanding Einstein-Vlasov LRS Bianchi models.

**Acknowledgements** First and foremost, I am grateful to J. Mark Heinzle who suggested this topic to me and provided guidance during the whole project. I am also thankful for the discussions I had with S. Calogero and C. Uggla during the workshop ‘Dynamics of General Relativity’ at the Erwin Schrödinger Institute for Mathematical Physics in Vienna in summer 2011.

## 6 Appendix: fixed points at infinity

To find the fixed points of (2), (8) and (9) at infinity, a method presented in [12, 3.10] is adopted in a slightly modified way:

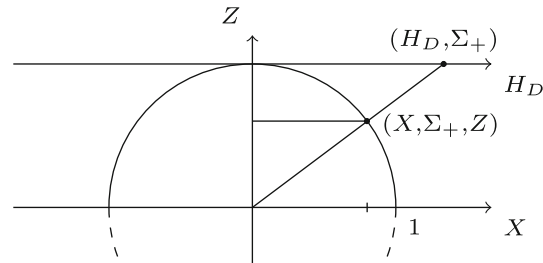
### 6.1 In two dimensions

Consider a two-dimensional system

$$\begin{bmatrix} H_D \\ \Sigma_+ \end{bmatrix}' = \begin{bmatrix} P(H_D, \Sigma_+) \\ Q(H_D, \Sigma_+) \end{bmatrix}$$

<sup>9</sup> One can use the same arguments as in Sect. 3.5 and Appendix 6 for each  $l = \text{const}$  hypersurface to prove that all orbits can be trapped in a compact subset of  $\mathbb{R}^4$ .

**Fig. 18** Projection onto the ‘Poincaré cylinder’



where  $P$  and  $Q$  are polynomials of degree  $n$  and  $m$  in  $H_D$  respectively, satisfying  $n \leq m + 1$ . One can write this system as

$$Q(H_D, \Sigma_+)dH_D - P(H_D, \Sigma_+)d\Sigma_+ = 0, \quad (15)$$

where however the information about the direction of the flow is lost. Next the  $H_D$  coordinate is formally compactified by projecting the state space onto the ‘Poincaré cylinder’ as depicted in Fig. 18. The corresponding coordinate transformation  $(H_D, \Sigma_+) \rightarrow (X, \Sigma_+, Z) : X^2 + Z^2 = 1$  is given by  $H_D = \frac{X}{Z}$ . Applying this to (15) and multiplying by  $Z^{m+2}$  yields

$$Z^{m+1}Q(X/Z, \Sigma_+)dX - Z^{m+2}P(X/Z, \Sigma_+)d\Sigma_+ - XZ^mQ(X/Z, \Sigma_+)dZ = 0, \quad (16)$$

which defines a flow on the ‘Poincaré cylinder’; cf. [12, p. 267]. Points at infinity in the original state space correspond to points on the ‘equator’  $X = 1, Z = 0$  on the ‘Poincaré cylinder’. Furthermore, evaluating (16) with  $X = 1, Z = 0$  gives the flow on the ‘equator’, which corresponds to the flow at infinity,

$$(Z^m Q(X/Z, \Sigma_+))|_{X=1, Z=0}dZ = 0. \quad (17)$$

Note that the first two terms of (16) vanish since they are at least proportional to  $Z$ . This is not true however for the third term of (16). From (17), for  $(Z^m Q)|_{X=1, Z=0} \neq 0$  it follows that  $dZ = 0$ , which corresponds to trajectories through a regular point on the ‘equator’, where the sign of  $(Z^m Q)|_{X=1, Z=0}$  determines the flow direction. Fixed points on the ‘equator’ correspond to solutions of  $(Z^m Q)|_{X=1, Z=0} = 0$ ; cf. [12, p. 268 Thm 1]. Solving this equation for  $Q$  in the context of (8) and (9) yields  $\Sigma_+ = \pm 1$  for the fixed points at infinity in  $\mathcal{V}_{\text{VII}}$  and  $\mathcal{B}_{\text{III}}$  respectively, i.e.  $T_\infty := [\infty, -1]^T$  and  $Q_\infty := [\infty, 1]^T$ .

## 6.2 In three dimensions

The generalisation to three or more dimensions is straightforward; cf. [12, p. 277 ff]. Consider a three dimensional system

$$\begin{bmatrix} H_D \\ \Sigma_+ \\ M_1 \end{bmatrix}' = \begin{bmatrix} P(H_D, \Sigma_+, M_1) \\ Q(H_D, \Sigma_+, M_1) \\ R(H_D, \Sigma_+, M_1) \end{bmatrix}$$

where  $P$ ,  $Q$  and  $R$  are polynomials of degree  $l$ ,  $n$  and  $m$  in  $H_D$  respectively, satisfying  $n + 1 \geq l \leq m + 1$ . One can write this system as

$$\begin{aligned} Q(H_D, \Sigma_+, M_1)dH_D - P(H_D, \Sigma_+, M_1)d\Sigma_+ &= 0 \\ R(H_D, \Sigma_+, M_1)dH_D - P(H_D, \Sigma_+, M_1)dM_1 &= 0, \end{aligned} \quad (18)$$

where however the information about the direction of the flow is lost. Again the  $H_D$  coordinate is formally compactified by means of a projection on the ‘Poincaré cylinder’, i.e. by a coordinate transformation  $(H_D, \Sigma_+, M_1) \rightarrow (X, \Sigma_+, M_1, Z) : X^2 + Z^2 = 1$  given by  $H_D = \frac{X}{Z}$ . Applying this to (18), multiplying by  $Z^{m+2}$  and  $Z^{n+2}$  respectively and evaluating the resulting expressions at the ‘equator’  $X = 1, Z = 0$  yields

$$\begin{aligned} (Z^m Q(X/Z, \Sigma_+, M_1))|_{X=1, Z=0} dZ &= 0 \\ (Z^n R(X/Z, \Sigma_+, M_1))|_{X=1, Z=0} dZ &= 0. \end{aligned}$$

Trajectories through a regular point on the ‘equator’ corresponds to  $dZ = 0$ , where the flow direction is determined by the signs of  $(Z^m Q(X/Z, \Sigma_+, M_1))|_{X=1, Z=0}$  and  $(Z^n R(X/Z, \Sigma_+, M_1))|_{X=1, Z=0}$ . Fixed points on the ‘equator’ correspond to solutions of the system of equations  $\{(Z^m Q)|_{X=1, Z=0} = 0, (Z^n R)|_{X=1, Z=0} = 0\}$ . Solving this for  $Q$  and  $R$  in the context of (2) yields  $\Sigma_+ = \pm 1, M_1 = 0$  for the fixed points at infinity in  $\mathcal{X}_{\text{VIII}}$ , i.e.  $T_\infty := [\infty, -1, 0]^T$  and  $Q_\infty := [\infty, 1, 0]^T$ .

## References

1. Heinzle, J.M., Uggla, C., Röhr, N.: The cosmological billiard attractor. *Adv. Theor. Math. Phys.* **13**(2), 293–407 (2009). International Press. Preprint: arXiv:gr-qc/0702141v1
2. Calogero, S., Heinzle, J.M.: Dynamics of Bianchi type I solutions of the Einstein equations with anisotropic matter. *Annales Henri Poincaré* **10**(2), 225–274 (2009). Springer-Verlag/Birkhäuser Science. Preprint: arXiv:0809.1008v2 [gr-qc]
3. Calogero, S., Heinzle, J.M.: Bianchi cosmologies with anisotropic matter: locally rotationally symmetric models. *Phys. D. Nonlinear Phenom.* **240**(7), 636–669 (2010). Elsevier. Preprint: arXiv:0911.0667v1 [gr-qc]
4. Calogero, S., Heinzle, J.M.: Oscillations toward the singularity of locally rotationally symmetric Bianchi type IX cosmological models with Vlasov matter. *SIAM J. Appl. Dyn. Syst.* **9**(4), 1244–1262 (2010). Society for Industrial and Applied Mathematics. Preprint: arXiv:1011.3982v1 [gr-qc]
5. Rendall, A.D., Uggla, C.: Dynamics of spatially homogeneous locally rotationally symmetric solutions of the Einstein Vlasov equations. *Class. Quantum Gravity* **17**(22), 4697–4713 (2000). Institute of Physics Publishing. Preprint: arXiv:gr-qc/0005116v1
6. Wald, R.M.: *General Relativity*. The University of Chicago Press, Chicago (1984)
7. Wainwright, J., Ellis, G.F.R. (eds.): *Dynamical Systems in Cosmology*. Cambridge University Press, Cambridge (1997)
8. Heinzle, J.M., Röhr, N., Uggla, C.: Matter and dynamics in closed cosmologies. *Phys. Rev. D.* **71**(8), 083506-1–083506-17 (2005). American Physical Society. Preprint: arXiv:gr-qc/0406072v1
9. Wainwright, J., Hsu, L.: A dynamical systems approach to Bianchi cosmologies: orthogonal models of class A. *Class. Quantum Gravity* **6**(10), 1409–1431 (1989). Institute of Physics Publishing
10. Ringström, H.: The future asymptotics of Bianchi VIII vacuum solutions. *Class. Quantum Gravity* **18**(18), 3791–3823 (2001). Institute of Physics Publishing. Preprint: arXiv:gr-qc/0103107v1

- 
11. Horwood, J.T., Hancock, M.J., The, D., Wainwright, J.: Late-time asymptotic dynamics of Bianchi VIII cosmologies. *Class. Quantum Gravity* **20**(9), 1757–1777 (2003). Institute of Physics Publishing. Preprint: arXiv:gr-qc/0210031v2
  12. Perko, L.: *Differential Equations and Dynamical Systems*, second edition. Texts in applied Mathematics **7**. Springer, Berlin (1996)

## Part 3

# Plotting interactive flow diagrams with Maple

### **Remark**

This part is supplemented by a Maple document with the same content as presented here and working examples. It is available online; [1]. The document was written in Maple 15. The compatibility with other Maple versions cannot be guaranteed.



## Some basic Maple

This chapter serves as a short introduction to the computer algebra system Maple with a focus on the commands and features that are needed to create interactive flow diagrams, which is then the subject of chapter 7. Section 1 serves to get familiar with the Maple surface. After a discussion of some Maple commands in section 2, section 3 discusses the use of the basic tools to create interactive features in Maple documents, embedded components.

### 1. The Maple surface

Figure 10 shows the Maple surface with an open document which is displayed in the main window. Here the user can type in text and math input, and Maple displays the output of executed commands. By default Maple displays math in a fashion close to handwriting, which is Maple internally called 2D-math. On the contrary the more classical code-like fashion to display commands is called 1D-math and can be used optionally. For instance the 1D-math input

$$\sin(1/\text{sqrt}(x-1)) \quad \text{corresponds to} \quad \sin\left(\frac{1}{\sqrt{x-1}}\right) \quad \text{1D- versus 2D-math}$$

in 2D-math. In this text I will present all Maple code in 2D-math, with little exceptions where 1D-math is required. All math input is case sensitive. If one wishes to suppress the output of a maple command one has to end it with a colon. Several inputs can be collected in a single execution group, which are then all evaluated together. Here one has to end each input except for the last one with either a colon or a semicolon, where the semicolon would indicate that the output of the respective input shall be displayed. One can also split up inputs into two or more lines by pressing [alt]+[enter]. The toolbar at the top of the document offers buttons to choose between math and text input and offers several layout options.

The toolbar on the left contains a list of palettes. Each palette contains clickable items. For instance the ‘Expression’ palette contains clickable templates for often used math expressions, while the ‘Components’ palette contains tools for embedding interactive features into the document; cf. section 3.

palettes

The toolbar at the top of the Maple window contains shortcuts for frequently used features, like saving files or executing the document.

### 2. Some basic commands

A colon followed by an equation sign is used to assign values to variables. For instance the command  $\beta := 2.5$  assigns the value 2.5 to the variable  $\beta$ , but one could also assign other types of data to a variable, such as a matrix or a text string. To clear a single variable one can assign the respective text string to it, e.g. by  $\beta := \beta$ . The *restart* command clears the internal memory (for instance all assignments to variables) such that Maple behaves essentially as if just started. So it is common praxis to begin a maple document with this command to ensure that no complications occur due to prior executed code.

assigning and clearing variables

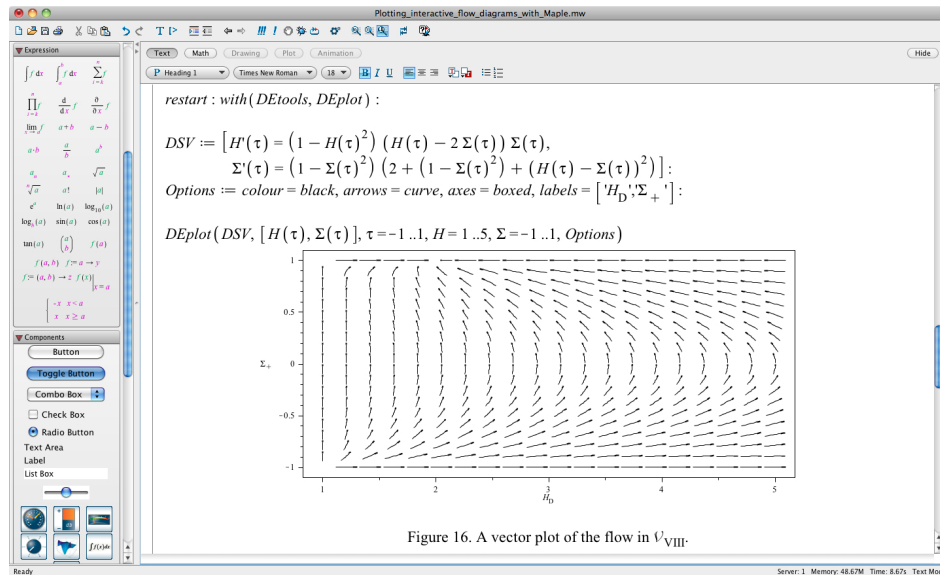


FIGURE 10. The Maple surface.

sets, lists and  
sequences

the Maple help

packages

procedures

The syntax for most mathematical commands is oriented close to mathematical handwriting: Multiplication can be entered with either a space or with the \*-key, in which case it is displayed as a dot;  $ab$  or  $a \cdot b$ . A map  $f$  that maps an  $x$  to an  $f(x)$  is defined with the syntax  $f := x \rightarrow f(x)$ , where the arrow is typed as  $\rightarrow$ . Derivatives can be entered in several ways, for instance for functions  $f : \mathbb{R} \rightarrow \mathbb{R}$  very simple with the prime notation;  $f'(x)$ . A set is entered by  $\{\dots, \dots, \dots\}$ . An ordered set is in Maple called a list, and is entered like a set, just with square brackets;  $[\dots, \dots, \dots]$ . The  $n^{\text{th}}$  element of a list  $A$  can be addressed by  $A_n$ . The *seq* command is often useful to create sets or lists. For instance the command  $[seq(3n, n = 1..3)]$  would create the list  $[3, 6, 9]$ . As an additional option a step size for  $n$  can be given to the *seq* command. The graph of a function  $f : \mathbb{R} \rightarrow \mathbb{R}$  can be plotted with  $plot(f(x), options)$ . Maple provides a very good help system. One can call the help page of a specific command, say *plot*, directly from the document by executing the code  $?plot$ .

The most basic commands are available in Maple straight away. More specific commands are organised in packages. To use them one has to either load the command from the package, load the whole package or address the package together with the command. For instance  $with(plots)$  would load the whole *plots* package while  $with(plots, display)$  would just load the *display* command from this package. Without loading the package or the command, it can be used with the syntax  $plots:-display$  or alternatively  $plots[display]$ . For some older packages, like *DEtools*, only the latter syntax works. It should be noted that there are packages which are not compatible with each other.

Maple also offers the user to create his own commands, called procedures, with the **proc** command. For example, the following code would define a new command *lineplot* with two arguments  $k$  and  $d$ , that would plot the graph of the straight line  $kx + d$ :

```
restart :
```

```
lineplot := proc(k, d)
```

```
  local x, y :
```

```
    plot(k x + d, x = -10..10, y = -10..10, thickness = 2, colour = grey)
```

```
end proc:
```

The **local** command therein is used to declare  $x$  and  $y$  as local variables within the procedure. This ensures that no problems occur when the same variables are also used outside of the procedure for other purposes. Save programming of procedures therefore means to declare all internally used variables that should not interfere with the rest of the document as local.

local variables within  
procedures

### 3. Embedded components

Maple offers a variety of interactive components that can be embedded in the document. They can be found in the ‘Components’ palette in the toolbar on the left. As a demonstrative example should serve the plot of the line  $x + d$  in a plot component where the offset  $d$  is adjustable with a slider component:

components pallet

For this one first has to add the components to the document by clicking on the respective icons in the palette. The properties of each component can be set by right clicking on it and choosing ‘Component Properties...’ from the appearing drop-down menu. The properties can then be set in the respective opening window; cf. figure 11.

component  
properties

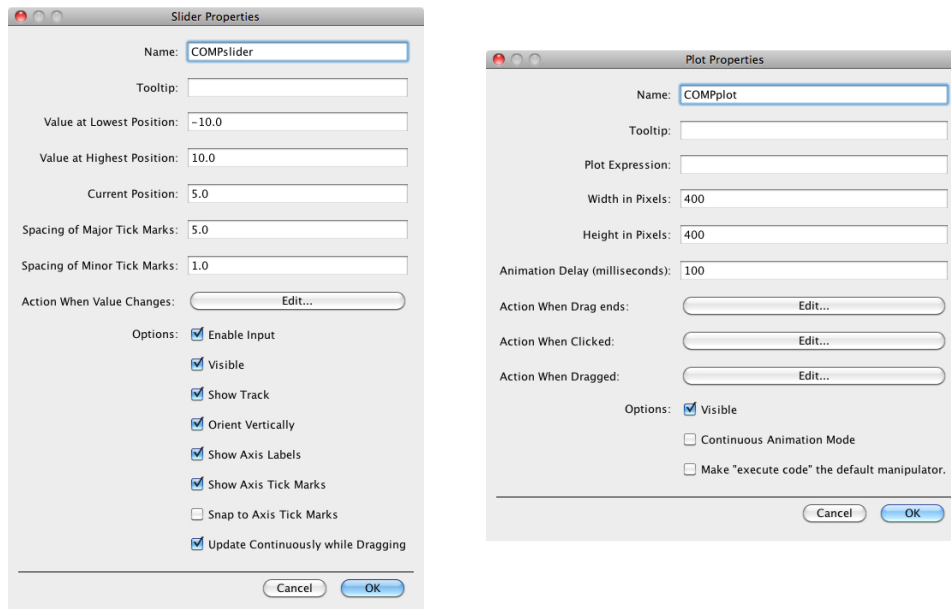


FIGURE 11. The properties windows of the slider and plot components.

Most options are self-explanatory. For instance names can be assigned to the components. Here they shall be called **COMPSlider** and **COMPplot** respectively. In the present example the graph in the plot component is supposed to react on a change of the slider position. The respective code must therefore be entered in the

code window that appears after clicking the ‘Edit...’ button of the ‘Action When Value Changes’ property of the slider component; cf. figure 12.

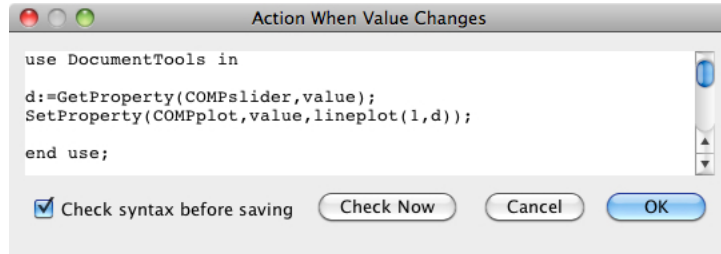


FIGURE 12. The code for the slider’s ‘Action when value changes’.

The code is thereby placed between the lines `use DocumentTools in` and `end use;` and can be entered in 1D-math only. Each input except for the last has to be ended with a semicolon or colon. The first command line in figure 12 reads out the current slider position and assigns this value to the variable `d` by use of the `GetProperty` command. The second line then draws the plot in the plot component by use of the `SetProperty` command. The `lineplot` command used therein is the procedure defined at the end of section 2. After saving the code by clicking ‘Ok’, the plot reacts to the adjustments of the slider in the desired manner. An example plot is shown in figure 13.

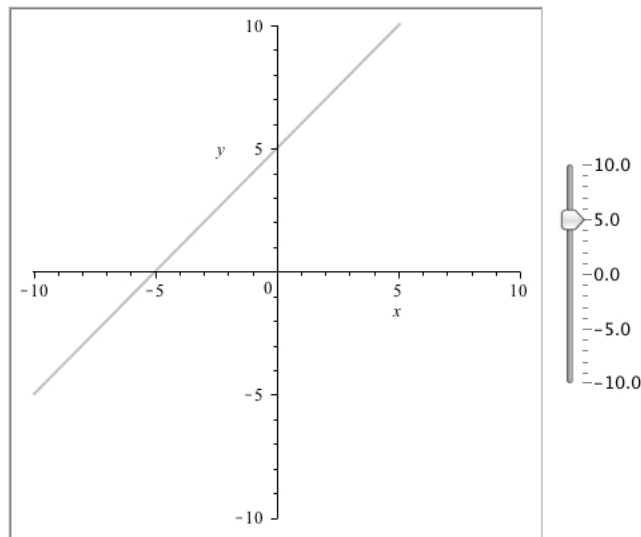
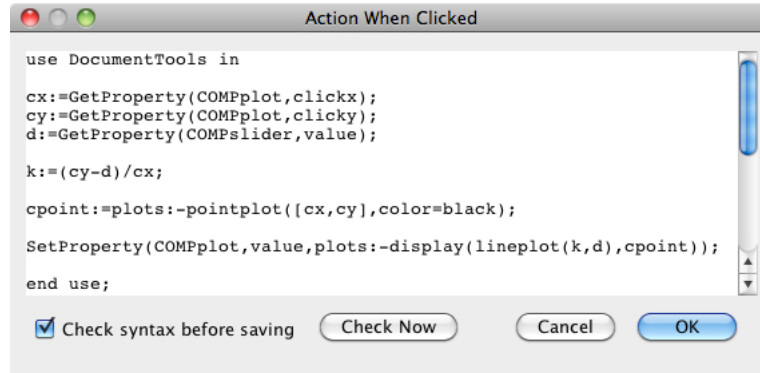


FIGURE 13. The plot component shows a plot of the line  $x + d$ , where  $d$  is adjusted with the slider component.

action when clicked

An interesting feature of the plot component is its ‘Action When Clicked’ property; cf. figure 11. For a demonstration the previous example shall be modified such that the plotted line goes through the point in the plot on which is clicked. The respective code is shown in figure 14:



```

use DocumentTools in
cx:=GetProperty(COMPplot,clickx);
cy:=GetProperty(COMPplot,clicky);
d:=GetProperty(COMPslider,value);


k:=(cy-d)/cx;

cpoint:=plots:-pointplot([cx,cy],color=black);
SetProperty(COMPplot,value,plots:-display(lineplot(k,d),cpoint));
end use;


```

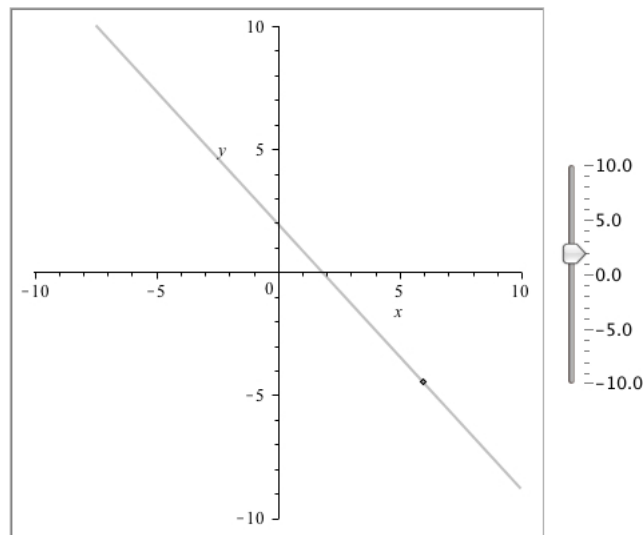
Check syntax before saving    Check Now    Cancel    OK

FIGURE 14. The code for the plot's 'Action When Clicked'.

The position at which the plot was clicked is read out from the `clickx` and `clicky` property of the plot component, and stored in the variables `cx` and `cy`. The value of `d` is still read out from the slider component. Together these variables then serve to compute the slope `k` of the line, after which the line can be plotted as before. The `pointplot` is added to mark the clicked point by a dot. Since the plot shall still react on adjustments of the slider, the code of figure 14 must also be entered for the slider's 'Action When Value Changes'. An example plot of the resulting interactive graph is shown in figure 15. It is important to note that, in order to perform a click that executes the 'Action When Clicked', one has to use the 'Execute click and drag code' tool . It can be found in the toolbar above the code window when the plot is selected.

`clickx` and `clicky` properties

the 'Execute click and drag code' tool 

FIGURE 15. The plot component shows a plot of the line  $kx + d$  that goes through the point on which the plot was clicked last (black dot), and where  $d$  is adjusted with the slider component.



## Plotting flow diagrams

This chapter now shows how to plot flow diagrams of dynamical systems in Maple. Section 1 introduces the *DEplot* command and shows how to plot simple flow diagrams with it. Section 2 then shows how one can draw interactive flow diagrams by making use of embedded components, which were introduced in section 3 of the previous chapter.

### 1. Simple flow diagrams

Maple offers a very simple and convenient way to plot a flow diagram with the *DEplot* command which is contained in the *DEtools* package. I should however outline that there are other possibilities to plot flow diagrams as well. In fact the *DEplot* command is not ideal in the matter of computing efficiency when drawing interactive plots or animations. Other approaches are more efficient; cf. [2]. For the present purposes it is however easily fast enough and has the advantage of being the most simple way, where only one command is needed. To plot a flow diagram with *DEplot* the command has to be fed arguments as follows:

*DEplot*(*dynamical system*, *dynamical quantities*, *time range*, *options*) the *DEplot* command

The first argument is the dynamical system entered as a list or set of ordinary differential equations. The second argument is a list or set of the dynamical quantities, while the third argument fixes the range of the time variable over which the system shall be integrated. All following arguments are optional. The simple use of the command shall be demonstrated by means of the dynamical system ((8) in part 2)

$$\begin{bmatrix} H_D \\ \Sigma_+ \end{bmatrix}' = \begin{bmatrix} (1 - H_D^2)(H_D - 2\Sigma_+)\Sigma_+ \\ (1 - \Sigma_+^2)(2 + (1 - \Sigma_+^2) + (H_D - \Sigma_+)^2) \end{bmatrix}$$

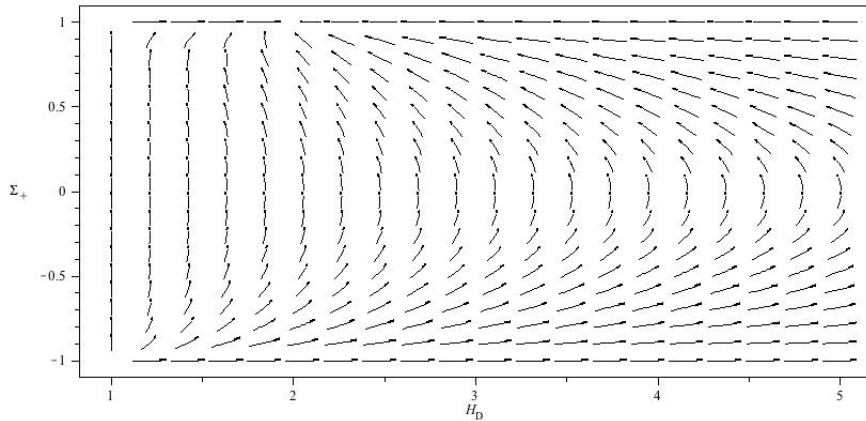
in the state space  $\mathcal{V}_{\text{VIII}}$  given by  $H_D \in (1, \infty)$  and  $\Sigma_+ \in (-1, 1)$ ; cf. figure 1 and section 3.1 in part 2. The following code then produces the vector plot depicted in figure 16: vector plots

*restart* : *with*(*DEtools*, *DEplot*) :

*DSV* := [*H'*( $\tau$ ) = (1 -  $H^2$ )( $H - 2\Sigma$ ) $\Sigma$ ,  
 *$\Sigma'$* ( $\tau$ ) = (1 -  $\Sigma^2$ )(2 + (1 -  $\Sigma^2$ ) + ( $H - \Sigma$ ) $^2$ )] :

*Options* := *color* = *black*, *arrows* = *curve*, *axes* = *boxed*, *labels* = [ $H_D$ ,  $\Sigma_+$ ] :

*DEplot*(*DSV*, [*H*( $\tau$ ),  *$\Sigma$* ( $\tau$ )],  $\tau = -1..1$ ,  $H = 1.5$ ,  $\Sigma = -1..1$ , *Options*)

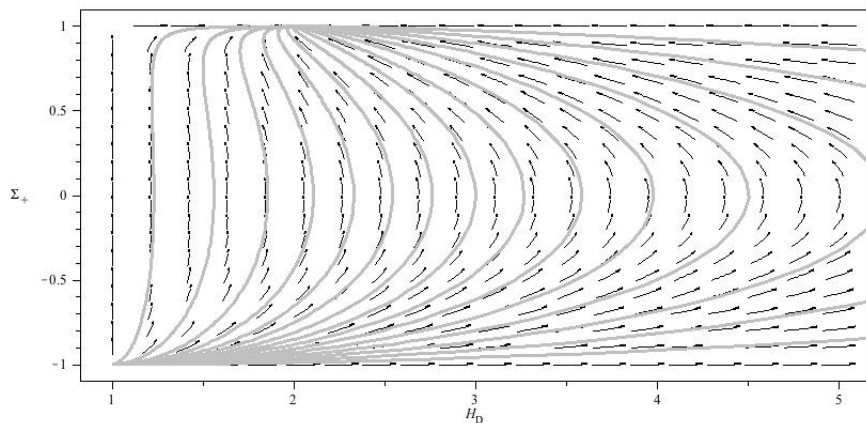
FIGURE 16. A vector plot of the flow in  $\mathcal{V}_{VIII}$ .

The arrows point in the direction of the flow at a grid of points in the state space and already give a good impression on how the flow lines look and where fixed points are located, especially when the option *arrows = curve* or *arrows = comet* is used.

adding flow lines,  
initial conditions

However one would also want to add actual flow lines to this plot. For this one has to give initial conditions as an additional argument to the *DEplot* command right after the argument for the time range. These have to be entered in the form of a set or list of lists. For instance  $[[H(0) = 2, \Sigma(0) = 0], [H(0) = 4, \Sigma(0) = 0]]$  would draw two flow lines through these initial points for  $\tau$  in the entered range. (When initial conditions are entered, the use of the variables with their subscripts, i.e.  $H_D$  and  $\Sigma_+$ , would cause an error.) The following code then produces the plot depicted in figure 17 where the initial data points are distributed along the straight line that goes from the upper left to the lower right corner of the plot region:

```
InitCond := [seq(H(0) = i, \Sigma(0) = -.5i + 1.5, i = 1..4.75, .25)] :
Options2 := Options, numpoints = 500, linecolour = grey, obsrange = false :
DEplot(DSV, [H(\tau), \Sigma(\tau)], \tau = -1..1, InitCond, H = 1.5, \Sigma = -1..1, Options2)
```

FIGURE 17. A vector plot with flow lines of the flow in  $\mathcal{V}_{VIII}$ .



The *numpoints* option can be used to adjust the accuracy to which the solution curves are integrated. A too low value would lead to edgy lines. High values in turn produce smooth flow lines but also increase the computational costs. The *obsrange* option specifies if the integration of a solution should be stopped once the solution curve has left the plot region. The default is *true*. In this case it is set to *false* since there are flow lines which return to the plot region. The plot in figure 17 is to be compared with the analytical result; cf. figure 4 in part 2.

## 2. Interactive flow diagrams

Except for the system in the vacuum boundary  $\mathcal{V}_{\text{VIII}}$ , part 2 dealt with systems that depend on the matter parameters  $(w, \beta)$  out of the parameter space  $\mathbb{P} := (-\frac{1}{3}, 1) \times \mathbb{R}$ . In these cases one could of course draw flow diagrams as described in section 1 for fixed parameter values. However to investigate how the flow changes with the parameters one would like to have an interactive flow diagram in which the parameters would be adjustable in an intuitive fashion, and where one would directly see the change in the flow in reaction of a change of the parameters. This can be achieved by the use of embedded components which were introduced in section 3 of chapter 6.

The goal of this section is to create an interactive flow diagram of both the system ((9) in part 2)

$$\begin{bmatrix} H_D \\ \Sigma_+ \end{bmatrix}' = \begin{bmatrix} -(1 - H_D^2) \left( 2 - \frac{3}{2}(1 - w)(1 - \Sigma_+^2) - H_D \Sigma_+ \right) \\ -(1 - \Sigma_+^2) \left( (1 - H_D^2) + \frac{3}{2}(1 - w)(H_D \Sigma_+ + \beta) \right) \end{bmatrix}$$

in the Bianchi III boundary  $\mathcal{B}_{\text{III}}$  specified by  $H_D \in (1, \infty)$  and  $\Sigma_+ \in (-1, 1)$ , and

$$\begin{bmatrix} M_1 \\ \Sigma_+ \end{bmatrix}' = \begin{bmatrix} M_1 \left( \frac{3}{2}(1 - w)\Sigma_+^2 - 4\Sigma_+ + \frac{1+3w}{2} \left( 1 - \frac{M_1^2}{12} \right) \right) \\ \frac{M_1^2}{6}(2 - \Sigma_+) - \frac{3}{2}(1 - w) \left( 1 - \Sigma_+^2 - \frac{M_1^2}{12} \right) \left( \Sigma_+ - \frac{\beta}{2} \right) \end{bmatrix}$$

in the boundary  $\mathcal{S}_{\sharp}$  given by  $M_1 \in (0, \sqrt{12(1 - \Sigma_+^2)})$  and  $\Sigma_+ \in (-1, 1)$ . The latter system is obtained from the full system ((2) in part 2) for  $H_D = 0$ . The result should be in the fashion of the analytical results; cf. figures 5 to 17 of Part 2.

Clearly two plot components are needed that displays the flow plots. They shall be called `COMPflowB` and `COMPflowS` respectively. The parameters could for example be adjusted with two sliders. A more fancy way however is to use a second plot component which displays a part of the parameter space  $\mathbb{P}$ , and to use it's 'Action When Clicked' to pick a value for  $(w, \beta)$ . This shall be named `COMPparameters`. The plot of  $\mathbb{P}$  shall also display the bifurcation lines which correspond to qualitatively different flows on  $\mathcal{B}_{\text{III}}$  and  $\mathcal{S}_{\sharp}$ ; cf. figure 3 of part 2. The relevant bifurcation lines are  $\pm 1, \beta_{\pm}(w)$  and  $\beta_{\sharp}(w)$  for the flow in  $\mathcal{B}_{\text{III}}$ , as well as  $\pm 2$  and  $\beta_{\sharp}(w)$  for the flow in  $\mathcal{S}_{\sharp}$ . These have to be plotted in `COMPparameters` each time `COMPparameters` is clicked. Hence it is smart to prepare the respective code in procedures to keep the necessary code in the 1D-math environment of the 'Action When Clicked' to a minimum:

setting up the components

code to plot the bifurcation lines

*restart* :

*BifurcLinesB* := `proc()`

**local** *w, Options, Options1, Options2* :

*Options* := *thickness* = 2, *colour* = black, *labels* = ['w', 'β'] :

*Options1* := *Options*, *view* = [-1/3..1, -3..3], *discont* = true :

*Options2* :=  $w = -1/3..-.2$ , *Options* :

*plots*:-display( $\left( \text{plot} \left( \left[ -1, 1, \frac{2w}{1-w} \right], \text{Options1} \right), \right.$   
 $\left. \text{plot} \left( \left[ \text{seq} \left( \frac{-1+\sigma \sqrt{-3+(1-3w)^2}}{3(1-w)}, \sigma = [-1, 1] \right) \right], \text{Options2} \right) \right)$

**end proc:**

*BifurcLinesS* := **proc**()

**local**  $w, \text{Options}$  :

*Options* := *thickness* = 2, *colour* = grey,  
*labels* = ['w', 'β'], *view* = [-1/3..1, -3..3] :

$\text{plot} \left( \left[ -2, 2, \frac{8-2\sqrt{(3(1-w))^2+4(1+3w)}}{3(1-w)} \right], w = -1/3..1, \text{Options} \right)$

**end proc:**

code to plot the  
flow diagrams

Equally the process of plotting the flow diagrams shall be prepared as procedures that takes the values of  $w$  and  $\beta$  as arguments:

*FlowPlotB* := **proc**( $w, \beta$ )

**local**  $DSB, H, \Sigma, \tau, \text{InitCond}, \text{Options}$  :

*InitCond* := [seq([ $H(0) = i, \text{Sigma}(0) = -.5i + 1.5$ ],  $i = 1..4.75, .25$ )] :

*Options* := *colour* = black, *arrows* = curve, *axes* = boxed,

*labels* = [ $H_D, \Sigma_+$ '], *numpoints* = 500,

*linecolour* = grey, *obsrange* = false :

$DSB := \left[ H'(\tau) = -(1 - H(\tau)^2) \left( 2 - \frac{3}{2}(1 - w) (1 - \Sigma(\tau)^2) - H(\tau) \Sigma(\tau) \right), \right.$   
 $\left. \Sigma'(\tau) = -(1 - \Sigma(\tau)^2) \left( (1 - H(\tau)^2) + \frac{3}{2}(1 - w) (H(\tau) \Sigma(\tau) + \beta) \right) \right] :$

with(*DEtools*, *DEplot*) :

*DEplot*(*DSB*, [ $H(\tau), \Sigma(\tau)$ ],  $\tau = -1..1, \text{InitCond}, H = 1..5, \Sigma = -1..1, \text{Options2}$ )

**end proc:**

*FlowPlotS* := **proc**( $w, \beta$ )

**local**  $DSS, M, \Sigma, \tau, \text{InitCond}, \text{Options}$  :

*InitCond* := [seq([ $M(0) = i/3, \text{Sigma}(0) = 0$ ],  $i = -10..1$ )] :

*Options* := *colour* = black, *arrows* = curve, *axes* = boxed,

*labels* = [ $-M_1, \Sigma_+$ '], *numpoints* = 500, *linecolour* = grey :

$DSS := \left[ M'(\tau) = M(\tau) \left( \frac{3}{2}(1 - w) \Sigma(\tau)^2 - 4\Sigma(\tau) + \frac{1+3w}{2} \left( 1 - \frac{M(\tau)^2}{12} \right) \right), \right.$   
 $\left. \Sigma'(\tau) = \frac{M(\tau)^2}{6} (2 - \Sigma(\tau)) - \frac{3}{2}(1 - w) \left( 1 - \Sigma(\tau)^2 - \frac{M(\tau)^2}{12} \right) \left( \Sigma(\tau) - \frac{\beta}{2} \right) \right] :$

```
plots:-display(DEplot(DSS, [M(τ), Σ(τ)], τ = -1..3,
  InitCond, M = -√12..0, Σ = -1..1, Options),
plots:-implicitplot(M = -√12(1 - Σ²),
  M = -√12..0, Σ = -1..1, colour = black, thickness = 2))
```

**end proc:**

To provide the possibility to read the chosen value of  $(w, \beta)$  from the plot of  $\mathbb{P}$ , the clicked point shall be marked by a dot and trace lines. This is prepared in yet another procedure:

```
TraceClick := proc(cw, cb)
```

```
  local cpoint, clines, Options, w, β :
```

```
  Options := w = -1/3..1, β = -3..3, colour = black :
```

```
  cpoint := plots:-pointplot([cw, cb], colour = black) :
```

```
  clines := plots:-implicitplot([w = cw, β = cb], Options) :
```

```
  plots:-display(cpoint, clines) :
```

**end proc:**

What is left to do is to type the code for the ‘Action When Clicked’ of COMPparameters, where the above procedures are called; cf. figure 18: code for the ‘Action When Clicked’

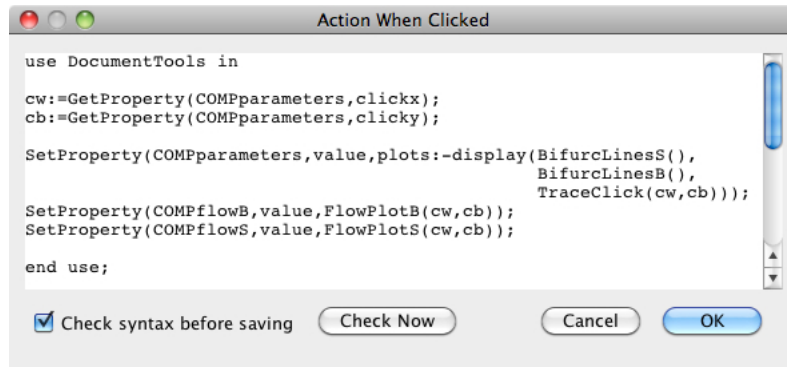
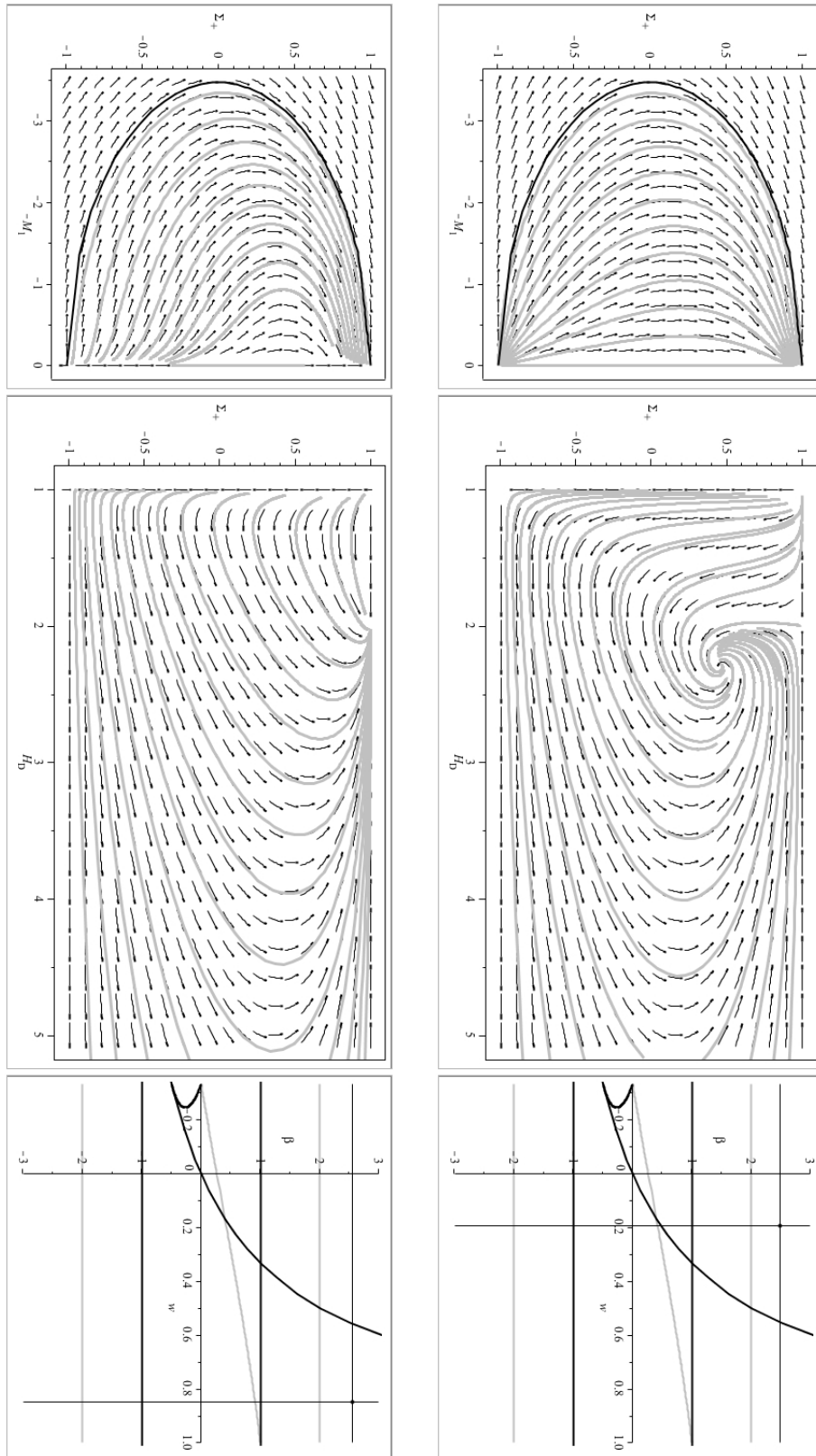


FIGURE 18. The code for the ‘Action When Clicked’ of the plot of  $\mathbb{P}$ .

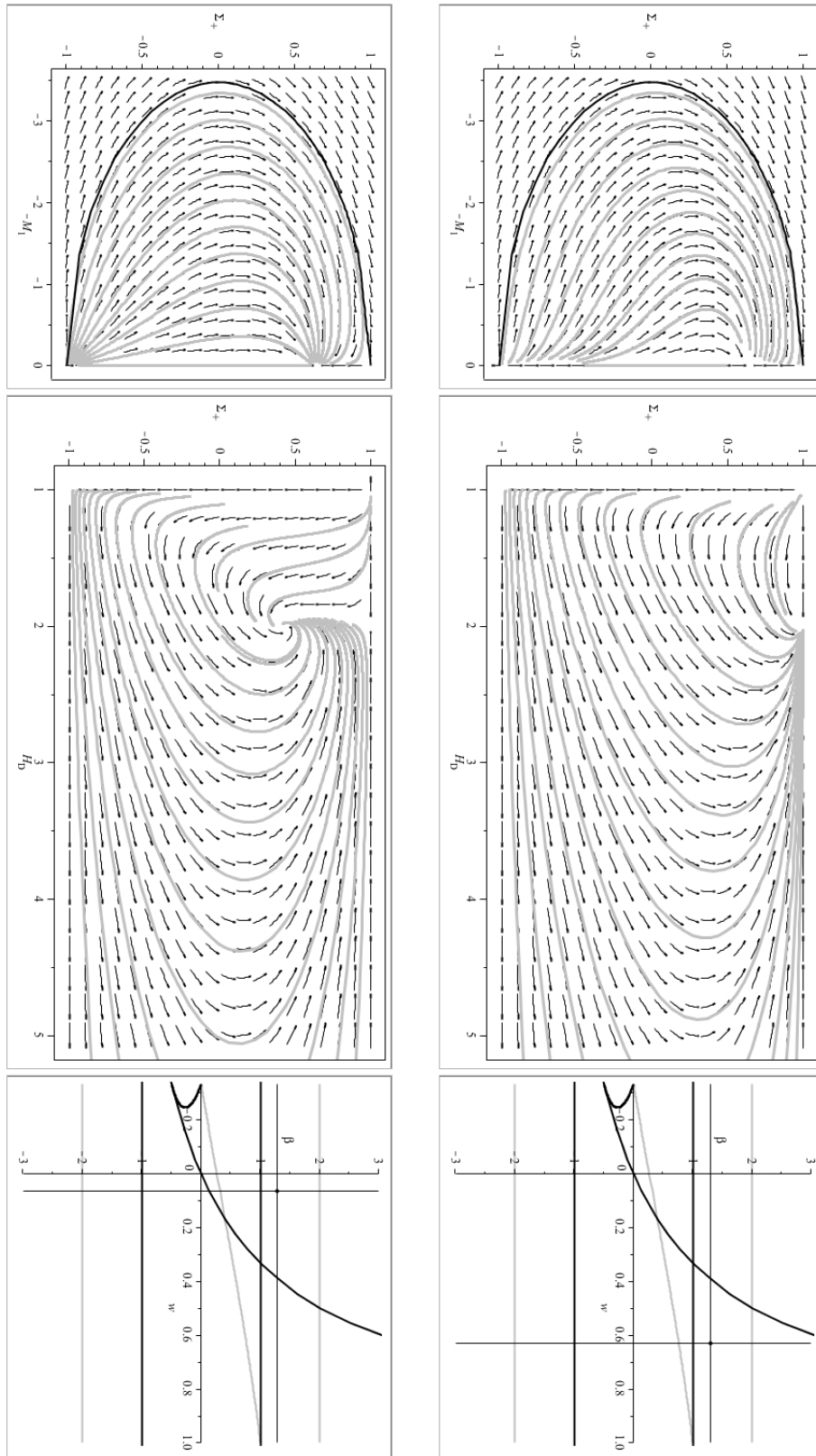
Figures 19 to 24 show example plots of the resulting interactive flow diagram. These are to be compared with the analytical results in figures 5 to 17 of part 2. Since the Maple plots do not contain the flow in the Bianchi I boundary  $\mathcal{X}_1$ , there are two cases less here than in part 2.



(A) corresponds to figure 5 of part 2

(B) corresponds to figure 6 of part 2

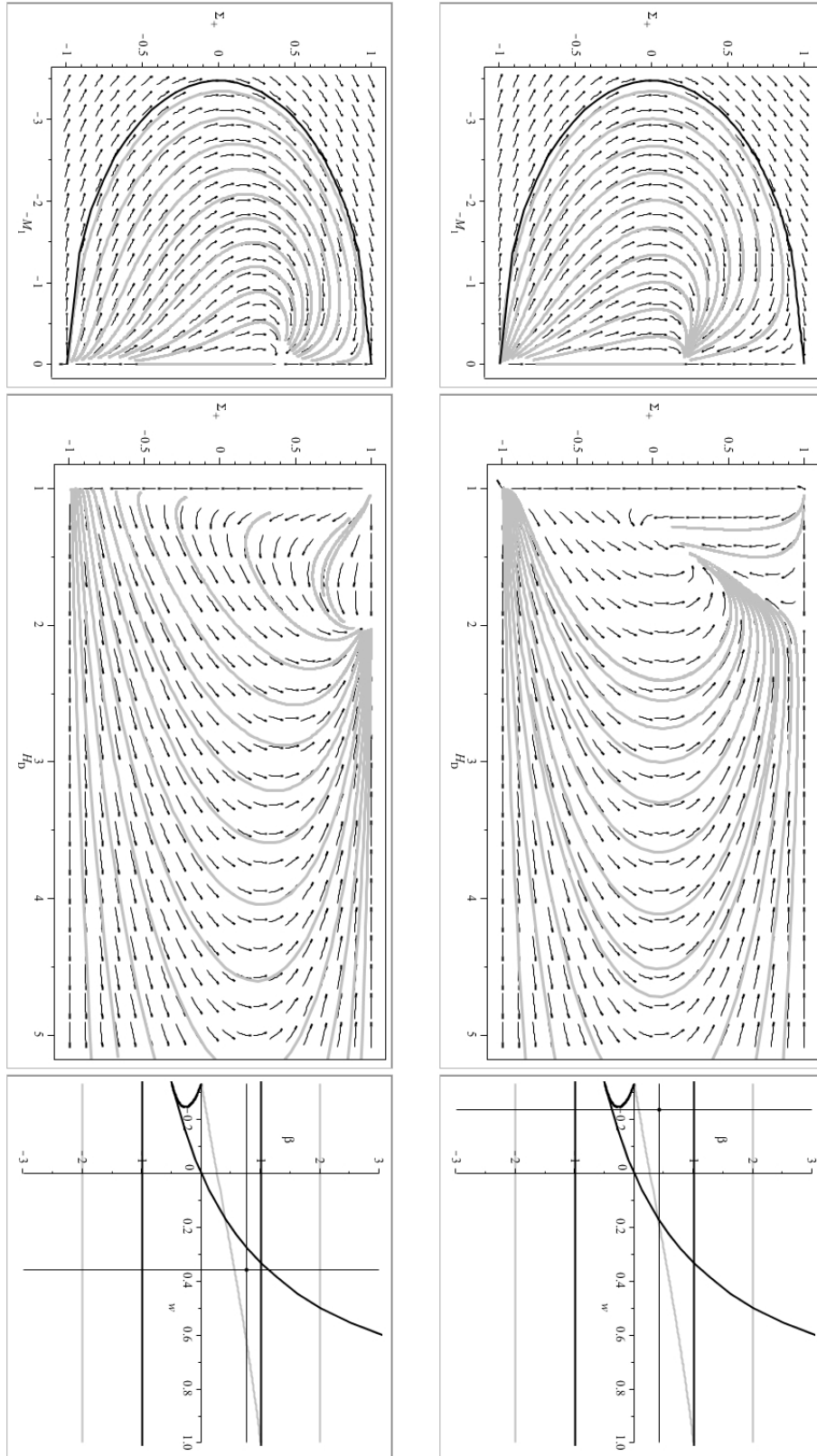
FIGURE 19. Example plots of the interactive flow diagram. The labels refer to the corresponding diagrams of the analytical results in part 2, of which the respective plot is a representative.



(A) corresponds to figure 7 of part 2

(B) corresponds to figure 8 of part 2

FIGURE 20. Example plots of the interactive flow diagram. The labels refer to the corresponding diagrams of the analytical results in part 2, of which the respective plot is a representative.

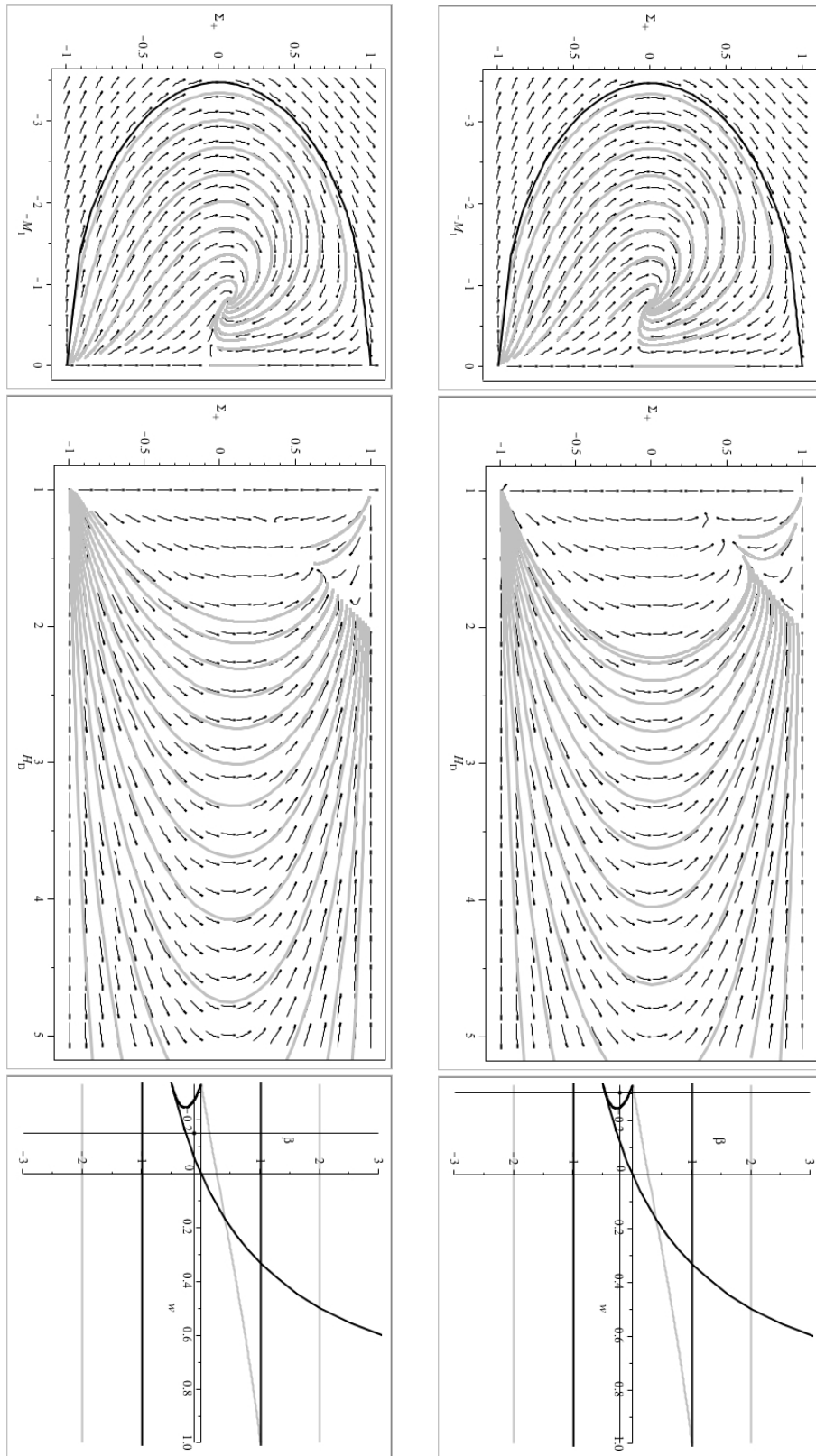


(A) corresponds to figure 9 of part 2

(B) corresponds to figure 10 of part 2

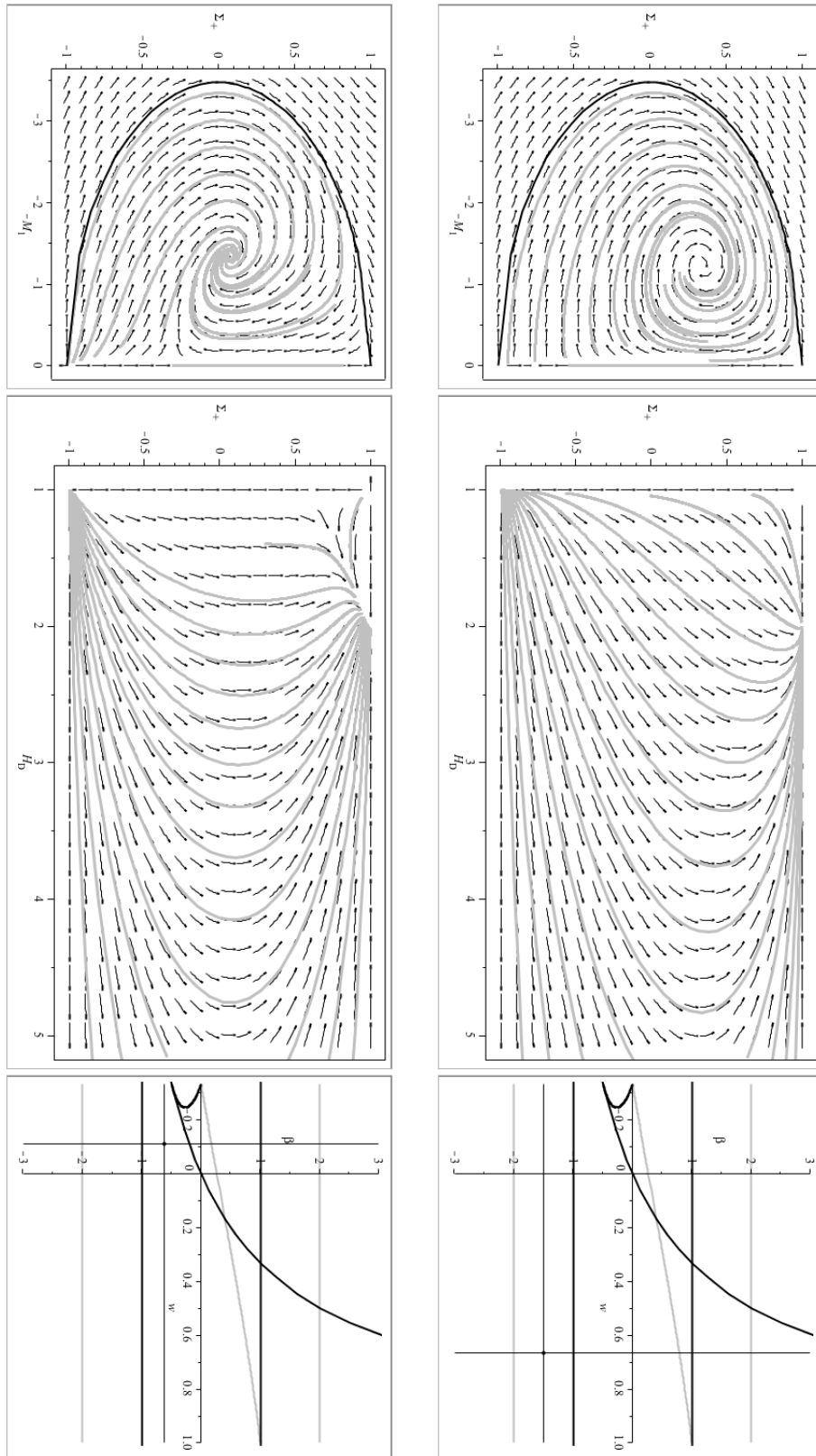
FIGURE 21. Example plots of the interactive flow diagram. The labels refer to the corresponding diagrams of the analytical results in part 2, of which the respective plot is a representative.





(A) corresponds to figure 11 and 13 of part 2 (B) corresponds to figure 14 of part 2

FIGURE 22. Example plots of the interactive flow diagram. The labels refer to the corresponding diagrams of the analytical results in part 2, of which the respective plot is a representative.



(A) corresponds to figure 12 and 15 of part 2 (B) corresponds to figure 16 of part 2

FIGURE 23. Example plots of the interactive flow diagram. The labels refer to the corresponding diagrams of the analytical results in part 2, of which the respective plot is a representative.



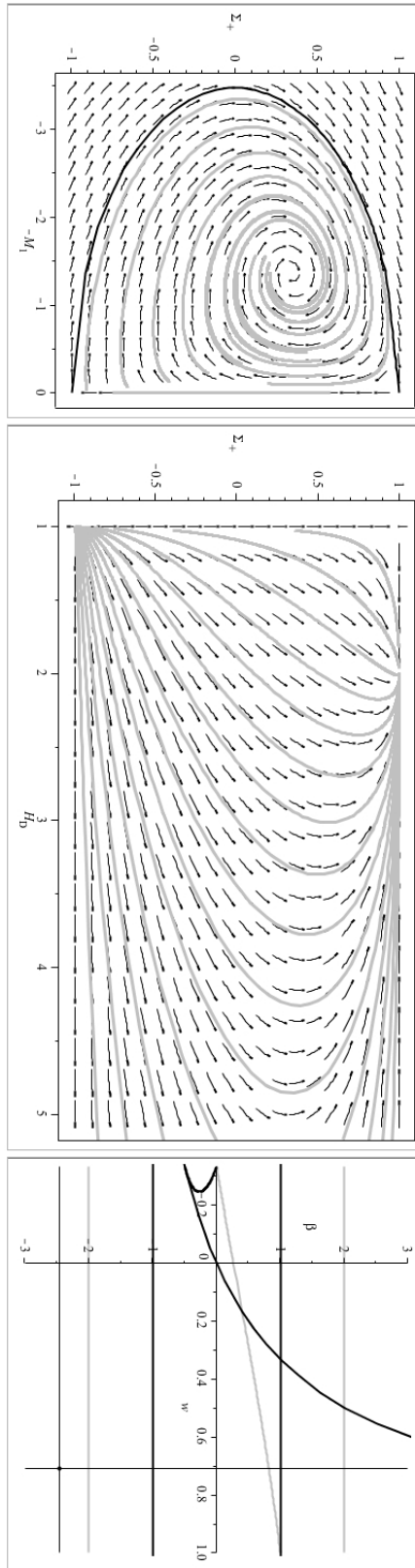


FIGURE 24. Example plot of the interactive flow diagram. This plot is a representative of the analytical result of figure 17 of part 2.



## References and online resources

- [1] Heißel G: `Plotting_interactive_flow_diagrams.mw`; Maple 15 document (2012).  
[https://www.dropbox.com/s/ssdzhpt00awz2wu/Plotting\\_interactive\\_flow\\_diagrams.mw](https://www.dropbox.com/s/ssdzhpt00awz2wu/Plotting_interactive_flow_diagrams.mw)

(In the case that the name of the downloaded file does not end with ‘.mw’ it might be necessary to manually rename the file so it has the proper ‘.mw’ ending, in order to open it with Maple.)

This document is a supplement to part 3 with the same content and working examples. It was created with Maple 15. The compatibility with other Maple versions cannot be guaranteed. In case that problems occur with the download, or the above link is not supported anymore at some time, feel free to contact me at either [Gernot.Heissel@Mac.com](mailto:Gernot.Heissel@Mac.com) or [Gernot.Heissel@GMX.at](mailto:Gernot.Heissel@GMX.at).

Cited on page 62

- [2] acer (forum user): faster than DEplot; post in the MaplePrimes forum (2011).  
<http://www.MaplePrimes.com/posts/119858-Faster-Than-DEplot>

[www.MaplePrimes.com](http://www.MaplePrimes.com) is a forum site funded by Maplesoft. It provides a community platform for Maple users and is a good address for constructive communication. This particularly interesting post discusses an alternative to the `DEplot` command in using a combination of the commands `plots:-odeplot` and `plots:-fieldplot`. It contains working examples and comparisons of the different approaches, and shows that the alternative approach, in turn for the price of being more complicated, is superior in terms of the computing efficiency.

Cited on page 69



# Appendix



## Abstract

This thesis is organised in three parts: Part 1 is concerned with a short introduction to spatially homogenous cosmology and the use of methods from the mathematical theory of dynamical systems in this research field. It aims to help the reader who is just starting to become acquainted with spatially homogenous cosmology to get a good overview and to become familiar with the basic ideas and concepts. After the lecture of part 1 the reader should then be able to read and understand part 2 at least along general lines. Part 2 is a reprint of my research article *Dynamics of locally rotationally symmetric Bianchi type VIII cosmologies with anisotropic matter* which was published by Springer in 2012 in the journal *General Relativity and Gravitation*. It deals with the analysis of one particular class of spatially homogenous cosmologies. The therefor chosen matter contents are in general anisotropic and comprise a larger family of models in which for instance also perfect fluids are contained as special cases. The results allow to draw conclusions on how the grade of anisotropy of the matter content effects the past and future asymptotic evolution of these models. Part 3 gives a tutorial on how to visualise the solutions of the evolution equations examined in part 2 in an interactive flow diagram with the computer algebra system Maple. The such produced diagrams allow the user to see a change in the behaviour of the solutions as a direct reaction to the change in the matter parameters, where one of them essentially gives the grade of matter anisotropy. They are therefore well suited to clearly represent the complex space of solutions, and most notably to present the physical conclusions which were drawn out of the analysis in a comprehensible fashion. Part 3 is also supplemented by a Maple document, which has the same content than presented in this part, with working examples.





## Zusammenfassung (German abstract)

Diese Arbeit besteht aus drei Teilen: Teil 1 gibt eine kurze Einleitung in die räumlich homogene Kosmologie und in die Anwendung von Methoden aus der mathematischen Theorie der dynamischen Systeme auf diesem Gebiet. Sie ist an den Leser gerichtet der gerade damit beginnt sich mit der räumlich homogenen Kosmologie vertraut zu machen, und soll ihm helfen einen guten Überblick über dieses Gebiet zu erlangen, und die grundlegenden Ideen und Konzepte zu verstehen. Nach der Lektüre von Teil 1 sollte es dem Leser dann möglich sein Teil 2 zu lesen und zumindest im Kern zu verstehen. Teil 2 ist ein Abdruck meines Aufsatzes *Dynamics of locally rotationally symmetric Bianchi type VIII cosmologies with anisotropic matter* welcher 2012 von Springer in der Zeitschrift General Relativity and Gravitation veröffentlicht wurde. Er befasst sich mit der Analyse einer bestimmten Klasse von räumlich homogenen kosmologischen Modellen. Die hierfür gewählten Materieinhalte sind im allgemeinen anisotrop, und umschließen eine größere Familie von Modellen in der etwa auch ideale Flüssigkeiten als Spezialfall enthalten sind. Die Resultate erlauben es Schlüsse darüber zu ziehen in welcher Weise sich der Grad der Anisotropie des Materieinhaltes auf die asymptotische Dynamik in der fernen Vergangenheit und Zukunft auswirkt. Teil 3 gibt eine Anleitung zur Visualisierung der Lösungen der in Teil 2 behandelten Bewegungsgleichungen in einem interaktivem Flussdiagramm mit dem Computer Algebra System Maple. Die so erstellten Diagramme erlauben es dem Benutzer eine Änderung im Verhalten der Lösungen als direkte Reaktion auf eine Änderung der Materieparameter wahrzunehmen, von denen einer im Wesentlichen den Grad der Anisotropie bestimmt. Sie eignen sich daher sehr gut dazu den komplexen Lösungsraum übersichtlich darzustellen und vor allem auch um die aus der Analyse gezogenen physikalischen Schlüsse verständlich zu präsentieren. Teil 3 ist zudem durch ein Maple Dokument ergänzt, welches den Inhalt dieses Teils mit ausführbaren Beispielen wiedergibt.



## Curriculum vitae

### Profile

Name	Gernot Heißel
Academic degree	Bachelor of Science (BSc)
Date of birth	08.07.1985
Place of birth	Rum in Tyrol, state of Austria
Nationality	Austria
Contact	Gernot.Heissel@Mac.com, Gernot.Heissel@GMX.at



### Education at school

- 1991–1995 Attendance of the primary school Volksschule Innsbruck-Siebererstraße
- 1995–1999 Attendance of the secondary school Bundesgymnasium & Bundesrealgymnasium Innsbruck-Sillgasse
- 1999–2004 Attendance of the technology-oriented higher college Höhere Technischen Bundes-Lehr- und Versuchsanstalt (HTL) Anichstraße Innsbruck in the college of Electronics specialising in Technical Computer Science; Graduation with distinction (mit gutem Erfolg)

### Education at university

- 2005–2009 Student of Physics at the University of Innsbruck; Graduation with the Bachelor of Science (BSc)
- 2009–2012 Student of Physics in the Master's programme at the University of Vienna.

### Academical and pertinent practical experience

- 08-09/2006 Four weeks work experience in seismic surveying at the geophysics company GeoExpert AG, based in Embrach in Switzerland.
- 07/2007 Three weeks science hands-on training at the University of Innsbruck with the project of designing and building a staff balancing machine in the form of a double pendulum
- 2010–2012 Position as tutor to the lectures *Mathematical Methods of Physics 1* (winter semesters 2010/11 and 2011/12) and *Mathematical Methods of Physics 2* (summer semester 2011) at the University of Vienna

02/2012 Participation to the second *Central European Relativity Seminar* at the Jagiellonian University in Kraków with a talk on the results of my Master's thesis.

### **Further occupations**

07-08/2000 Respectively four weeks work experience at the IT department of the  
07-08/2001 government of Tyrol

2004–2005 Military service at the Österreichisches Bundesheer (Austrian Armed Forces) for eight months

### **Scientific interests**

I am generally interested in very fundamental questions of physics. I want to discover what nature is all about. As a consequence of this, there results on the one hand my strong interest in the two fundamental pillars of theoretical physics; quantum field theory for the description of particles, and general relativity for the description of spacetime. On the other hand, from that results also my strong interest in those fields of physics, in which these two theories are brought together to reach a better understanding and description of nature. With this I particularly mean fields like astroparticle physics and cosmology.

### **Further interests and hobbies**

In my free-time I read physics textbooks and interdisciplinary science magazines. Outside science, I like to listen to good music or to watch a good movie. I am also interested in sound synthesis and try to be creative in this respect with my synthesiser. I enjoy being out in nature, and like to be in the mountains in winter, especially on the snowboard or the barrow.